2017년도 2월
박사학위 논문

The mechanism of cellular senescence and neuronal differentiation in human bone marrow mesenchymal stem cells

조 선 대 학 교 대 학 원

생 명 과 학 과

정 신 구

The mechanism of cellular senescence and neuronal differentiation in human bone marrow mesenchymal stem cells

인간 유래 골수 줄기세포의 노화 및 신경 분화 기전 연구

2017 년 2 월 24 일

조 선 대 학 교 대 학 원

생 명 과 학 과

정 신 구

The mechanism of cellular senescence and neuronal differentiation in human bone marrow mesenchymal stem cells

지도교수 조광원

이 논문을 이학박사학위 신청 논문으로 제출함

2016 년 10월

조 선 대 학 교 대 학 원

생 명 과 학 과

정 신 구

정신구의 박사학위논문을 인준함

위원장 조선대학교 부교수 전택중 (인)

위 원 조선대학교 조교수 송상기 (인)

위 원 조선대학교 조교수 온탁범 (인)

위 원 한양대학교 교 수 채영규 (인)

위 원 조선대학교 부교수 조광원 (인)

2016년 12월

조선대학교 대학교

CONTENTS

List of Tables

List of Figures

[Part. I]

(Chapter 1)

(Chapter 2)

(Chapter 3)

[Part. II]

(Chapter 1)

(Chapter 2)

Abbreviations

ALS	Amyotrophic lateral sclerosis
AP	Alkaline phosphatase
ATM	Ataxia-telangiectasia mutated
Bcl-2	B cell lymphoma-2
BHA	Butylated hydroxyanisole
BM-	Bone marrow-mesenchymal stromal cells
CAT	Catalase
CNS	Central nervous system
CNS	Central nervous system
CREB	cAMP response element-binding protein
DCFH-	2'-7'-Dichlorodihydrofluorescein diacetate
ERK1/2	Extracellular signal-regulated protein kinase
FBS	Fetal bovine serum
FOXO1	Forkhead box O1
GV	*Gracilaria vermiculophylla*
HDAC	Histone deacetylase
HDAC6	Histone deacetylase 6
HSC	Hematopoietic stem cells
MAPK	Mitogen activated protein kinase
MDM2	Mouse double minute 2 homolog

MSCs	Mesenchymal stromal cells
MTs	Microtubules
PBS	Phosphate-buffered saline
PCR	Polymerase chain reaction
PD	Population doublings
PDL	Population doubling level
PTM	Post-translational modification
ROS	Reactive oxygen species
ROS	Reactive oxygen species
RT	Room temperature
SA	Sodium arsenite
Sirt2	Sirtuin 2
SOD	Superoxide dismutase
TSA	Trichostatin A
TubA	Tubastatin A
UP	*Undaria pinnatifida*

Abstract

The mechanism of cellular senescence and neuronal differentiation in human bone marrow mesenchymal stem cells

Sin-Gu Jeong

Advisor : Associate Prof. Goang-Won Cho, Ph.D.

Department of life science,

Graduate school of Chosun University

Adult stem cells have been used for cell therapy in patients with aging related diseases such as degenerative disorder. A sufficient quantity of stem cells is necessary to maximize therapeutic efficacy. For this reason, isolated stem cells must be amplified under *in vitro* culture conditions. However, stem cells undergo replicative senescence during long-term culture. Cellular senescence causes functional decline of cells due to cumulative damages in DNA, proteins, lipids, and carbohydrates. Thus, stem cell expansions increase the risk of cellular senescence, resulting in reduced therapeutic efficacy or the failure of stem cell therapies.

In this study, first, I examined alteration of intracellular ROS and

apoptotic signaling pathway in senescent stem cells. Senescent stem cells resisted oxidative damage induced by hydrogen peroxide, and the expression of the apoptotic molecules (Bax, Bcl-2, cleaved caspase-3 and p53) did less change in response to apoptotic stimulation in senescent stem cells compared to young stem cells. In addition, I detected increasing ROS levels and decreasing antioxidant proteins (SOD1, SOD2, and catalase) in senescent stem cells. These senescence phenotypes were partially recovered by scavenging excess ROS by treatment with the antioxidant reagent ascorbic acid. Thus, control of excessive ROS production during the long-term expansion may yield better quality of cells which may lead to improved therapeutic efficacy in stem cell therapy.

Next, I observed the anti-oxidant and anti-senescent effects through the treatment of trichostatin A (TSA), *Undaria pinnatifida* extracts (UP-Ex), or *Gracilaria vermiculophylla* extracts (GV-Ex) to stem cells. When the senescent cells were treated with TSA, UP-Ex, or GV-Ex, the expression of anti-oxidant proteins (SOD1, SOD2, and catalase) was significantly restored, and the excessive ROS was reduced. The expression of senescence related proteins (p53, p21, and p16) were decreased and differentiation potency was restored. This study suggests that stem cell cultures with TSA, UP-Ex, and GV-Ex may improve the efficiency of cell therapy by preventing stem cell senescence.

Mesenchymal stem cells (MSCs) have the potential to differentiate into neuronal cells, and have been used for cell therapy in neurological

diseases. Many researchers have tried to improve the efficiency of differentiation through the epigenetic approach and the pattern analysis of the genes during the neuronal differentiation process. This means that genetic and epigenetic regulations are important for the neuronal differentiation. In this study, I investigated the role of histone deacetylase Sirt2 and stress granules (SGs) which were involved with post-transcriptional modification in neuronal differentiation process. I observed that acetylation of α-tubulin expression levels gradually decreased from 2 to 6 h and then returned to baseline at 12 h during neuronal differentiation, while the expression of Sirt2 was significantly increased. Sirt2 regulates the expression of neural specific proteins NF-M and MAP-2 via ERK-CREB pathway activation. I observed that the SGs were significantly increased between 1 and 2 h during neuronal differentiation and then gradually decreased after 2 h, whereas neural specific protein NF-M expression was begun to increase after 6 h. Taken together, it was concluded that Sirt2 and SGs may play an important role in the neuronal differentiation. Therefore, specific roles of Sirt2 and SGs in neuronal differentiation need to be further investigated.

국문초록

인간 유래 골수 줄기 세포의 노화 및 신경 분화 기전 연구

성체 줄기세포는 퇴행성 질환과 같은 노화 관련 질환의 세포치료제로서 사용되어왔다. 줄기세포의 충분한 양의 확보는 치료 효율성의 증가를 위해 필수적이다. 이러한 이유로, 분리된 줄기세포는 기내 배양을 통해 충분한 세포의 양을 확보해야 한다. 그러나 장기간의 배양 동안 줄기 세포는 복제 노화를 겪는다. 세포 노화는 DNA, 단백질, 지질, 그리고 탄수화물의 누적된 손상으로 인해 세포의 기능적 감소를 유발한다. 이와 같이, 줄기세포의 장기간 배양은 세포 노화를 증가시키고 이로 인해 세포 치료의 실패 또는 효율성의 감소를 야기시킨다.

본 연구는 첫째로 노화된 줄기 세포에서 세포 사멸 경로의 변화와 활성 산소를 관찰하였다. 노화된 줄기 세포는 과산화수소에 의해 유도된 손상에 저항하였고, 세포 사멸 단백질 (Bax, Bcl-2, cleaved caspase-3와 p53)의 발현이 젊은 줄기 세포에 비해 노화된 줄기 세포에서 스트레스 반응에서 발현이 적은 변화를 보였다. 또한 노화된 줄기 세포에서 세포 내 활성 산소 수준의 증가를 관찰하였고, 항-산화 단백질인 SOD1, SOD2, catalase의 발현의 감소를 관찰하였다. 항-산화 물질인 아스코르브산을 처리한 결과, 항-산화 단백질의 유의한 회복을 통해 축적된 활성 산소가 감소하는 것을 관찰하였다. 이는 활성 산소의 제어가 세포 노화의 제어와 세포 치료의 효율성을 높이기 위해 중요한 요인인 것을 의미한다.

다음으로 활성산소의 제어를 위해 항-산화 효능을 갖는 물질을 찾고자 연구를 진행하였다. 본 연구에서는, 노화된 줄기 세포에서 trichostatin A (TSA)와 참미역 추출물 그리고 꼬물꼬시래기 추출물의 처리를 통하여 항-산화 및 항-노화 효과를 관찰하였다. TSA, 참미역 추출물 그리고 꼬물꼬시래기 추출물을 노화된 세포에 처리 하였을 때, 노화로 인해 감소되었던 항-산화 단백질의 발현이 유의하게 회복됨을 관찰하였고, 세포 내 축적되었던 활성 산소의 양이 유의하게 감소됨을 관찰하였다. 또한 노화 표지 단백질인 p53, p21 그리고 p16의 발현이 감소하는 것을 관찰하였고, 분화-능 역시 회복됨을 관찰하였다. 이 연구는 줄기세포 배양액과 함께 TSA, 참미역 추출물 그리고 꼬물꼬시래기 추출물을 처리 하였을 때 줄기세포의 노화를 억제하여 세포 치료의 효율성을 증가시킬 수 있음을 의미한다.

중간엽 줄기세포는 신경세포로 분화 할 수 있는 능력이 있고, 신경계 질환의 치료제로 사용 되어왔다. 많은 연구자들은 신경 분화 과정 동안 후생 유전적 접근과 분화 과정 동안의 유전자 패턴의 분석을 통해 분화 효율성을 높이고자 하였다. 이는 유전적 및 후생유전적 조절이 신경세포의 분화에 중요하게 작용하는 것을 의미한다. 본 연구는 히스톤 탈아세틸화 효소인 Sirt2와 전사 후 변형에 관여하는 스트레스 그래뉼의 신경 분화 과정 동안의 역할을 연구하였다. 신경 분화 과정동안 α-tubulin의 아세틸화가 2시간에서 6시간에 감소하였다가 회복되는 것을 관찰하였고, 이를 조절하는 Sirt2의 발현이 유의하게 증가하는 것을 관찰하였다. Sirt2를 억제하였을 때 분화 과정 동안 신경 특이적 단백질인 NF-M과 MAP-2의 발현은 유의하게 감소하였고 이는 Sirt2가 ERK와 CREB의 인산화를 통해

신경분화를 조절하는 것을 나타낸다. 스트레스 그래뉼의 형성은 신경 분화 동안 1시간에서 2시간 사이에 유의하게 증가되었고 2시간 이후부터 점진적으로 감소하는 것을 관찰하였다. 반면에 신경 특이적 단백질인 NF-M의 발현은 6시간부터 증가되는 것을 관찰하였다. 종합적으로, Sirt2와 스트레스 그래뉼은 신경 세포로의 분화 기전에 있어서 중요한 역할을 할 수 있다. 그러므로 신경분화에 있어서 Sirt2와 스트레스 그래뉼의 정확한 역할에 대한 연구는 진행 되어야 한다.

I. Introduction

1. Stem cells as a biomedicine

Human bone marrow-mesenchymal stem cells (hBM-MSCs) can differentiate into various cell types (Caplan, 2007; Jeong et al., 2013; Pittenger et al., 1999). hBM-MSCs also secrete a number of trophic/growth factors and act as trophic mediators (Cho et al., 2010; Nagai et al., 2007), which provide protection against oxidative stress and inflammation. These features suggest that hBM-MSCs are an excellent candidate for stem cell medicine.

2. Cellular senescence in stem cells

Stem cells and their microenvironmental niches regulate tissue homeostasis (Singh, 2012). Stem cells are exposed to factors that lead to age-related changes in their replicative or post-mitotic progeny. Their numbers gradually decrease with progressive aging, resulting in the deterioration of homeostasis and the accumulation of senescent cells. Stem cells gradually enter into a senescence phase, with telomere shortening and a decline of telomerase (TERT) activity, called the Hayflick limit (Hayflick and Moorhead, 1961; Allsopp et al., 1992). Stem cells undergo replicative senescence, which is characterized by typical phenotypes including morphological enlargement (a flat, fried egg morphology), reduced secretion of growth factors/cytokines, reduced

differentiation potential, epigenetic modification, and telomere shortening (Harley et al., 1990; Maegawa et al., 2010; Mastri et al., 2012).

3. Reactive oxygen species (ROS)

Steady-state, intracellular ROS provides a number of beneficial effects, including enhancing cell proliferation and migration (Hoidal, 2001; Irani, 2000). However, excessive ROS production causes devastating effects, including degradation of DNA, protein, and lipid and suppresses the transcription of genes involved in cellular differentiation and mitochondrial function (Chiarugi and Buricchi, 2007; Geissler et al., 2012). Previous studies, excessive intracellular ROS impair the DNA repair and cellular signaling as a means of accelerating cellular senescence (Hart and Setlow, 1974; Koga et al., 2011). Elevation of intracellular ROS up-regulates the tumor suppressor genes p53 and p21 (Jung et al., 2004; Macip et al., 2002). Thus, ROS are a major cause of functional decline during typical cellular senescence.

4. Microtubules (MTs)

Microtubules (MTs) are an important component of the cytoskeleton that can influence the cell structure, cell division, intracellular transport, and differentiation (Bowne-Anderson et al., 2013; Gelfand and Bershadsky, 1991; Howard and Hyman, 2003). MTs are generally composed of 13 profilaments, each constructed from asymmetric heterodimers of αβ-

tubulin. MTs switch between slow growth and rapid shrinkage, known as dynamic instability (Howes et al., 2014). The dynamic instability of MTs can be explained empirically by two parameters: growth rate, shrinkage rate (Al-Bassam and Corbett, 2012). The MT dynamic is mediated by post-translational modifications (PTM) of the tubulin subunits (α- and β-tubulin), such as acetylation, phosphorylation, detyrosination, and ubiquitination (de Forges et al., 2012; Mitchison and Kirschner, 1984). The acetylation/deacetylation of α-tubulin at lysine 40 (K40) contributes to MT modification (Al-Bassam and Corbett, 2012; Howes et al., 2014).

5. Stress granules (SGs)

In eukaryotic cells, untranslated mRNAs can accumulate in cytoplasmic mRNP granules, such as processing bodies (P-bodies) and stress granules (SGs). SGs are ribonucleoprotein (RNP) complexes consist of arrested translation initiation complexes (Anderson and Kedersha, 2008), RNA binding proteins, miRNAs, and various proteins involved with signaling of cell metabolisms (Anderson and Kedersha, 2009b). Moreover, SGs are related to germ cell granules, somatic cell granules, and neuronal granules. SGs play important roles in the translation of mRNA and localization (Yamasaki and Anderson, 2008). SGs assembly occurred from an incomplete assembly of translation initiation factors eIF4E, eIF4G, eIF5A, poly-A binding protein (PABP), eIF3, eIF2, and 43S pre-initiation complex (PIC) (Yamasaki and Anderson, 2008). 43S PIC is repressed by

phosphorylation at serine 51 (S51) of eukaryotic initiation factor 2α (eIF2α), an important element of eIF2–GTP–$tRNA^{Met}$ ternary complex for assembly of 43S PIC (Yamasaki and Anderson, 2008).

II. Materials and Methods

1. Human BM-MSCs and culture conditions

The hBM-MSCs were purchased from CEFO (Cell Engineering For Origin; Seoul, Korea). Cells were tested for viral infections and mycoplasma contamination and confirmed to be negative. Flow cytometric analysis of the cells revealed a CD73+, CD105+, CD31- phenotype. The hBM-MSCs (0.9×10^3 cells/cm^2) were cultured in hBM-MSC growth media (DMEM; Gibco; Grand Island, NY, USA), containing mesenchymal cell growth supplements, L-glutamine, penicillin, and streptomycin, without any stimulatory supplements or vitamins. Cells were maintained in a humidified incubator at 37 °C, using a standard mixture of 95% air and 5% CO_2. Cells were subcultured once every 5 days and medium was changed every three days. Long-term cell growth in vitro was monitored by counting the cell number with a hemocytometer. The cumulative population doubling (PD) was calculated with the formula PD level (PDL) = 3.22 × log(Ne)−log(Nb), where Nb indicates the cell number at the beginning of the incubation time and Ne indicates the cell number at the end of the incubation time.

2. Senescence-associated β-galactosidase (SA-β-gal) staining

Senescence-associated beta-galactosidase (SA-β-gal) staining was carried out using the Senescence β-Galactosidase Staining Kit (Cell Signaling Technology Inc.; Danvers, MA, USA) according to the

manufacturer's instructions. The MSCs were seeded into 6-well plates at a density of 1 × 10^4 cells/well and incubated until the appropriate confluence was reached. The cells were washed with PBS and fixed with 2% formaldehyde and 0.2% glutaraldehyde in distilled water for 15 min at room temperature. The cells were then washed twice with PBS containing 1 mM $MgCl_2$ (pH 7.2) and stained overnight in β-galactosidase staining solution [1 mg/mL X-gal, 5 mM $K_3Fe[CN]_6$ (potassium ferricyanide), 5 mM $K_4Fe[CN]_6$ (potassium ferrocyanide), 2 mM $MgCl_2$, 40 mM citric acid/sodium phosphate (pH6.0), and 150 mM NaCl in distilled water] at 37°C without CO_2. The stained cells were then visualized by microscopy (Nikon Eclipse TS100; Tokyo, Japan). Images were captured by a digital camera (Canon i-Solution IMTcam3; Tokyo, Japan).

3. Detection of intracellular ROS

Intracellular ROS levels were measured using the cell permeable substrate 2′,7′-dichlorofluorescin diacetate (DCFH-DA; Sigma-Aldrich; St. Louis, MO, U.S.A), which converts to the fluorescent product 2′,7′-dichlorodihydrofluorescein (DCF) for ease of detection. MSCs were treated with/without ascorbic acid for 2 days at 37 °C and then were incubated with 20 μM DCFH-DA at 37 °C for 1 h. After washing with PBS, the cells were fixed with 4 % paraformaldehyde for 10 min and mounted with 40,6-diamidino-2-phenylindole (DAPI) containing mounting solution (ProLong Gold antifade reagent; Molecular Probes; Eugene, OR, U.S.A). The cells

then were visualized by fluorescence microscopy with a Nikon Eclipse 80Ti microscope (Nikon; Tokyo, Japan). Cell images were taken with a DS-RI1 digital camera (Nikon; Tokyo, Japan).

4. Quantitative PCR (real-time PCR)

MSCs were harvested and total RNA was extracted using RNAiso reagent (TAKARA, Japan) according to the manufacturer's instructions. A Primescript II 1st strand cDNA synthesis kit (TAKARA, Japan) was used to reverse transcribe 3-5 μg of total RNA with 0.2 μg of random primers (TAKARA, Japan), 1 mM dNTPs, and the supplied buffer. For real-time PCR, first strand cDNAs were amplified using Power SYBR Green PCR master mix (Applied Biosystems Inc., USA) with gene-specific primers for human *AP, FABP4, RUNX2, Matrilin, musashi, nestin, HDAC6, MAP-2, NF-M, Sirt2,* or *β-actin*. Real-time PCR cycling parameters were 95°C for 10 min, followed by 40 cycles of 15 s at 95°C, and 1 min at 58°C. Primers were synthesized by GenoTech (GenoTech Corp., South Korea).

Table 1. Oligonucleotides used for RT-PCR

Target		Sequence (5' → 3')
Alkaline phosphatase (AP)	F	GCACCATGAAGGAAAAGCCA
	R	TGTGAAGACGTGGGAATGGT
FABP4	F	GGCATGGCCAAACCTAACAT
	R	CCTGGCCCAGTATGAAGGAA
RUNX2	F	TCTGACCGCCTCAGTGATTT
	R	TGCCTGGGGTCTGTAATCTG
Matrilin	F	GGTGGGCATTGTCTTCACTG
	R	GGCTCTGAGGCTATTTCCCT
Musashi	F	ATAAAGTGCTGGCGCAATCG
	R	TCGTTCGAGTCACCATCTTGG
Nestin	F	AGCCCTGACCACTCCAGTTT
	R	GCTGCTTACCACTTTGCCCT
MAP-2	F	GAGGTGGGTCAATCACCAGGT
	R	AGACTGCAGTGGTGCAATCTC
NF-M	F	GTGAACCACGAGAAGGCTCA
	R	AGGTAGTCTTTGCGCTCCAC
HDAC6	F	ACTGAGACCATCCAAGTCCA
	R	ATGATGCCGAGGTGACTTTC
Sirt2	F	GGAGGCTCAGGACTCAGAT
	R	CCAAACAGATGACTCTGCGA
β-actin	F	ATCCGCAAAGACCTGTACGC
	R	TCTTCATTGTGCTGGGTGCC

5. MTT assay

The protective effects of GV-Ex in hBM-MSCs were evaluated by 3-(4,5-dimethylthiazol-2-yl)-2,5-diphenyltetrazolium bromide (MTT) assay (Sigma-Aldrich) according to the manufacturer's instructions. Briefly, hBM-MSCs were seeded in 96-well plates (8×10^3 cells/well). The next day, the cells were incubated with 0-10 μg/mL of GV-Ex for 24 h, treated with 0-3 mM H_2O_2 for 1 h, and then analyzed by MTT assay.

6. Osteocyte and adipocyte differentiation

The ability to differentiate into osteocytes and adipocytes was evaluated in P-17 UP-Ex-treated hBM-MSCs (UP-Ex-MSCs) according to previously described procedures [20,21]. For osteogenic differentiation, hBM-MSCs were cultured for 14 days with osteogenic medium containing DMEM (Gibco), 10% fetal bovine serum (FBS; Hyclone, Logan, Utah, USA), 100 nM dexamethasone (Cayman Chemical, Ann Arbor, Michigan, USA), 100 μM L-ascorbic acid (Sigma-Aldrich), and 10 mM beta-glycerophosphate (Sigma-Aldrich). The medium was replaced every 3 days. After induction of osteogenic differentiation, the efficiency of differentiation was examined by alizarin red S staining. The staining solution was prepared by dissolving 1 mg alizarin red S powder (Sigma-Aldrich) per mL of distilled water. Cells were fixed in 4% PFA for 15 min, stained with 1% alizarin red S for 20 min at room temperature, and then the staining solution was removed. For adipogenic differentiation, cells were

seeded in 24-well plates and then incubated for 14 days with adipogenic medium, composed of DMEM, 10% FBS, 500 μM 3-isobutyl-1-methylxanthin (Cayman Chemical), 1 μM dexamethasone, 100 μM indomethacin (Cayman Chemical), and 10 μg/mL insulin (Tocris Bioscience, Bristol, UK). The differentiation ratio was evaluated by staining with oil red O staining solution (0.7 g oil red O powder in 200 mL of 100% isopropanol). Cells were washed with PBS and fixed with 4% PFA for 15 min. After washing twice with distilled water, cells were stained with oil red O for 10 min at room temperature, and then the solution was removed. All stained cells were then visualized by microscopy with a Nikon Eclipse TS100 microscope. Images were captured with a Canon i-Solution IMTcam3 digital camera (Canon, Tokyo, Japan).

7. Immunoblot analysis

Proteins were extracted with 400 μL RIPA buffer containing 2 mM phenylmethylsulfonyl fluoride, 1 mM sodium orthovanadate, and protease inhibitor cocktail (Santa Cruz Biotechnology, Dallas, TX, USA) for 30 min at 4 °C and centrifuged at 16,000 ×*g* for 20 min. Total protein (50 μg) was resolved by 10% sodium dodecyl sulfate-polyacrylamide gel electrophoresis and then transferred to PVDF membranes (AGFA, Mortsel, Belgium). The membranes were blocked with 5% skim milk and immunoblotted with specific antibodies to test the experiment target protein for 16 h at 4 °C. The appropriate horseradish peroxidase-

conjugated secondary antibodies (Jackson ImmunoResearch Laboratories, West Grove, PA, USA) were used for enhanced chemiluminescence detection (GE Healthcare, Buckinghamshire, UK).

Table 2. Primary antibodies used for western blotting

1st antibody	2nd antibody	1st Ab Dilution ratio
Acetylated α-tubulin	Donkey anti-Mouse IgG	1 : 500
ATM	Donkey anti-Mouse IgG	1 : 500
Bax	Donkey anti-Rabbit IgG	1 : 500
Bcl-2	Donkey anti-Mouse IgG	1 : 500
Catalase	Donkey anti-Goat IgG	1 : 500
Cleaved caspase-3	Donkey anti-Rabbit IgG	1 : 500
CREB	Donkey anti-Rabbit IgG	1 : 500
eIF2α	Donkey anti-Rabbit IgG	1 : 500
ERK	Donkey anti-Rabbit IgG	1 : 500
FoxO1	Donkey anti-Rabbit IgG	1 : 500
G3BP	Donkey anti-Mouse IgG	1 : 200
MAP-2	Donkey anti-Mouse IgG	1 : 500
NF-M	Donkey anti-Goat IgG	1 : 200
p16	Donkey anti-Mouse IgG	1 : 200

p21	Donkey anti-Rabbit IgG	1 : 500
p53	Donkey anti-Rabbit IgG	1 : 500
p-ATM	Donkey anti-Mouse IgG	1 : 500
p-CREB	Donkey anti-Goat IgG	1 : 500
p-eIF2α	Donkey anti-Rabbit IgG	1 : 500
p-ERK	Donkey anti-Mouse IgG	1 : 500
p-FoxO1	Donkey anti-Rabbit IgG	1 : 500
p-p53	Donkey anti-Rabbit IgG	1 : 500
Pro-caspase-3	Donkey anti-Rabbit IgG	1 : 500
SOD1	Donkey anti-Goat IgG	1 : 1000
SOD2	Donkey anti-Rabbit IgG	1 : 1000
Tia	Donkey anti-Goat IgG	1 : 200
α-tubulin	Donkey anti-Rabbit IgG	1 : 1000
β-actin	Donkey anti-Mouse IgG	1 : 5000

8. Preparation of *Gracilaria vermiculophylla* extract and *Undaria pinnatifida* extract

G. vermiculophylla was harvested from the East Sea (Kang won do, Republic of Korea), washed two or three times with tap water to remove residual salts, and dried at room temperature. The dried seaweed powder was extracted by soaking the seaweed in 80% ethanol (20× volume) for 7 days, then filtering the ethanol through a 150 mm diameter Qualitative Filter Paper (Hyundai Micro, Gyeonggi-do, Korea). The ethanol was then evaporated using a Rotary Evaporator (Eyela, Tokyo, Japan), and the resulting extract was stored at −70 °C for one day. After freezing, the final dried extract was obtained by lyophilization for 3 days in a freeze dryer (Ilshin Lab. Co. Ltd., Gyeonggi-do, Korea). The stock solutions for experimental assays were prepared by solubilizing 20 mg of dried extract with 1 mL of either a mixture of equal parts dimethyl sulfoxide and ethanol (GV-crude; GV-Cr), or distilled water (GV-H_2O; GV-H), or acetone (GV-acetone; GV-Ac).

U. pinnatifida was harvested from the East Sea (Kang won do, Republic of Korea), washed 2 or 3 times with tap water, drained after elimination of residual salts, and dried at room temperature. The dried seaweed powder was extracted with 80% ethanol (20 times volume) for 1 week and filtered through 150-mm Qualitative Filter Paper (Hyundai Micro, Gyeonggi-do, Korea). The ethanol was evaporated using a Rotary Evaporator (Eyela, Tokyo, Japan), and the dried extract stored at −70°C

for one day. After freezing, the final, dried extract was obtained by lyophilizing for 3 days in a freeze dryer (Ilshin Lab., Gyeonggi-do, Korea). The stock solutions for experimental assays were prepared by solubilizing 20 mg of UP-Ex in 1 mL of DMSO/ethanol (ratio = 1:1).

9. Immunocytochemical staining

MSCs were grown on poly-L-lysine-coated coverslips (Fisher Scientific, USA) and induced to differentiate into neuron-like cells. Cells were then fixed with fixation solution containing 4% paraformaldehyde in phosphate-buffered saline (PBS) for 15 min at room temperature (RT). After three washes with 500 μL PBS, cells were permeabilized with ice-cold methanol for 5 min at RT. Cells were then washed three times with PBS and incubated with blocking buffer (5% normal horse serum in PBS containing 0.02% sodium azide) for 1 h at RT. Cells were incubated with antibodies against MAP-2 or NF-M (Santa Cruz Biotechnology, USA) diluted 1:200 in blocking buffer overnight at 4°C. After three washes in 500 μL PBS-A, cells were incubated with an Alexa 488-conjugated donkey anti-mouse IgG or donkey anti-goat IgG antibody (Molecular Probes Inc., USA) diluted 1:500 in Hoechst 33342 (Molecular Probes Inc., USA) for 1 h at RT, then washed three times with PBS, and mounted with a drop of mounting solution (ProLong Gold antifade reagent, Molecular Probes Inc., USA). The cells were visualized with fluorescence microscopy using a Nikon Eclipse 80Ti microscope (Nikon, Japan). Cell images were taken with

a DS-RI1 digital camera (Nikon, Japan).

10. Neuronal differentiation

hBM-MSCs were exposed to pre-induction media containing 10% FBS, 10 ng/ml bFGF, and 500 μM β-mercaptoethanol for 24 hours. The media were replaced with induction media containing 100 μM butylated hydroxyanisole (BHA), and 2% DMSO in FBS-free media for 6 hours. The cell images were taken with a microscope (Olympus IX71, Japan) and a digital camera (Olympus U-LS30-3, Japan). Neurite lengths were measured using the ImageJ program (NIH, USA).

11. Evaluation of apoptotic cells and senescent cells

Hoechst 33342 (Molecular Probes Inc., Eugene, OR, USA) staining and SA-β-gal assays were performed simultaneously to evaluate apoptosis in senescent cells. MSCs at different passages (P-7, P-14, and P-17) were treated with 0 or 1 mM H_2O_2 for 1 h. Cells were then analyzed using the Senescence β-Galactosidase Staining Kit (Cell Signaling Technology Inc.) according to the manufacturer's instructions. After the completion of SA-β-gal staining, cells were washed with PBS twice, and incubated with PBS containing Hoechst33342 for 1 h at room temperature. The stained cells were observed using a Nikon Eclipse 80Ti fluorescence microscope. Apoptotic cells, identified as those exhibiting the morphological criteria for apoptosis (e.g., DNA fragmentation, nuclear condensation, and

segmentation), were counted in 200 randomly selected cells in each experiment (n = 3). Images were taken with a microscope (Olympus IX71; Tokyo, Japan) and a digital camera (Olympus U-LS30-3).

12. Activity analysis of caspase-3, caspase-8, and caspase-9

The activities of caspase-3, caspase-8, and caspase-9 were measured using the Caspase Colorimetric Assay Kit (Biovision, San Francisco, CA, USA) according to the manufacturer's instructions. hBM-MSCs were resuspended in 50 μL of lysis buffer and incubated on ice for 10 min. After centrifugation, the supernatant was transferred to a fresh tube. Each lysate protein (50 μg) was mixed with 50 μL of reaction buffer (1% NP-40, 20 mM Tris-HCL pH 7.5, 137 mM NaCl, and 10% glycerol) containing 200 μM caspase-3, caspase-8, or caspase-9 substrate. Samples were then incubated at 37°C for 2 h. Caspase activity was assessed using a microplate reader (Thermo Fisher Scientific Inc., Waltham, MA, USA) at an absorbance of 405 nm.

13. Statistical analysis

The data are represented as means ± standard deviation (SD) of the means from three or more independent experiments. Statistical comparisons between groups were made using independent *t*-tests. A p-value of less than 0.05 was considered statistically significant.

III. The Main Subject

Part I. Cellular senescence and Reactive oxygen species

Chapter 1. Accumulation of apoptosis-insensitive human bone marrow-mesenchymal stem cells after long-term expansion

1. Introduction

The life span of mature cells in the human body varies depending on their environmental status and biological function. As cells die, new cells are born to maintain the appropriate cell count in each tissue or organ (Biteau et al., 2011). Stem cells and their microenvironmental niches regulate tissue homeostasis (Singh, 2012). However, their numbers gradually decline with progressive aging, resulting in the decrease in homeostasis and the accumulation of senescent cells. Thus, organs and tissues in the aged human body have reduced biological function.

Adult stem cells have been used for cell therapy in patients with aging-related diseases such as degenerative disorders (Augello et al., 2007; Barry and Murphy, 2013; Farini et al., 2014; Kan et al., 2007; Kim et al., 2014; Wollert et al., 2004). A sufficient quantity of stem cells is necessary to optimize therapeutic efficacy. However, it is difficult to acquire enough cells from a donor. For this reason, isolated stem cells have to be

expanded under in vitro culture conditions. However, during long-term expansion, stem cells undergo replicative senescence, which is characterized by typical phenotypes including morphological enlargement (a flat, fried egg morphology), reduced secretion of growth factors/cytokines, reduced differentiation potential, epigenetic modification, and telomere shortening (Harley et al., 1990; Maegawa et al., 2010; Mastri et al., 2012). This senescence is caused by the accumulation of cellular damage induced by oxidative stress. Thus, stem cell expansions increase the risk of cellular senescence, resulting in reduced therapeutic efficacy or the failure of stem cell therapies (Cho et al.; Heeschen et al., 2004; Rossi et al., 2007).

Previous studies have provided evidence that p53 mediates cellular responses to DNA damage resulting from reactive oxygen species (ROS) and antagonizes oncogenic transformation (Gambino et al., 2013; Johnson et al., 1996). The stabilization and activation of p53 are highly regulated by post-translational modifications including phosphorylation, ubiquitination, and acetylation. Mdm2 (mouse double minute 2 homolog), an E3 ubiquitin ligase, interacts with p53 and degrades it by ubiquitination of the C-terminal lysine residues (Moll and Petrenko, 2003). Non-ubiquitinated p53 is degraded in a proteasome-dependent manner. Ataxia-telangiectasia mutated (ATM) (Saito et al., 2002) and Mdm2 are hypophosphorylated in response to oxidative DNA damage, leading to p53 stabilization and activation. Thus, activated p53 causes cell cycle arrest via transcriptional

regulation of p21, and subsequent processes lead to DNA repair or apoptosis.

Apoptosis (i.e., programmed cell death) occurs via two signaling pathways, the intrinsic and extrinsic apoptosis pathways. The intrinsic apoptosis pathway plays a pivotal role in development and tissue homeostasis to maintain an appropriate cell number (Biteau et al., 2011). If an excess of cells experience apoptosis, degenerative diseases may occur over time. B cell lymphoma-2 (Bcl-2) family members modulate apoptosis by altering the mitochondrial membrane permeabilization, leading to the release of cytochrome C to promote apoptosome formation and activation of cysteine proteases, caspase-9 and -3 (Strasser et al., 2000). p53 also participates in intrinsic apoptosis and permanent cell cycle arrest, which is a senescence response. It stimulates pro-apoptotic proteins and suppresses anti-apoptotic proteins (Walensky, 2006).

In this study, I established replicative senescent cells from the long-term expansion of human bone marrow mesenchymal stromal cells (hBM-MSCs). The apoptotic signaling pathway of the cells was characterized under oxidative stress. I demonstrated that apoptotic-insensitive cells accumulated during the long-term expansion of hBM-MSCs.

2. Result

(1) Long-term expansion of MSCs results in cellular senescence phenotypes

Human BM-MSCs were cultured under standard growth conditions until the development of replicative senescence. The PD for each passage gradually declined (Fig. 1A, left panel). The cumulative PDL increased until 20 passages, after which no significant differences among passages were observed (Fig. 1A, right panel). To determine replicative senescence at the molecular level, I examined the expression level of the senescence markers p16 and p53. The expression of these proteins was low after 7 passages (P-7), increased at P-14, and increased further at P-17 (Fig. 1B). In SA-β-gal assays, the number of SA-β-gal-positive cells increased depending on the passage number, from 30% at passage 7 (P-7) to 79% at passage 17 (P-17) (Fig. 1C; *t*-test, $*p < 0.01$, mean ± SD, n = 3). The cells were classified as early passage (≤7), middle passage (12 to 14), or late passage (≥15) based on the data shown in Figure 1.

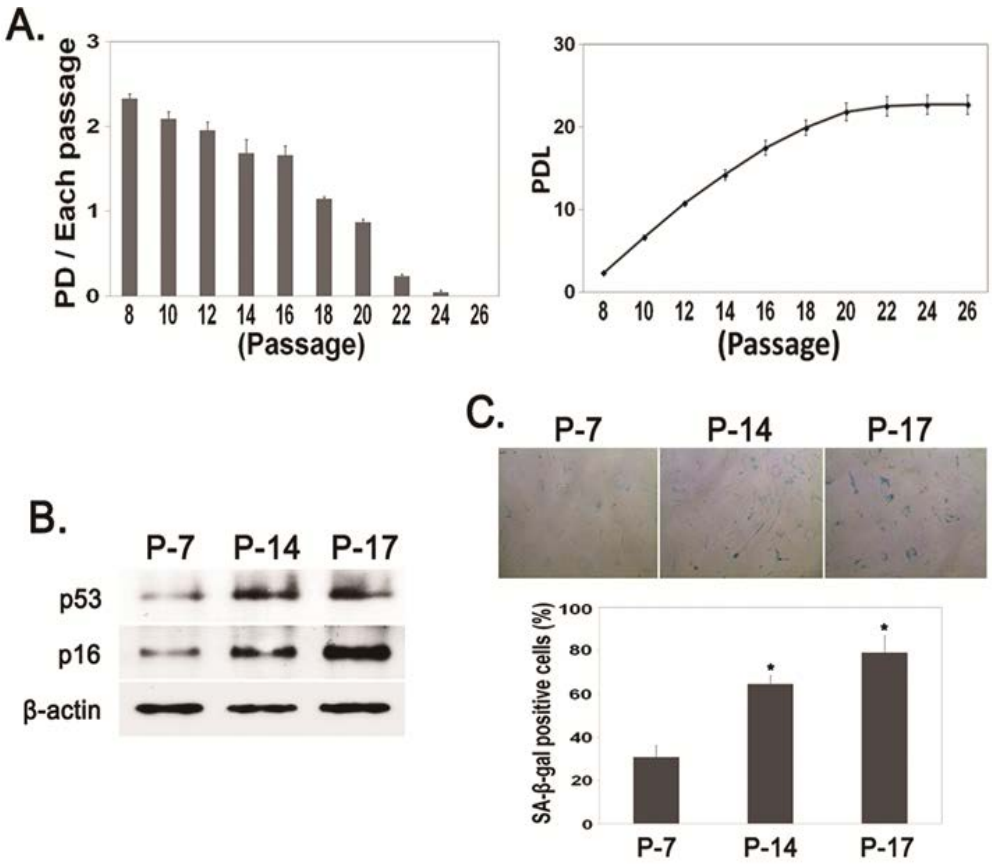

(Chapter 1) Fig. 1.

Figure 1. Replicative senescence in long-term cultured MSCs.

(A) Cells from each passage were counted to determine the population doublings (PD/ passage) (left panel). PDs were summed and the resulting PD level (PDL) is shown (right panel). (B) The expression levels of senescence marker proteins p53 and p16 were elevated in long-term cultured MSCs. (C) Senescence-associated β-galactosidase-positive cells (green color) increased in a passage-dependent manner for hBM-MSCs.

(2) Resistance to oxidative damage in long-term cultured MSCs

To verify the cell protective effects against oxidative stress, hMSCs at different passages were exposed to H_2O_2 (0–2 mM) and examined by MTT assays. Interestingly, late- and middle-passage MSCs had greater protective effects than early-passage MSCs (Fig. 2A, upper panel; *t*-test, $*p < 0.05$, mean ± SD, n = 4). Based on the immunoblot analysis, cleaved caspase-3 was almost undetectable in the P-17 cells exposed to 0.5–1 mM H_2O_2, but increased in a dose-dependent manner in P-7 cells (Fig. 2A, lower panel). Similar results were obtained using sodium arsenite (20 μM), which is another compound that causes oxidative damage (Fig. 2B; *t*-test, $*p < 0.05$, mean ± SD, n = 4). In the caspase activity assay with 0 or 1 mM H_2O_2, the resistance was mediated by caspase-9 and -3 rather than by capsase-8 (Fig. 2C). These results suggest that the late-passage cells are less sensitive to cellular damage caused by oxidative stress.

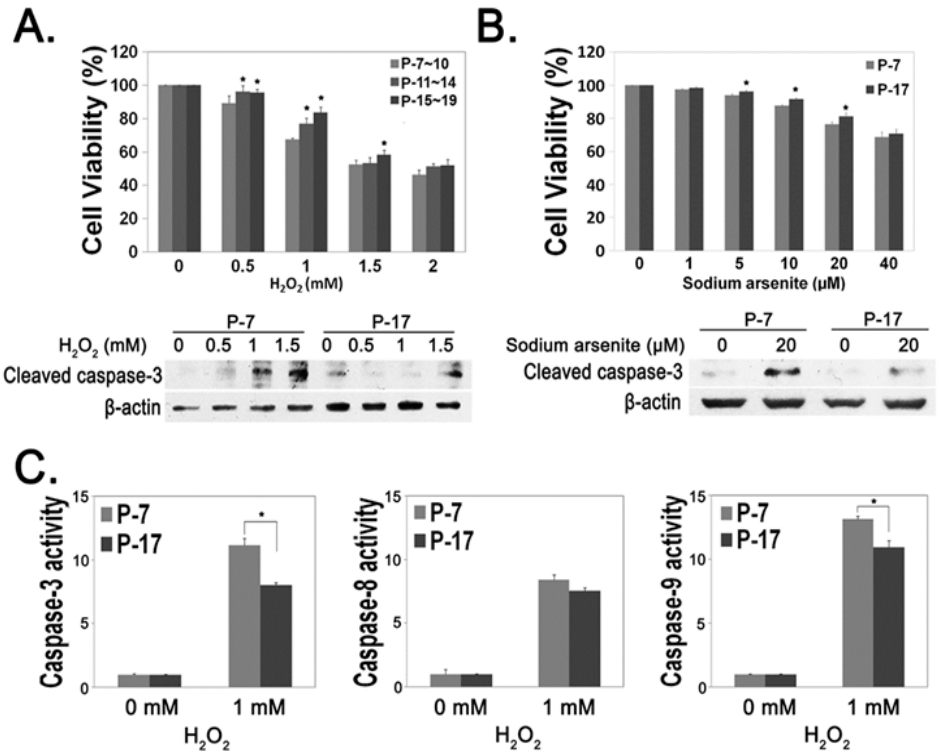

(Chapter 1) Fig. 2.

Figure 2. Resistance to oxidative damage in long-term cultured MSCs.

(A) MSCs were exposed to H_2O_2 (0-2 mM) for 1 h and cell viability was examined by MTT assays. Long-term cultured MSCs were more protective (upper panel). H_2O_2-exposed MSCs were extracted and total proteins were measured by immunoblot analyses with cleaved scaspase-3 antibody (lower panel). (B) Similarly, cells were exposed to 0-40 μM sodium arsenite and subjected to cell viability assays (upper panel) and immunoblot analysis (lower panel). (C) The caspase activity assays were performed with 0 or 1 mM H_2O_2-exposed MSCs.

(3) Apoptosis-resistant cells accumulated in long-term cultured MSCs

To determine the accumulation of resistant cells during long-term expansion, MSCs were treated with 0-1 mM H_2O_2 and co-stained with Hoechst33342 and SA-β-gal to distinguish the apoptotic cells from senescent MSCs based on nuclear morphology. A nuclear morphology typical of apoptosis (condensation and fragmentation of nuclear chromatin) was observed in β-gal-negative cells (Fig. 3A). β-gal-positive cells increased, while apoptotic cells decreased in a passage-dependent manner (Fig. 3B, left panel). The numbers of apoptotic β-gal-positive or β-gal-negative cells are presented in Figure 3B (middle and right panel; Supplemental Table 1 and 2). The non-apoptotic β-gal-positive cells significantly increased (Fig. 3B, middle panel; P-7: -14: -17 = 19.52: 51.08: 58.55%). These data suggest that apoptosis mainly occurred in β-gal-negative cells, and non-apoptotic cells accumulated in late-passage MSCs.

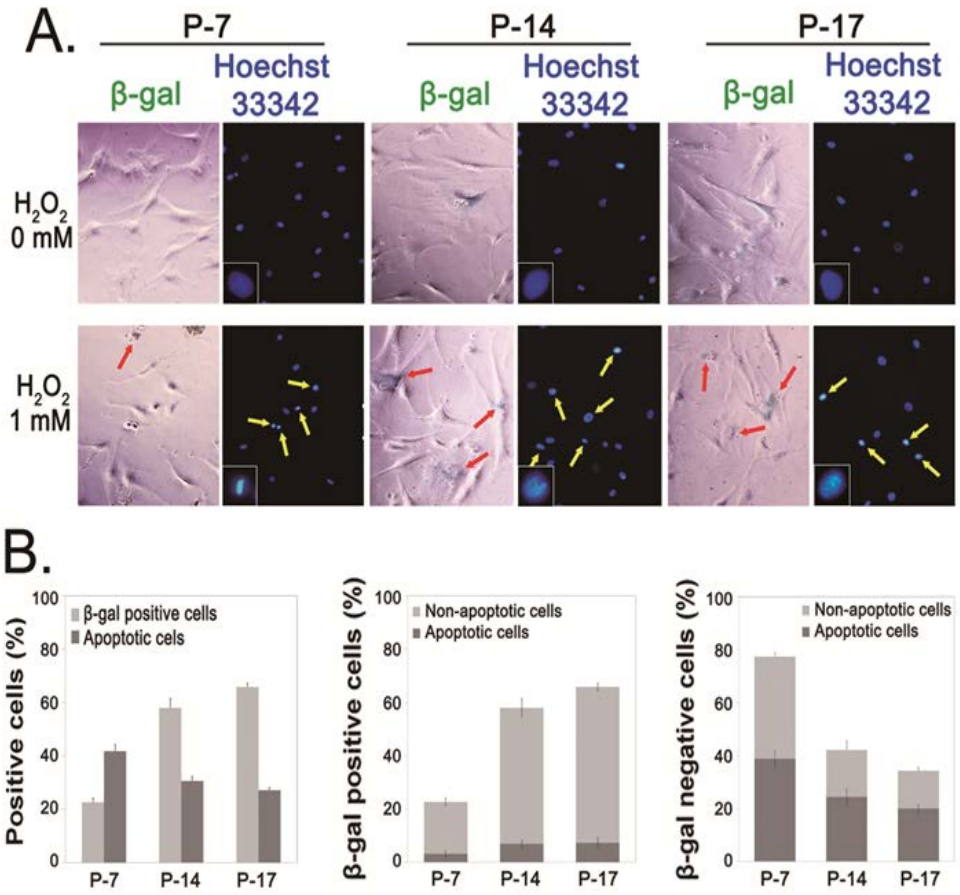

(Chapter 1) Fig. 3.

Figure 3. Accumulation of apoptotic-resistant cells in long-term cultured MSCs.

(A) MSCs at different passages were co-stained with SA-β-gal (green color) and Hoechst33342 (blue color) to assess the percentage of apoptotic cells among senescent MSCs. β-gal-positive cells are indicated by red arrows, apoptotic cells are indicated by yellow arrows. (B) SA-β-gal-positive cells and apoptotic cells were counted (left panel). The apoptotic β-gal-positive (middle panel) and β-gal-negative cells (right panel) are presented.

(4) Early-passage MSCs respond to oxidative stress, but not late MSCs

To evaluate the resistance at the molecular level, oxidative stress-responsive proteins ATM and p53 were quantified by immunoblot analysis. Cells of different passage were treated with 0–1.5 mM H_2O_2. The expression of p-ATM and p-p53 increased in either the 7- and 17-passage MSCs (Fig. 4A). The expression of the pro-apoptotic protein Bax increased, while that of the anti-apoptotic protein Bcl-2 decreased at P-7 and -17 (Fig. 4B; *t*-test, $*p < 0.05$, mean ± SD, n = 3), suggesting that late-passage MSCs were less sensitive to stress-induced apoptosis.

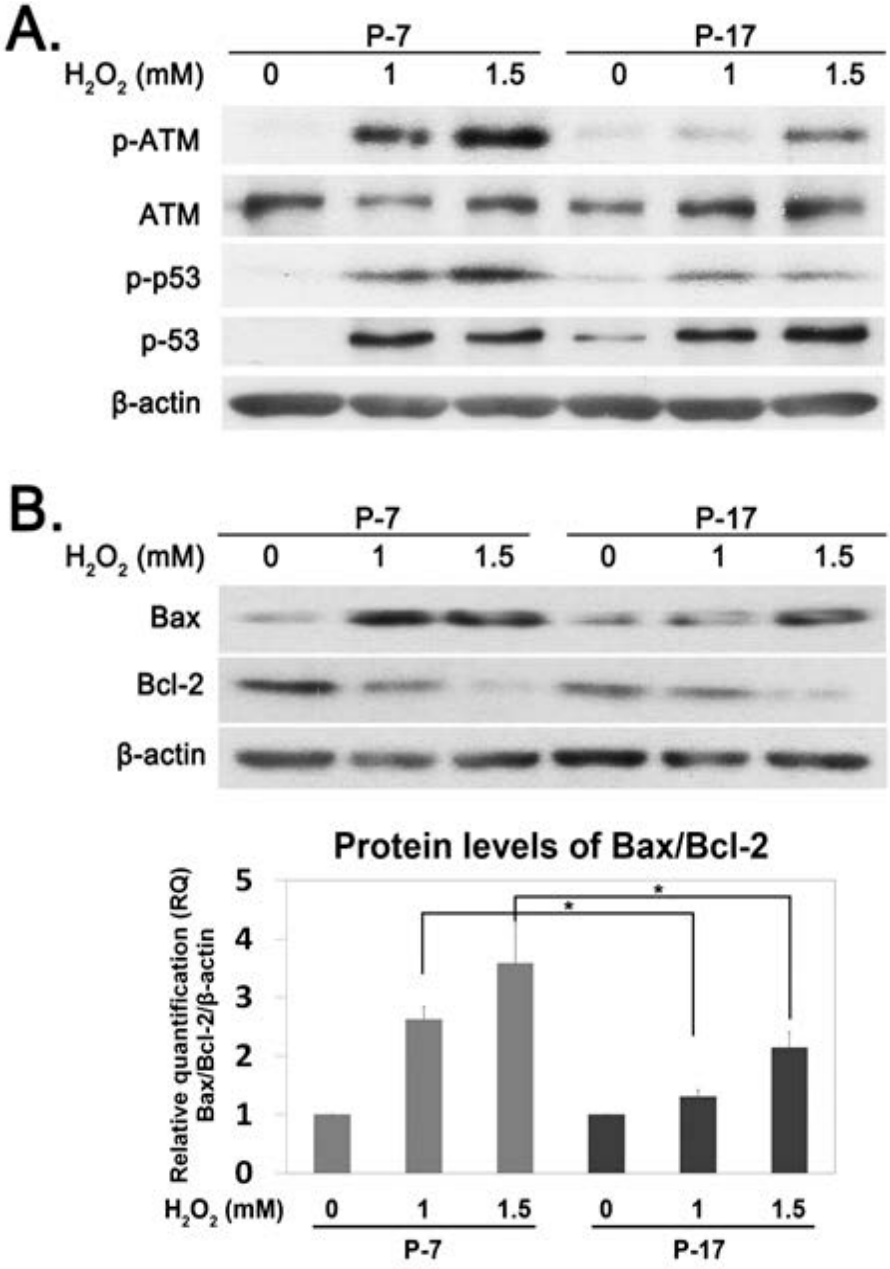

(Chapter 1) Fig. 4.

Figure 4. Insensitivity to stress-induced apoptosis signaling in long-term cultured MSCs.

(A) MSCs (P-7 and P-17) were exposed to H_2O_2 (0-1.5 mM) and the total proteins were extracted and measured by immunoblot analyses with specific antibodies against ATM, p-ATM, p53, p-p53, and β-actin. (B) Similarly, H_2O_2-exposed cells were subjected to immunoblot analyses with Bax, Bcl-2, and β-actin. Protein expression data were quantified and normalized with β-actin using the ImageJ software.

3. Discussion

I established replicative senescent cells from in vitro long-term cultured human BM-MSCs and identified a passage-dependent decline in PD (Fig. 1). The cells were classified into three groups, early (7-10), middle (11-14), and late (~15) passages, consistent with a previous study (Stenderup et al., 2003). The expression of senescence proteins p53, p16, and SA-β-gal increased in the late-passages MSCs (Fig. 1B and 1C).

Since long-term cultured MSCs are associated with reduced secretion of trophic/growth factors (Cho et al.; Mastri et al., 2012), which reduces differentiation ability and cellular protective effects, late-passage MSCs may have a weak protective effect against diverse cellular damage. To examine this, cells were injured by oxidative stress (stimulated by H_2O_2 or sodium arsenite) and their viability was estimated. I demonstrated that the rates of cellular protection are higher in late-passage MSCs than early-passage MSCs, and this result was confirmed by MTT assay and immunoblot analysis with cleaved caspase-3 (Fig. 2A and 2B). The intrinsic apoptotic pathway (capase-3 and -9) participates in this protective effect, suggesting that intrinsic cell death signaling may be less sensitive to oxidative stress in late-passage MSCs.

Previous studies have shown that the accumulating senescent cells caused by a loss of tissue homeostasis (Kuilman et al., 2010; Singh, 2012) induces a functional decline in those and surrounding cells (Coppe et al., 2008; Rodier and Campisi, 2011). Deursen and colleagues used transgenic mice that induce the elimination of p16Ink4a-postive senescent cells and found that a late-life clearance of these cells attenuated the progression of age-related disorders

(Baker et al.). They suggested that senescent cells accumulated in various tissues and organs as aging progressed. In this study, I showed that the apoptosis-resistant cells (i.e., the non-apoptotic cells in Fig. 3B, middle panel) accumulated in *in vitro* long-term cultures, and that these cells were mostly SA-β-gal-positive (Fig. 3B, middle and right panel).

Excessive intracellular ROS causes oxidative damage of cellular DNA, proteins, lipids, and carbohydrates (Evans and Halliwell, 1999). When unrecoverable damage accumulates, apoptosis is triggered to avoid further impairment of the surrounding healthy cells or the development of oncogenic transformation (Cerutti, 1985). This type of apoptosis is trigged by ATM and p53 (Moll and Petrenko, 2003; Saito et al., 2002). Their signals mediate the activity of Bcl-2 family members, which are transferred to the mitochondrial membrane; cysteine proteases eventually induce chromatin condensation, internucleosomal DNA cleavage, blebbing of the plasma membrane, and surface exposure of "eat me signals" (Strasser et al., 2000). To characterize the apoptotic-resistant cells at the cell signaling level, i examined the oxidative stress-sensitive proteins ATM and p53 (Moll and Petrenko, 2003; Saito et al., 2002), apoptosis molecules Bax and Bcl-2 (Walensky, 2006), and caspase proteases. The expression of phosphorylated p-ATM and p-p53 and pro-apoptotic protein Bax increased and the anti-apoptotic protein Bcl-2 decreased in early-passage MSCs, whereas there were no responses to the stimulations in late-passage MSCs (Fig. 4), suggesting that apoptotic signaling was not triggered by oxidative stress in long-term cultured MSCs.

Cellular senescence is strongly associated with excessive intracellular ROS

production (Cadenas and Davies, 2000), which is generated by a multiplicity of factors including aerobic energy metabolism, xenobiotics, solar ultraviolet radiation, and ionizing radiation (Evans and Halliwell, 1999; Pryor et al., 2006). ROS can cause cellular damage, which leads to loss of cell function or cell death when it exceeds the physiological concentration limit. In this study, I established replicative senescent MSCs from long-term culture and identified the accumulation of apoptotic-resistant cells during stem cell expansion. These cells are insensitive to oxidative stress-induced apoptosis. Taken together, I propose that excessive intracellular ROS causes random damage to cellular molecules and induces apoptotic cell death. However, some cells that are accidently impaired by damage to the apoptotic signaling molecules may avoid apoptosis and accumulate in long-term culture dishes. These cells may accelerate the progressive senescence of healthy neighboring cells and rarely progressed to oncogenic transformation. The control or selective elimination of these cells may enable the accumulation of healthy stem cells by cell expansion. These cells may possess better stem cell potency, which may assure therapeutic efficacy in stem cell therapy.

Chapter 2. Elevation of endogenous ROS levels in replicative senescence-human bone marrow mesenchymal stem cells

1. Introduction

Human bone marrow-mesenchymal stromal cells (hBM-MSCs) have the potential to differentiate into diverse cell types (Caplan, 2007; Jeong et al., 2013; Pittenger et al., 1999). hBM-MSCs also act as trophic mediators, by secreting a number of trophic/growth factors (Cho et al., 2010; Nagai et al., 2007) which provide protection against oxidative stress and inflammation. These features suggest that hBM-MSCs are an excellent candidate for stem cell medicine. However, the efficacy of stem cell therapy markedly differs depending on the donor's health and age (Chambers et al., 2007; Cho et al., 2010; Fan et al., 2013), suggesting that stem cells need to be enhanced prior to use in stem cell therapy.

Primary culture cells from human tissues have a limited life span when cultured *in vitro*. Primary culture cells gradually enter into a senescence phase, with telomere shortening and a decline of telomerase (TERT) activity (Allsopp et al., 1992; Harley et al., 1990), called the Hayflick limit (Hayflick, 1965; Hayflick and Moorhead, 1961). In recent studies, replicative senescence was defined as the cellular damage of DNA (Hart and Setlow, 1974), proteins (Koga et al., 2011; Rodriguez et al., 2010),

lipids, and carbohydrates, induced by excessive intracellular reactive oxygen species (ROS) that impair DNA repair and cellular signaling as a means of accelerating cellular senescence. Many researchers have used antioxidant reagents to attenuate progressive senescence in different types of cultured primary cells (Kondo et al., 2014; Ludlow et al., 2014), and have suggested that removing excessive intracellular ROS may improve replicative senescence.

ROS are by-products of the metabolism of aerobic energy, and the levels of ROS regulate various cellular processes, including proliferation, apoptosis, differentiation, and cellular senescence (Hoidal, 2001; Irani, 2000). Excessive ROS production also suppresses the transcription of genes involved in cellular differentiation, cellular adhesion, and mitochondrial function (Chiarugi and Buricchi, 2007; Geissler et al., 2012). Elevation of intracellular ROS up-regulates the tumor suppressor genes p53 and p21 (Jung et al., 2004; Macip et al., 2002). Thus, ROS are a major cause of functional decline during typical cellular senescence.

The antioxidant enzymes superoxide dismutase 1 (SOD1/Cu-ZnSOD) and superoxide dismutase 2 (SOD2/MnSOD) play primary roles in scavenging endogenous ROS (Johnson and Giulivi, 2005). Mutation of SOD1 is associated with familial amyotrophic lateral sclerosis (ALS) and the subsequent impairment of mitochondrial function (Vehvilainen et al., 2014). Loss of SOD1 leads to age related pathology (Watanabe et al., 2014). Mutation of SOD2 in *Drosophila* causes a decline in heart function

that is induced by accumulated ROS (Piazza et al., 2009). Thus, cellular senescence is closely associated with defects in antioxidant enzymes and the accumulation of intracellular ROS levels.

In this study, I investigated intracellular ROS and the effects of antioxidant enzymes on long-term cultured MSCs.

2. Results

(1) Endogenous ROS increased in long term cultured MSCs

To evaluate the differences between early and late passage MSCs, endogenous ROS levels were examined and visualized by DCFH-DA staining. ROS levels increased in a passage-dependent manner (Fig. 1A). The results were quantified by fluorescence read ELISA (Fig. 1B; *t*-test, $*p < 0.01$, mean ± SD, n = 6). To further investigate the effects of ROS accumulation long term cultured MSCs, cells were subjected to immunoblot analysis with specific antibodies against p53, catalase, SOD1, SOD2, and FoxO1, which are associated with ROS modulation. The levels of p53, which functions as a gatekeeper against ROS damage, increased in long-term cultured MSCs (P-17), while levels of the antioxidant proteins SOD1, SOD2, and catalase decreased. Similar results were obtained for the phosphorylation of the ROS responsive transcription factor FoxO1 (Fig. 1C), suggest that excess intracellular ROS accompanies the reduction of antioxidant enzymes in long term cultured MSCs (P-17).

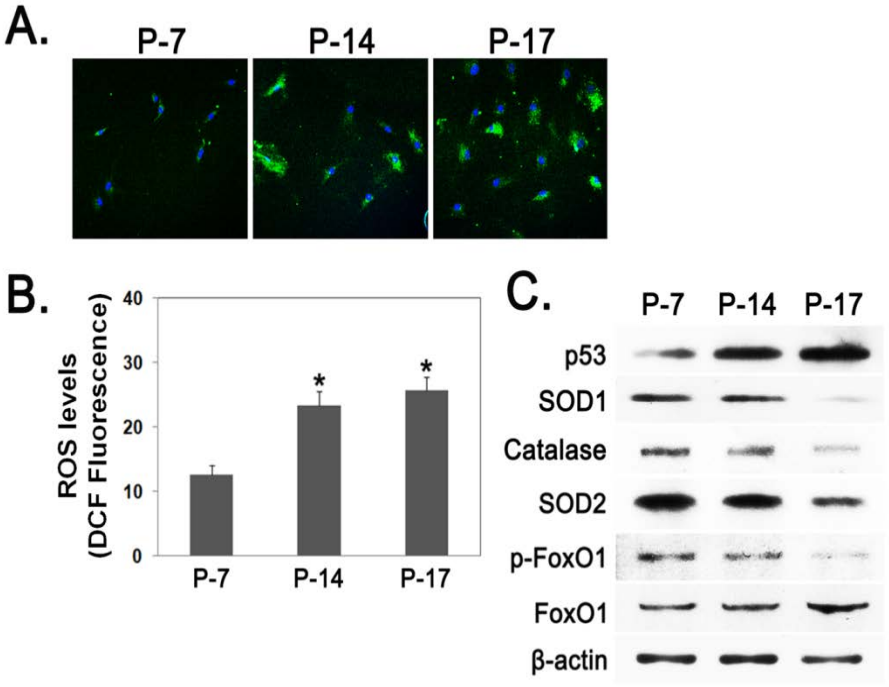

(Chapter 2) Fig. 1.

Figure 1. Increased endogenous ROS in long term cultured MSCs.

(A) Endogenous ROS levels (green color) were determined by staining with DCFH-DA and observed under fluorescence microscope. Nuclei were stained with DAPI (blue color). (B) Endogenous ROS were quantified using fluorescence read ELISA. (C) Total proteins were extracted from each of the different passages of MSCs (P-7, P-14, and P-17). The expression of p53, catalase, SOD1, SOD2, FoxO1, and p-FoxO1 proteins was measured by immunoblot analyses.

(2) Treatment with the antioxidant ascorbic acid restores signaling molecules in MSCs

Since long term cultured MSCs increase endogenous ROS and have decreased levels of the antioxidant enzymes, I used the antioxidant reagent ascorbic acid to remove the excess ROS (Guaiquil et al., 2001). P-17 MSCs were treated with ascorbic acid (0~2000 μM) for 2 days and intracellular ROS levels were measured with DCFH-DA staining. ROS decreased in MSCs treated with 500~2000 μM ascorbic acid (Fig. 2A). Cellular toxicity was not observed under these conditions, as tested by MTT assay (Fig. 2B).

To examine the effects of removing excess intracellular ROS from long term cultured MSCs, P-17 MSCs were treated with/without 500 μM ascorbic acid and antioxidant enzymes were measured by immunoblot analysis. The levels of catalase, SOD1, SOD2 and phosphorylated-FoxO1 (p-FOXO) from P-17 MSCs were reduced compared to the levels from P-7 MSCs, while these levels increased in ascorbic acid treated MSCs (P-17/AA; Fig. 2C). The levels of the senescence related protein, p53, decreased in P-17/AA MSCs compared to the levels in untreated P-17 MSCs (Fig. 2C). These data indicate that the antioxidant ascorbic acid decreases excessive ROS and partially restores the antioxidant enzymes, catalase, SOD1, SOD2, FoxO1, and p53 in long term culture MSCs.

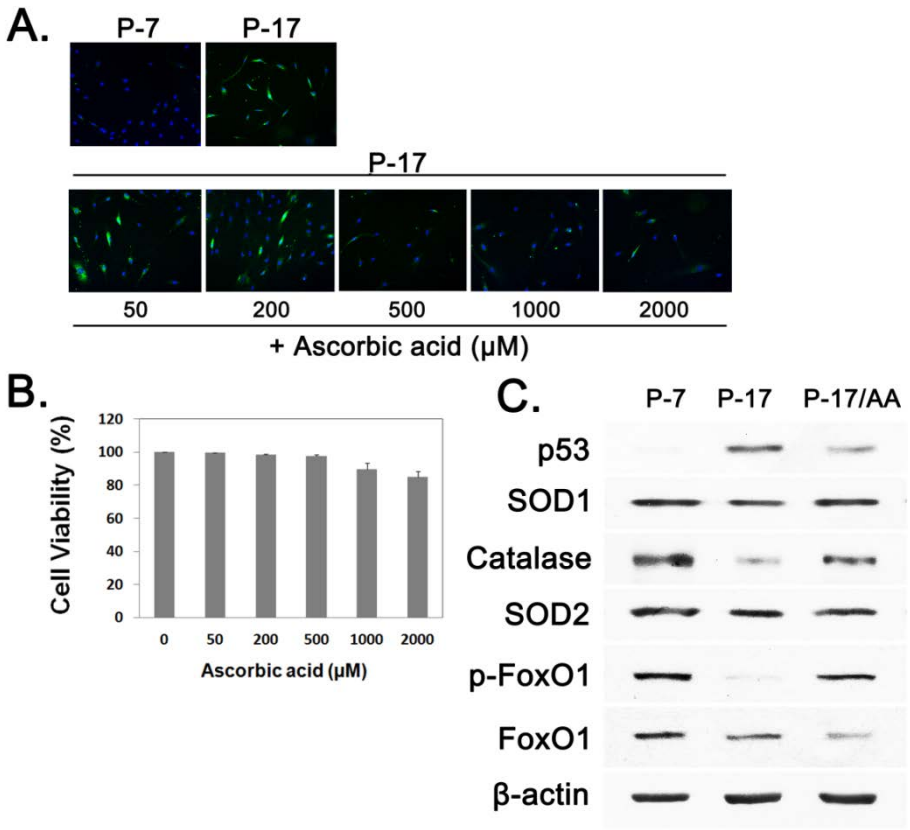

(Chapter 2) Fig. 2.

Figure 2. Modulation of excess ROS and antioxidant enzymes by ascorbic acid.

(A) Intracellular ROS was detected with ROS sensitive dye DCFH-DA in ascorbic acid (0~2000 μM) treated P-17 MSCs. (B) Cell viabilities in ascorbic acid treated MSCs were measured by MTT assay. (C) Total proteins were extracted from P-7, P-17, and ascorbic acid treated P-17 MSCS (P-17/AA). Catalase, SOD1, SOD2, FoxO1, p-FoxO1, p53 proteins were measured by immunoblot analyses.

(3) Restoration of potency in MSCs by treatment with ascorbic acid

BM-MSCs have the capacity to differentiation into diverse cell types including osteocytes and adipocytes (Pittenger et al., 1999). To determine if treatment with ascorbic acid restores the potential to differentiate in P-17 MSCs, the expression of tissue-specific progenitor marker genes was measured by quantitative PCR, including: *adiponectin*, *FABP4* for adipocyte; *AP*, *RUNX2* for osteocyte; *matrilin* for chondrocyte; *Musashi*, *nestin* for neuron. As shown in figure 4A, expression of all marker genes significantly decreased in P-17 MSCs compared to expression in P-7, while expression in P-17/AA MSC was equal to that in P-7 MSC, indicating that marker gene expression was restored by treatment with ascorbic acid (Fig. 3A; *t*-test, $*p < 0.05$, $**p < 0.005$, mean ± SD, n = 4). To verify these effects in long term cultured MSCs, P-17 and P-17/AA MSCs were stimulated to differentiate into osteocyte and adipocyte. P-17 MSCs showed a decrease in differentiation potency, while the differentiation potency of P-17/AA MSCs was similar to that of P-7 MSCs, indicating that differentiation potency was partially restored by ascorbic acid treatment. (Fig. 3B). These results suggest that the functional decline of differentiation capacity caused by excess ROS is restored through down-regulation of excessive ROS levels by treatment with the antioxidant ascorbic acid.

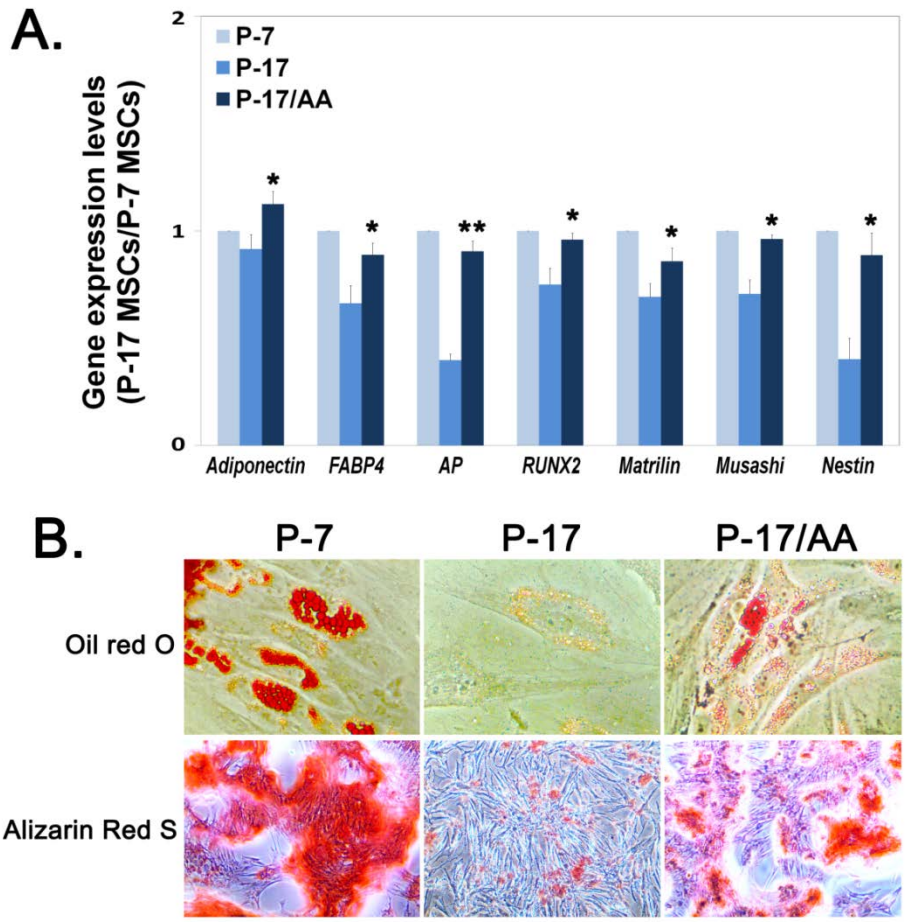

(Chapter 2) Fig. 3.

Figure 3. Restoration of differentiation capacity by ascorbic acid.

(A) The expression of progenitor marker genes was measured in P-7, P-17, and ascorbic acid treated P-17 MSCS (P-17/AA), tested by quantitative PCR. (B) Cells were inducted to differentiate into adipocytes (upper panels) and osteocytes (lower panels), and stained by oil red O and alizarin red S solution.

3. Discussion

In stem cell therapy, reduced therapeutic efficacies have been reported, in a manner that is dependent on the status of stem cells, such the states of cellular senescence and functional decline (Chambers et al., 2007; Wagner et al., 2009). These risks increase when cells are expanded to *in vitro* long term cultures (Hayflick, 1965; Hayflick and Moorhead, 1961). In the present study, I have established replicative senescence cells from long term cultured human BM-MSCs and examined the relationship between ROS and stem cell potency. The replicative senescence cells established here had elevated levels of senescence markers and of p16 in passage-dependent manner (I-Fig. 1), and had a reduced ability to differentiate (Fig. 3), which suggests that the use of long term expanded MSCs may hinder therapeutic efficacy.

Steady-state, intracellular ROS provides a number of beneficial effects, including enhancing cell proliferation and migration (Kim et al., 2013), whereas, excessive ROS generation causes devastating effects, including progressive modification and degradation of DNA, protein, and lipid, which results in blocking gene expression and stimulating apoptosis (Lee et al., 2014; Song et al., 2010). Previous studies have shown that excess ROS disturbs stem cell differentiation (Fehrer et al., 2006; Owusu-Ansah and Banerjee, 2009). Thus, cumulative damages induced by ROS cause functional decline and cell death (Song et al., 2010). Here, I examined intracellular ROS levels in long term cultured MSCs. I have found that

endogenous ROS gradually accumulated during cell expansion (Fig. 1A and 1B). MSCs with excess ROS (P-17) have shown reduced expression of markers for a number of diverse progenitor cells and an impaired differentiation potency (Fig. 3A and 3B).

The antioxidant enzymes, SOD1, SOD2 and catalase, are known to be a key regulator of ROS levels (Johnson and Giulivi, 2005), and p53 also regulates the intracellular ROS levels via regulation of SOD (Hussain et al., 2004). Here, I demonstrated that expression of the SOD1, SOD2, and catalase proteins is down-regulated at passage 14 and passage 17 (Fig 1C). The transcription factor FoxO1 plays a role in modulating endogenous ROS level through the transcription of SOD2 (Adachi et al., 2007; de Candia et al., 2008). I examined the expression of phosphorylated FoxO1 (p-FoxO1) and found that it is also down-regulated at passage 14 and passage 17 (Fig. 1C). From these data, I suggest that the increased intracellular ROS in long term expanded MSCs may alter the levels of antioxidant enzymes which subsequently induces an additional increase in intracellular ROS.

Since intracellular ROS increased and caused senescence in long term cultured MSCs, disposing of excess ROS by using an antioxidant may remedy the functional decline. To test this possibility, ascorbic acid, which is widely applied as an antioxidant reagent, was used to moderate the excess ROS (Guaiquil et al., 2001; Liu et al., 2014). A significant decrease in endogenous ROS was observed in long term cultured MSCs (P-17),

which was maximized by treatment of 500 μM ascorbic acid for 2 days (Fig. 2A). In P-17/AA MSCs, expression of the antioxidant enzymes, catalase, SOD1, SOD2, and p-FoxO1, was recovered, as was the expression of p53 (Fig. 2C). These results suggest that cumulative ROS levels during cell expansion may partially be reduced by antioxidant reagents such as ascorbic acid.

If intracellular ROS was down-regulated following treatment with ascorbic acid as shown in figure 3, this may improve the differentiation capacity. As shown in figure 7A, expression of the specific progenitor markers related to stem cell differentiation increased in ascorbic acid treated MSCs (Fig. 3A). In the differentiation experiments, ascorbic acid pretreated P-17 MSCs differentiated more effectively into adipocytes or osteocytes (Fig. 3B). These results suggest that removing excess intracellular ROS by antioxidants can recover the functional decline caused by replicative senescence.

In this study, I have detected increased ROS levels and reduction in the expression of antioxidant enzymes in long term cultured human BM-MSCs. These senescence phenotypes were partially recovered by scavenging excess ROS by treatment with the antioxidant reagent ascorbic acid, which suggests that elevation of intracellular ROS levels may play crucial role in the progression of replicative senescence. Thus, control of excessive ROS during the long term expansion may yield better quality of cells which may lead to improved therapeutic efficacy in stem cell therapy.

Chapter 3. Trichostatin A modulates intracellular reactive oxygen species through SOD2 and FOXO1 in human bone marrow-mesenchymal stem cells

1. Introduction

Bone marrow-mesenchymal stromal cells (BM-MSCs) possess the capacity to differentiate into several cell types (Jeong et al., 2013; Pittenger et al., 1999). MSCs also secrete diverse trophic factors (Cho et al., 2010; Nagai et al., 2007), which provide a protective environment against oxidative stress and inflammation. This suggests that MSCs are good candidates for stem cell therapy. However, various levels of efficacy have been reported depending on the health and age of donors (Heeschen et al., 2004; Rossi et al., 2007; Sharpless and DePinho, 2004). Previous studies have shown that migration and adhesion were markedly decreased following engraftment of progenitor cells obtained from unhealthy patients (Rota et al., 2006; Tepper et al., 2002). In addition, the increase in intracellular reactive oxygen species (ROS) can contribute to progressive functional decline of MSCs (Geissler et al., 2012). These studies indicate that further research is needed to improve the capability of stem cells prior to their application in stem cell therapy.

ROS are increased in ischemic-injured tissues, inducing apoptosis of transplanted MSCs in stem cell therapy (Song et al., 2010). Recent studies

have shown that ROS production from injured tissues disrupts cell adhesion by impairing integrin contacts (Chiarugi and Buricchi, 2007). Thus, the imbalance of intracellular ROS by chronic oxidative stress would lead to functional decline and progress the rate of cell senescence (Back et al., 2012).

The antioxidant enzyme superoxide dismutase 2 (SOD2/MnSOD) plays a primary role in protecting cells against oxidative stress via scavenging of the reactive oxygen species (Johnson and Giulivi, 2005). The forkhead box O (FOXO) is known as transcription factor that transactivates ROS-detoxifying enzymes such as SOD2 and catalase (Huang and Tindall, 2007). Increased intracellular ROSs by oxidative stress decreases FOXO1, SOD2, and subsequently induces apoptosis (Huang and Tindall, 2007; Jung et al., 2014).

Histone deacetylases (HDACs) play a role in mediating the expression of various genes by regulating the proteins involved in chromatin modulation (Bolden et al., 2006; Minucci and Pelicci, 2006). HDAC inhibitors have been used as therapies in various diseases such as cancer (Minucci and Pelicci, 2006), mood disorders (Machado-Vieira et al., 2011), and neurodegenerative disorders (Govindarajan et al., 2013). Recent studies have shown that the HDAC inhibitor trichostatin A (TSA) improves ischemic brain injury (Yildirim et al., 2008). Another HDAC inhibitor, valproic acid, has been generally used for the treatment of epilepsy (Koch-Weser and Browne, 1980; Rogawski and Loscher, 2004) and bipolar

disorder (Drevets, 2000; Rajkowska, 2000). Therefore, the use of HDAC inhibitors could increase the therapeutic efficiency in treating these diseases.

The HDAC inhibitor TSA blocks the activities of HDAC 1, 3, 4, 6, and 10 at low molar concentrations (Vanhaecke et al., 2004). A recent study reported that treatment with TSA in a mouse model of amyotrophic lateral sclerosis improved pathological phenotypes of motor neurons and delayed disease progression (Yoo and Ko, 2011). Another study reported that TSA has protective effects against cisplatin-induced ototoxicity through the regulation of apoptosis-related genes (Wang et al., 2013), suggesting that TSA may enhance cellular protective effects against oxidative stress.

In this study, I investigated whether TSA modulates intracellular ROS levels induced by oxidative stress in human BM-MSCs. Indeed, I demonstrated that TSA treatment leads to a reduction in excessive ROS and cellular toxicity in MSCs.

2. Results

(1) Significant decrease in intracellular ROS in TSA-treated MSCs

To examine the intracellular ROS change by oxidative stress, hBM-MSCs were treated with H_2O_2 (0~3 mM) for 1 h and ROS levels were measured by using the cell-permeable substrate DCFH-DA. As shown in Figure 1A, intracellular ROS increased in an H_2O_2 dose-dependent manner (Fig. 1A). ROS-positive cells versus DAPI-positive cells (total cells) from each group were counted (Fig. 1B). Cell viability gradually decreased following treatment with H_2O_2 in hBM-MSCs (Fig. 1C), indicating that ROS induced by oxidative stress affects cell viability.

To investigate whether H_2O_2-induced intracellular ROS were regulated by TSA in hBM-MSCs, cells were treated with TSA (0~1000 nM) for 8 h, and then oxidative stress was induced with 1 mM H_2O_2. ROS levels were detected by DCFH-DA. In TSA-pretreated MSCs (TSA-MSCs, 100~500 nM), ROS levels were significantly decreased compared to non-TSA treated MSCs (Fig. 1D). In contrast, when cells were pretreated with 1000 nM TSA, a significant decrease in ROS was not observed (Fig. 1D). ROS-positive cells versus total cells from each group were counted and values are presented as the means from three independent experiments (Fig. 1E; *t*-test, $* p < 0.05$, mean ± SD, n = 3). These data suggest that intracellular ROS levels were effectively reduced following treatment with 100~500 nM TSA in hBM-MSCs.

To examine the effects of TSA in hBM-MSCs without oxidative stress, cells were incubated with TSA (0~5000 nM) for 8 h, following which ROS levels and cell viability were observed using the DCFH-DA and MTT assay, respectively. ROS levels and cell viability were not changed under the testing conditions compared to non-treated MSCs (Ctrl-MSCs; Fig 1F and 1G), indicating that TSA alone did not stimulate ROS and did not affect toxicity in hBM-MSCs.

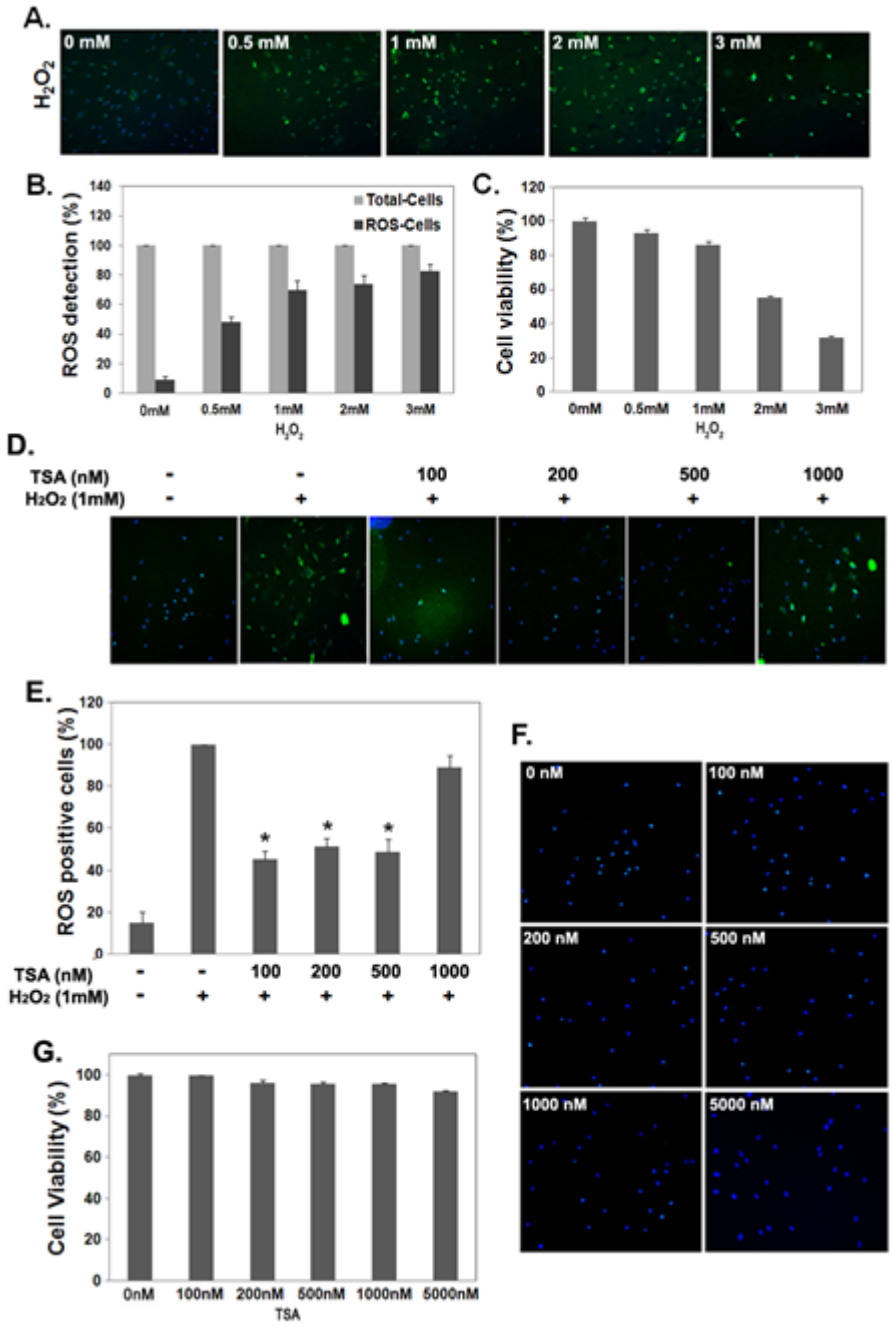

(Chapter 3) Fig. 1.

Figure 1. Regulation of intracellular ROS by TSA in MSCs.

(A) Intracellular ROS levels were visualized under a fluorescence microscope followed by treatment with H_2O_2 (0~3 mM) for 1 h. Green represents ROS and blue shows nuclei stained by DAPI. (B) Total cells (blue; DAPI-positive cells) and ROS containing cells (green) were counted. (C) Cell viability in H_2O_2-treated MSCs was examined by MTT assays. (D) Cells were treated with 1 mM H_2O_2 following pretreatment with TSA (0~1000 nM). The intracellular ROS (green) and nuclei (blue) were visualized under a fluorescence microscope. (E) ROS-positive cells (green) per total cells (blue) were counted (*t*-test, * $p < 0.05$, mean ± SD, n = 3). (F) Intracellular ROS levels were measured by fluorescence microscopy in TSA-treated MSCs without oxidative stress. (G) Cell viability was analyzed in TSA-treated MSCs by an MTT assay and compared with non-treated MSCs (Ctrl-MSCs; n = 3).

(2) TSA up-regulates antioxidant protein SOD2 in MSCs

To further investigate the effects of TSA in hBM-MSCs, cells were incubated with TSA (0~5000 nM) for 8 h and the SOD2 level was measured by immunoblot analysis. A large increase in protein expression was observed in 200 nM TSA-treated cells and only slightly increased in 1000 nm and 5000 nM TSA-treated MSCs (Fig. 2), indicating that pretreatment of cells with TSA resulted in increased expression of antioxidant protein SOD2.

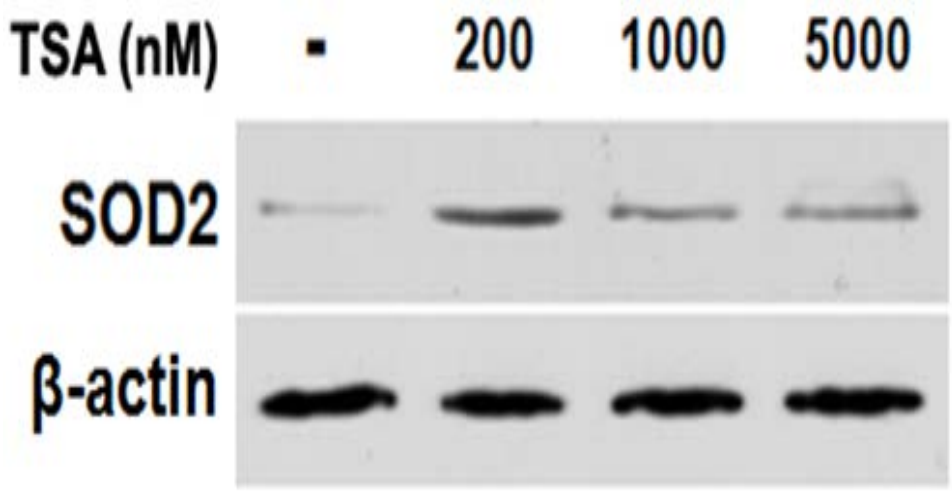

(Chapter 3) Fig. 2.

Figure 2. Increased SOD2 expression in TSA-treated MSCs.

MSCs were treated with TSA (0~5000 nM) for 8 h. Total proteins extracted from cells were subjected to immunoblot analysis with SOD2 antibody. SOD2 protein levels were increased in TSA-treated MSCs.

(3) Protective effects of TSA against oxidative injury in MSCs

Since TSA-treated MSCs (TSA-MSCs) increased SOD2 and suppressed H_2O_2-induced ROS generation, I examined the protective effects of TSA in treated cells. hBM-MSCs were treated with H_2O_2 (0~3 mM) followed by pretreatment with 200 nM TSA for 8 h. The viability of TSA-MSCs was significantly increased compared to non-treated MSCs (Ctrl-MSCs; Fig. 3A). Pre-incubation with various concentrations of TSA (0~10,000 nM or 50~500 nM) increased cell viability, whereas high doses of TSA (5000~10,000 nM) decreased cell viability (Fig. 3B), which is consistent with the results described above (Figs. 1E and 2). Similar results were obtained from activity assay for caspase-3 and -9 (Fig. 3C). These results suggest that cellular damage due to oxidative stress was reduced by the pre-incubation with low-dose TSA.

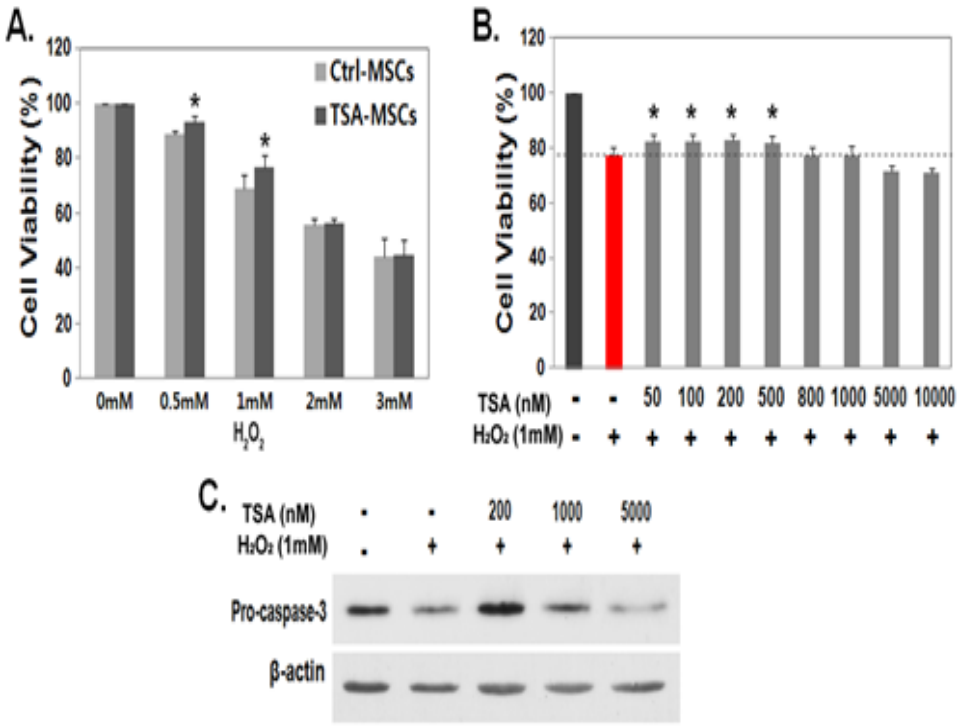

(Chapter 3) Fig. 3.

Figure 3. Cell protective effects of TSA in H_2O_2-treated MSCs.

(A) TSA-MSCs (200 nM of TSA for 8 h) were treated with 0, 0.5, 1, 2, or 3 mM H_2O_2 for 1 h, and their viability was determined by an MTT assay (*t*-test, * $p < 0.05$, mean ± SD, n = 3). (B) TSA-MSCs (50~10,000 nM of TSA for 8 h) were treated with 1 mM H_2O_2 for 1 h, and their viability was determined by an MTT assay (*t*-test, * $p < 0.05$, mean ± SD, n = 3). (C) Human BM-MSCs were pre-incubated with TSA (0~1000 nM) for 8 h and then treated with 1 mM H_2O_2 for 1 h. The activities of caspase-3, -9, and -8 was determined with colorimetric assays. The activities of caspase-3 and -9 were significantly decreased in 200 nM TSA pretreated MSCs compared to the H_2O_2-MSCs (*t*-test, * $p < 0.05$, mean ± SD, n = 3).

(4) TSA modulates FOXO1 and SOD2 in oxidative stress-induced MSCs

To further evaluate the effects of TSA, ROS-related targets (FOXO1, SOD2, p53, and pro-caspase-3) were quantified by immunoblot analysis. MSCs were treated with 1 mM H_2O_2 followed by pretreatment of TSA (0~5000 nM). Phospho-FoxO1 (p-FOXO1) and SOD2 levels were decreased in the H_2O_2-treated MSCs, but were significantly increased in TSA-pre-incubated MSCs (Fig. 4). These increases were maximized at 200 nM TSA-MSCs (Fig. 4). Similar results were obtained from immunoblot analyses for pro-caspase 3 (Fig. 4). p53, which is associated with cellular senescence, was increased in H_2O_2-treated MSCs and decreased in TSA-treated cells (Fig. 4). These data suggest that modulation of excessive ROS is suppressed by TSA through the action of FOXO1 and SOD2.

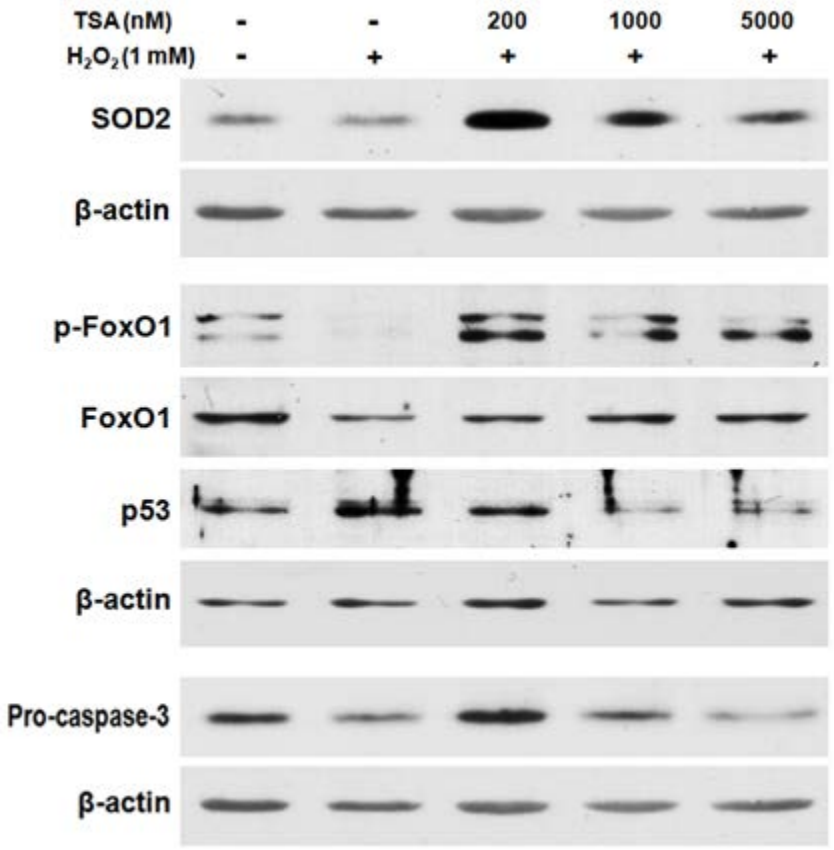

(Chapter 3) Fig. 4.

Figure 4. TSA modulates antioxidant proteins in oxidative stress-induced MSCs.

Human BM-MSCs were pre-incubated with TSA (0~5000 nM) for 8 h and then treated with 1 mM H_2O_2 for 1 h. The proteins were measured by immunoblot analyses with specific antibodies against SOD2, FOXO1, p-FOXO1, pro-capase-3, p53, and β-actin.

3. Discussion

Recently, many studies have shown that excessive ROS production is closely related to cellular senescence including functional decline and progression of cell death (Ben Mosbah et al., 2012; Song et al., 2010). In stem cell therapy, engraft cells are often damaged by ROS, resulting in a marked decrease of their beneficial efficacy (Ben Mosbah et al., 2012; Liu et al., 2010; Song et al., 2010). In this study, I examined intracellular ROS levels in hBM-MSCs exposed to H_2O_2. I observed a dose-dependent increase in intracellular ROS in H_2O_2-treated MSCs (Fig. 1A and 1B). Cell viability gradually decreased following an increase of ROS (Fig. 1C), consistent with previous studies (Kujoth et al., 2005; Liu et al., 2010; Song et al., 2010). These results suggest that stem cell therapy needs to be improved to offer better protective capability against harmful factors such as oxidative stress and inflammation prior to clinical usage.

Previous studies have demonstrated that HDAC inhibitors improve therapeutic efficacy in several diseases such as ischemic stroke (Xuan et al., 2012), cancer (Minucci and Pelicci, 2006), mood disorders (Machado-Vieira et al., 2011), and neurodegenerative disorders (Govindarajan et al., 2013). The HDAC inhibitor TSA attenuates cellular damage caused by alcohol-induced toxicity (Agudelo et al., 2011), and also provides a protective effect by suppressing inflammatory pathways (Yoo and Ko, 2011), suggesting the involvement of TSA in ROS regulation. Here, I showed that increased ROS induction induced by oxidative stress was

significantly decreased in TSA-pretreated MSCs (Fig. 1D and 1E).

The antioxidant enzyme SOD2 is known to be an important regulator of ROS levels and plays a primary role in protecting and preserving cells against oxidative stress via scavenging of the superoxide anion (Johnson and Giulivi, 2005). In this study, I have found that SOD2 expression was increased in low-dose (200 nM) TSA-treated MSCs and slightly increased with high-dose TSA treatment (1~5 μM; Fig 2). These data suggest that at high doses of TSA only weakly modulate ROS levels (Fig. 1D and 1E).

Previous reports have shown that the treatment of TSA at micromolar ranges induces growth inhibition and cell death followed by the increase of intracellular ROS in cancer cells (Chou et al., 2011; You and Park, 2013). In this study, I have shown that nanomolar ranges of TSA (100~500 nM) repressed excessive ROS generation, while high-dose TSA (1000 nM) did not (Fig. 1D and 1E). These effects were not due to cellular toxicity induced by a high dose of TSA (Fig. 1F and 1G). These differences between previous studies and present study may be due to the use of different TSA concentrations, which have varying effects on the expression of antioxidant enzymes such as SOD2 (Fig. 2). In addition, I have used primary cultured hBM-MSCs for this study.

Since TSA suppressed the production of intracellular ROS (Fig. 1D and 1E), I examined the cell protective effects against oxidative stress in TSA-MSCs. Cell viability of hBM-MSCs was improved by pretreatment with TSA compared to control MSCs (Fig. 3). This effect of TSA may be due to the

induced expression of SOD2 (Fig. 2).

The FOXO transcription factor family plays a pivotal role in the regulation of ROS levels (Adachi et al., 2007; de Candia et al., 2008). Previous studies have shown that FOXO1 (a FOXO family member) protects cells from oxidative stress and contributes to extending a cell's life span by lowering intracellular ROS through the upregulation of SOD2 (Adachi et al., 2007; de Candia et al., 2008; Honda and Honda, 1999). I have shown that SOD2 and phosphorylated FOXO1 (p-FOXO1) are down-regulated in oxidative stress-induced MSCs and up-regulated in TSA-treated MSCs (Fig. 4).

Excessive ROS induces apoptosis and is associated with various diseases and cellular senescence (Ben Mosbah et al., 2012; Song et al., 2010). Increased intracellular ROS also induces the expression of the ageing protein p53 (Liu et al., 2008). FOXO and SOD2 along with p53 are the main functional proteins that regulate cell death and senescence (Pani et al., 2009). Here, I examined the expression of p53 in TSA-pretreated MSCs and identified a reverse trend in expression compared to SOD2 and FOXO1. This indicates a correlation of p53 and intracellular ROS in TSA-MSC. NDA(P)H oxidase4 (NOX4) which is also a major source of oxidative stress (Kuroda et al., 2010), was increased the expression in the H_2O_2-treated MSCs, but significantly decreased in TSA-pre-incubated MSCs (Fig. S1), indicating that TSA pretreatment increases SOD2 expression and decreases NOX4 under oxidative stress. Taken together, these results

suggest that TSA may regulate intracellular ROS levels through modulating SOD2, FOXO1, NOX4, and p53. This modulation may be mediated by transcriptional activation of the antioxidant enzyme SOD2 and may rescue mitochondrial activity. I have presented in supplementary figure S2 that the schematic diagram of a model for the prevention of oxidative stress induced cellular toxicity by TSA (Fig. S2).

I demonstrated that TSA pretreatment of hBM-MSCs significantly reduces intracellular ROS. However, I was unable to confirm the identity of the genes that are directly involved in modulating intracellular ROS levels. Therefore, the relationship between TSA and gene regulation needs to be further examined, which should be the focus of next study.

In conclusion, I investigated cell protective effects of low-dose TSA in hBM-MSCs and confirmed its effect on improvement of cell viability under the peroxidative cell injury. This effect is achieved through SOD2 and FOXO1.

Chapter 4. Extracts from the red algae *Gracilaria vermiculophylla* prevent cellular senescence and improve differentiation potential in replicatively senescent human bone marrow mesenchymal stem cells

1. Introduction

Tissue homeostasis maintains the balance between cell death and cell proliferation within tissues and organs, and is one of the most important phenomena for human health (Biteau et al., 2011; Pellettieri and Sanchez Alvarado, 2007). Adult stem cells and their microenvironments play crucial roles in tissue homeostasis (Singh, 2012; Voog and Jones, 2010). However, most stem cell populations will gradually decline due to cellular senescence during the lifetime of an organism, eventually breaking the homeostatic balance and causing progressive tissue ageing (Liu and Rando, 2011; Rossi et al., 2008). A strategy to prevent adult stem cell senescence would be useful to attenuate the functional decline of tissues and organs, and help keep the aging body healthy.

An excess of reactive oxygen species (ROS) can lead to senescence and cellular pathologies such as protein misfolding, DNA damage, and gene dysregulation (Passos and von Zglinicki, 2005; Thannickal and

Fanburg, 2000). My previous studies have shown that a functional decline in stem cells can be caused by the accumulation of ROS during in vitro expansion, and that treatment with antioxidants such as ascorbic acid can delay stem cell senescence (Jeong and Cho, 2015a). Thus, the accumulation of harmful intracellular ROS (iROS) causes a functional decline in aging cells, including stem cells. Living cells normally produce excess ROS through aerobic energy metabolism (Hoidal, 2001). Cells use antioxidant enzymes such as superoxide dismutase 1 (SOD1), superoxide dismutase 2 (SOD2), and catalase (CAT) to dispose of harmful ROS (Jeong and Cho, 2015b; Johnson and Giulivi, 2005). Functional defects in these enzymes can lead to severe cellular damage resulting from the accumulation of iROS (Piazza et al., 2009; Vehvilainen et al., 2014; Watanabe et al., 2014). Cellular senescence may then accompany the chronic oxidative damage resulting from the abnormal accumulation of iROS. The elimination of excessive ROS is therefore crucial for maintaining proper cellular function.

Red algae of the genus *Gracilaria* are commonly found in bodies of water around the world. *Gracilaria* has been used as an agarophyte and an ingredient in Southeast Asian cuisine. Various species belonging to this genus have been commercially cultivated for human consumption (Mazarrasa et al., 2014). *Gracilaria* extracts have been found to have anti-hypercholesterolemic, antioxidant, anti-inflammatory, and antimicrobial effects (de Almeida et al., 2011; Yang et al., 2012). In this study, GV

extracts reduced the ROS levels in human bone marrow mesenchymal stem cells (hBM-MSCs) following chemically induced oxidative stress. Further, GV extracts restored the differentiation potential and reduced the ROS levels of replicatively senescent hBM-MSCs.

2. Results and Discussion

(1) Protective effects of *G. vermiculophylla* extracts against oxidative stress in MSCs

So far, several bioactive natural compounds have been isolated from red algae of genus *Gracilaria* (de Almeida et al., 2011; Yang et al., 2012). In this study, to test *G. vermiculophylla* extracts for cytotoxicity, hBM-MSCs were treated with GV-Cr, GV-H, or GV-Ac (0-50 μg/mL) for 24 h, and their viability was assessed by MTT assay. Cellular toxicity was not detected following treatment with up to 50 μg/mL GV-Cr, 30 μg/mL GV-H, or 30 μg/mL GV-Ac (Fig. 1A). To look for possible antioxidant effects, hBM-MSCs were treated with 1 mM H_2O_2 for 1 h after pre-treatment with 0-10 μg/mL of GV-Cr, GV-H, or GV-Ac for 24 h. Protective effects were observed in cells pre-treated with 1 μg/mL GV-Cr or GV-Ac, but not in cells pre-treated with GV-H (Fig. 1B, Fig. 1C). No protective effects were observed following treatment with GV-H, which suggests that some of the natural compounds important for these effects are likely not water soluble, but are soluble in organic solvents such as acetone, DMSO, and ethanol. To further investigate the impact of GV extracts on cell health, the levels of the apoptotic proteins p53 and cleaved caspase-3 were measured by immunoblot analysis. The levels of both p53 and cleaved caspase-3 in H_2O_2-treated hBM-MSCs were reduced when hBM-MSCs were pre-treated with 1 μg/mL GV-Cr or GV-Ac (Fig. 1D), suggesting that oxidative stress induced cell damage and apoptosis were prevented by GV extracts.

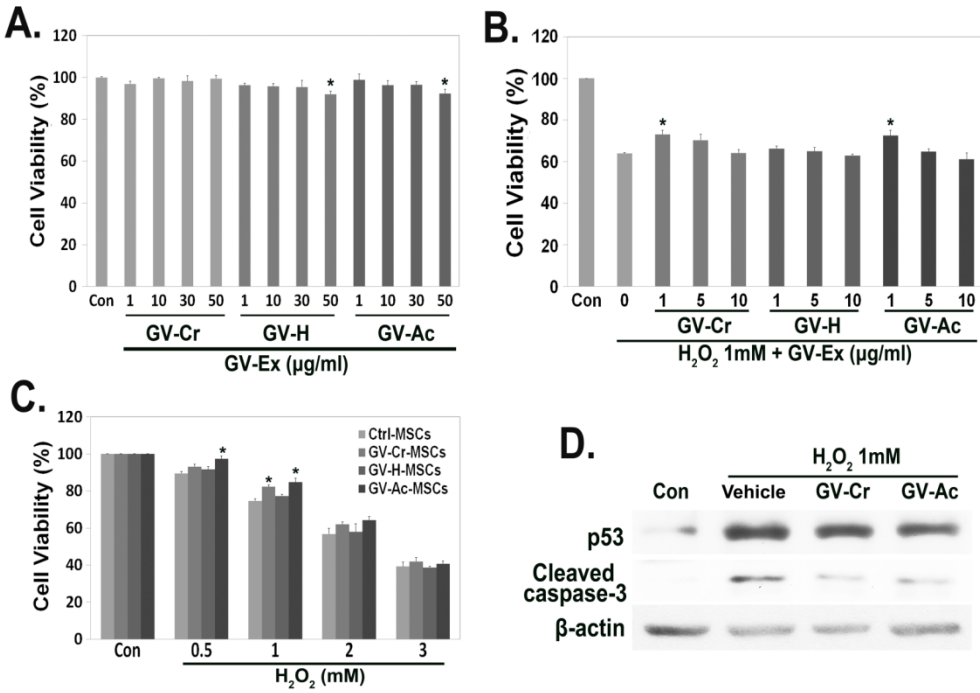

(Chapter 4) Fig. 1.

Figure 1. Protective effects of *G. vermiculophylla* extracts against oxidative stress in MSCs.

(A) hBM-MSCs were treated with 1, 10, 30, or 50 μg/mL GV-Cr, GV-H, or GV-Ac for 24 h (n=3). Cell viability was then measured by MTT assay. The graph shows the viability of cells under each treatment condition as a percentage of the viability of untreated cells (control), and * indicates a *p*-value of less than 0.05 in a paired t-test against the control. (B) hBM-MSCs were exposed to 1 mM H_2O_2 after incubation with each GV extract solution (0, 1, 5, or 10 μg/mL) for 24 h, then examined by MTT assay (n=4). The graph shows the viability of cells under each treatment condition as a percentage of the viability of untreated cells (control), and * indicates a *p*-value of less than 0.01 in a paired t-test against cells not given GV extract (0 column). (C) hBM-MSCs were treated with 1 μg/mL GV extract for 24 h, then treated with 0.5, 1, 2, or 3 mM H_2O_2 for 1 h, and the cell viabilities were determined using an MTT assay (n=4). The graph shows the viability of cells under each treatment condition as a percentage of the viability of untreated cells (control), and * indicates a *p*-value of less than 0.01 in a paired t-test against the control hBM-MSCs (no GV extract) from the same H_2O_2 treatment condition. Statistically significant protective effects were observed when GV-Cr or GV-Ac treatment preceded treatment with 1 mM H_2O_2. (D) hBM-MSCs were incubated with 1 μg/mL GV-Cr or GV-Ac, and then treated with 1 mM H_2O_2 for 1 h. Total protein extracts from the cells were then analyzed by western blot with antibodies against the apoptotic

proteins p53 and cleaved caspase-3. A β-actin antibody was used as a loading control. Vehicle indicates a mixture of equal parts DMSO and ethanol.

(2) GV-Ex moderates iROS levels through the regulation of antioxidant enzymes

Oxidative cellular damage and cellular senescence are mainly caused by excessive ROS production (Huang and Tindall, 2007; Jeong and Cho, 2015a). The activities of the antioxidant enzymes SOD1, SOD2, and CAT reduce the levels of harmful iROS (Johnson and Giulivi, 2005). Since GV-Ac treatment protected cells from oxidative stress, I hypothesized that it might modulate iROS levels. To examine this, iROS levels were measured in hBM-MSCs treated with GV extracts. The levels of iROS in hBM-MSCs after hydrogen peroxide exposure (1 mM) were significantly decreased by GV-Cr or GV-Ac pre-treatment (Fig. 2A). Conversely, the levels of iROS in hBM-MSCs not exposed to hydrogen peroxide did not change with GV extract pre-treatment (Fig. 2B). To further examine the effects of GV-Ac treatment, the levels of the antioxidant enzymes SOD1, SOD2, and CAT were measured by immunoblot analysis. The proteins were reduced in H_2O_2-treated hBM-MSCs (Vehicle), but partially recovered in hBM-MSCs pre-treated with GV-Cr or GV-Ac (Fig. 2C), suggesting that GV extracts may reduce excessive iROS caused by oxidative stress through modulating the levels of antioxidant enzymes.

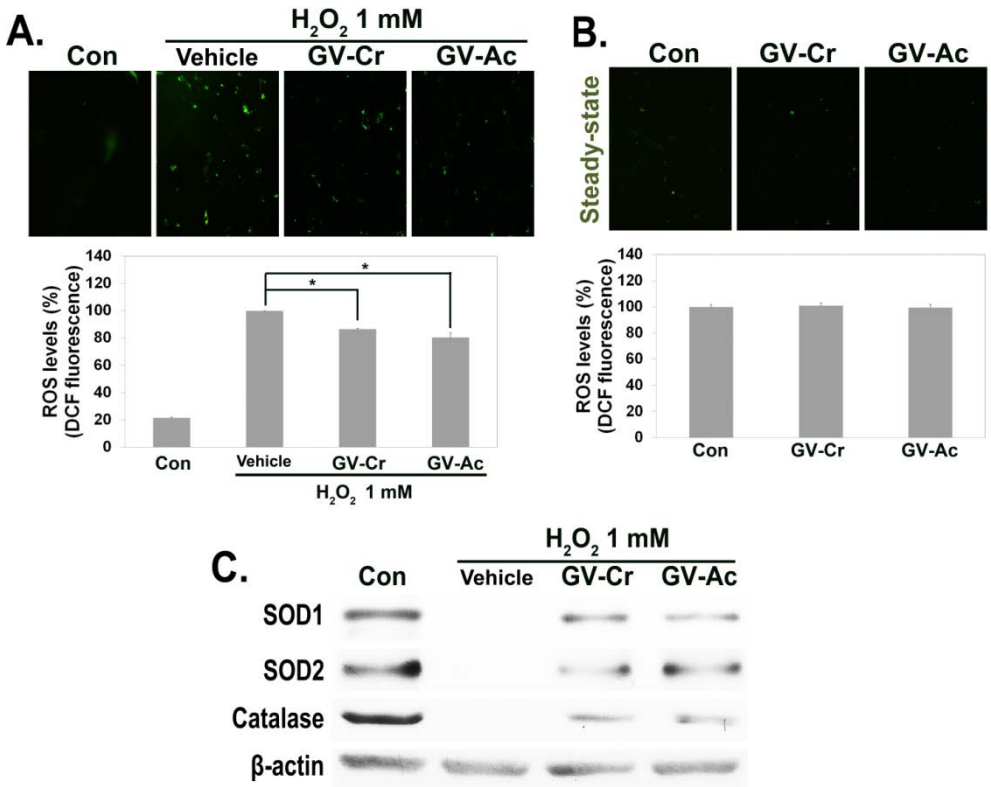

(Chapter 4) Fig. 2.

Figure 2. GV-Ex moderates intracellular ROS through the regulation of antioxidant enzymes.

(A) (Top) GV-Cr or GV-Ac pre-treated hBM-MSCs were treated with DCFH-DA for 1 h and then exposed to 1 mM H_2O_2 for 1 h before fixation. Fluorescence microscopy was then used to visual intracellular DCF production as a measure of iROS levels under each condition. The fluorescence intensities were then quantified for whole wells by an ELISA plate-reader (bottom). The graph shows the relative DCF fluorescence compared to vehicle treatment, and an * indicates a *p*-value of less than 0.01 in a paired t-test against the vehicle treated cells (n=3). (B) (Top) The iROS levels were visualized in GV extract treated hBM-MSCs that were not exposed to H_2O_2 (steady state), and the fluorescence intensities were then quantified for whole wells by an ELISA plate-reader (bottom). (C) GV extract pre-treated hBM-MSCs were treated with 1 mM H_2O_2 for 1 h. The levels of the anti-oxidant proteins SOD1, SOD2, and CAT were visualized by immunoblot. β-Actin was used as a loading control. Vehicle indicates a mixture of equal parts DMSO and ethanol.

(3) Restoration of the levels of antioxidant enzymes and senescence proteins by GV-Ex treatment in replicatively senescent MSCs

Long-term expansion of stem cells leads to accumulation of iROS, and cells progressively become senescent, with an accompanying reduction in antioxidant enzymes (Jeong and Cho, 2015a; Lu and Finkel, 2008; Nguyen et al., 2016). To evaluate whether GV-Ac moderates excessive iROS in senescent cells, hBM-MSCs were expanded up to passage 17 (P-17), and the iROS levels were compared with those of cells at passage 7 (P-7). ROS levels were significantly increased in P-17 hBM-MSCs compared to P-7 hBM-MSCs, but the increase was reduced when hBM-MSCs were pretreated with GV-Cr or GV-Ac (Fig. 3A). The decreased levels of antioxidant enzymes (SOD1, SOD2, and CAT) were restored in GV-extract treated hBM-MSCs (Fig. 3B). The senescence proteins p53, p21, and p16 were also increased in P-17 hBM-MSCs, but partly reduced by GV-Cr or GV-Ac treatment (Fig. 3C). These results indicate that GV-extract may prevent cellular senescence through the moderation of ROS levels in replicatively senescent hBM-MSCs.

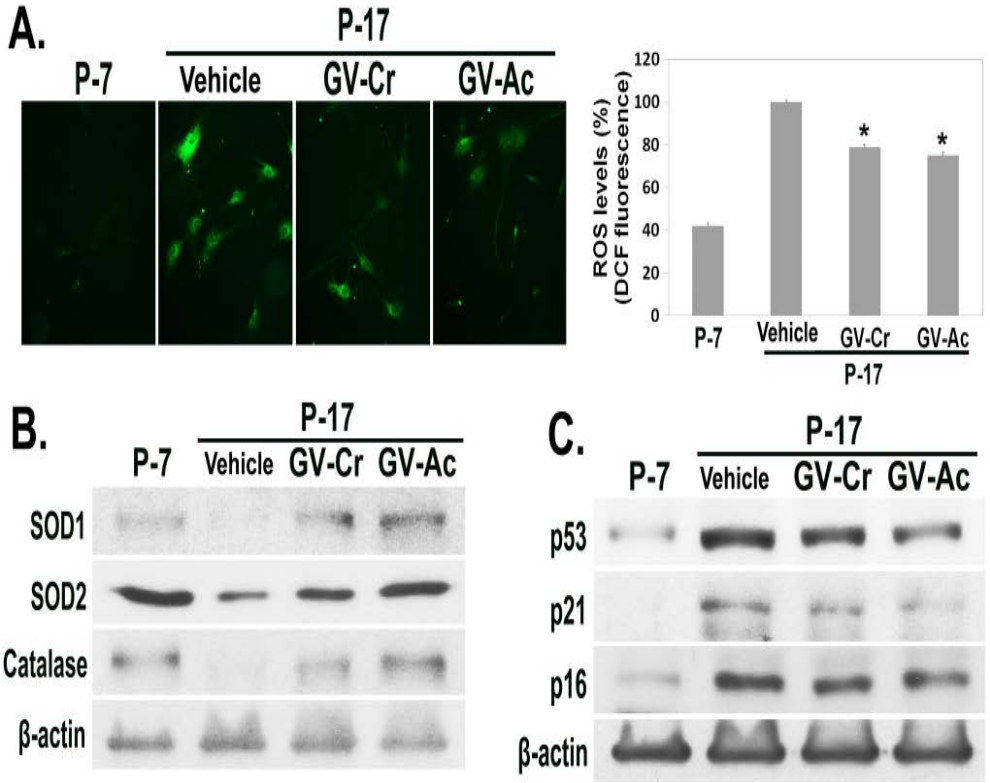

(Chapter 4) Fig. 3.

Figure 3. Restoration of antioxidant enzymes and senescent proteins by GV-Ex in replicatively senescent MSCs.

(A) (Left) Intracellular ROS levels were visualized by fluorescence microscopy following DCFH-Da treatment in hBM-MSCs at P-7, or under various pre-treatment conditions at P-17. Fluorescence intensities were quantified using an ELISA plate reader (right). The graph shows the relative DCF fluorescence compared to vehicle treatment, and an * indicates a *p*-value of less than 0.01 in a paired t-test against the vehicle treated cells (n=4). (B) Total soluble-lysates from P-7, P-17, and GV-extract treated P-17 hBM-MSCs were examined by immunoblot for SOD1, SOD2, and CAT protein levels. β-actin was used as a loading control. (C) The levels of senescence proteins such as p53, p21, and p16 were examined by immunoblot analysis with β-actin as a loading control. Vehicle indicates a mixture of equal parts DMSO and ethanol.

(4) GV-extract treatment reverses the functional decline in replicatively senescent MSCs

The ability of hBM-MSCs to differentiate into osteocytes and adipocytes has been well defined (Pittenger et al., 1999). This capacity is often used as a criterion to determine the functional activity of stem cells (Jeong and Cho, 2015a; Marcus et al., 2008). Since GV-extract treatment reduces ROS levels in replicatively senescent hBM-MSCs, it may prevent or reverse the functional decline of senescent stem cells. To examine this, P-17 hBM-MSCs treated with GV-extract were differentiated into osteocytes or adipocytes. The capacity for differentiation into both cell-types was decreased in P-17 hBM-MSCs, but restored by GV-extract treatment (Fig. 4). These results suggest that the decline in differentiation potential of replicatively senescent hBM-MSCs (P-17) was partially reversed or prevented by GV-extract treatment.

In this study, I examined the anti-senescent effect of extracts from the red algae *G. vermiculophylla* using hBM-MSCs. Treatment with *G. vermiculophylla* extracts moderated excessive iROS levels, increased or maintained the levels of the antioxidant enzymes SOD1, SOD2, and CAT, and decreased or maintained the levels of the senescence proteins p53, p21 and p16. I also found that GV-Cr and GV-Ac treatment restored the differentiation potency of replicatively senescent stem cells (P-17), suggesting that GV-extracts ameliorate the functional decline of senescent stem cells. These results suggest that combining GV-extract treatment with

stem cell treatment may improve the therapeutic efficacy of stem cell therapy.

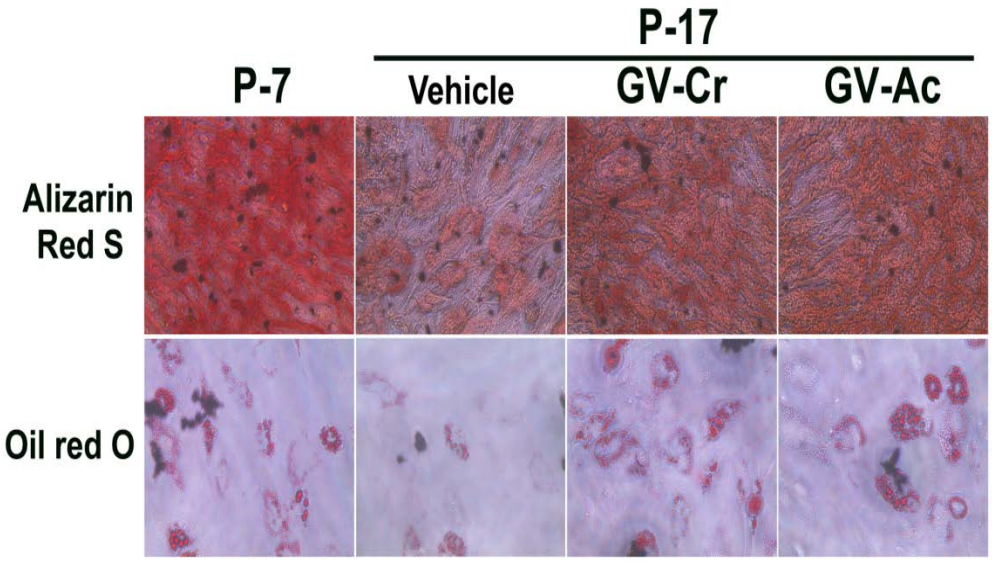

(Chapter 4) Fig. 4.

Figure 4. GV-Ex restores differentiation potential in replicatively senescent MSCs.

(A) hBM-MSCs (P-7, P-17, and GV-extract treated P-17) were induced to differentiate into osteocytes (upper panels) or adipocytes (lower panels). Differentiation capacities were measured by staining with alizarin red S (osteocytes) and oil red O (adipocytes).

Chapter 5. Functional restoration of replicative senescent mesenchymal stem cells by the brown alga *Undaria pinnatifida* extracts

1. Introduction

The steady-state level of intracellular reactive oxygen species (iROS) regulates several cellular signaling pathways, including those related to proliferation, differentiation, and inflammation, independently of cell type (Chiarugi and Buricchi, 2007; Hoidal, 2001; Irani, 2000), while excessive ROS damage DNA, proteins, and lipids, which leads to functional decline and cellular senescence (Back et al., 2012; Geissler et al., 2012; Jung et al., 2004). Long-term *in vitro* expansion of stem cells also leads to their entering senescence with accumulation of iROS (Jeong and Cho, 2015a; Macip et al., 2002), suggesting that the strict control of ROS is required to yield healthy stem cells during long-term expansion.

The antioxidant enzymes superoxide dismutase 1 (SOD1; Cu-ZnSOD), SOD2 (MnSOD), and catalase play crucial roles in the maintenance of iROS homeostasis (Johnson and Giulivi, 2005). The excessive ROS production induced by oxidative stress accompanies reduction of these enzymes' activities, and progressively induces apoptosis (Huang and Tindall, 2007; Jung et al., 2015). Thus, the actions of antioxidant enzymes are closely related to ROS homeostasis and cellular protection.

The brown alga *Undaria pinnatifida* has been commercially cultivated for human consumption and used in East Asian traditional foods and health-care diets (Murata et al., 2002; Schultz Moreira et al., 2013). Recent studies have reported that the compound fucoxanthin isolated from *U. pinnatifida* has anti-obesity effects by inducing the expression of uncoupling protein 1 in white adipose tissue (Maeda et al., 2005). Another compound, fucoidan, which was found in several species of brown algae, has a broad range of biological activities such as anti-inflammatory, antitumor, and antimetastatic (Atashrazm et al., 2015; Kim and Lee, 2012; Wang et al., 2014). *U. pinnatifida* also contains an abundance of eicosapentaenoic acid, one of the omega-3 fatty acids associated with the prevention of inflammation, cardiovascular disorders, and mental disorders (Khan et al., 2007; van Ginneken et al., 2011).

Replicative senescence is defined as the presence of compromised DNA repair and abnormal cellular signaling, and is induced by excessive iROS. Antioxidants protect cells from these impairments and attenuate cellular senescence. In the present study, I examined the antisenescence and anti-oxidative effects of *U. pinnatifida* ethanol extract. This results show that this extract reduced excessive iROS accumulation and inhibited cellular senescence in human bone marrow mesenchymal stem cells (hBM-MSCs).

2. Results

(1) Protective effects of UP-Ex against oxidative stress in MSCs

To examine cytotoxicity, hBM-MSCs were treated with UP-Ex (0-50 μg/mL) for 24 h, and cell viability was measured by an MTT assay. Toxicity was not detected at ≤ 10 μg/mL UP-Ex treatment (Fig. 1A; $p < 0.05$, n = 4). To examine the anti-oxidative effect of UP-Ex, cells were exposed to 1 mM H_2O_2 for 1 h following preincubation with UP-Ex (0-10 μg/mL) for 24 h. The viability was significantly increased in UP-Ex-MSCs compared to untreated hBM-MSCs (Fig. 1B; $p < 0.05$, n = 3). Similarly, 5 μg/mL UP-Ex protected hBM-MSCs exposed to 1 or 2 mM H_2O_2 (Fig. 1C; $p < 0.05$, n = 3). To further examine these protective effects at the molecular level, apoptosis-related proteins (p53 and cleaved caspase-3) were measured by immunoblot analysis. The expression of p53 and cleaved caspase-3 was decreased in UP-Ex-MSCs compared to untreated hBM-MSCs (Fig. 1D), which suggests that cellular damage from oxidative stress was reduced by treatment with UP-Ex.

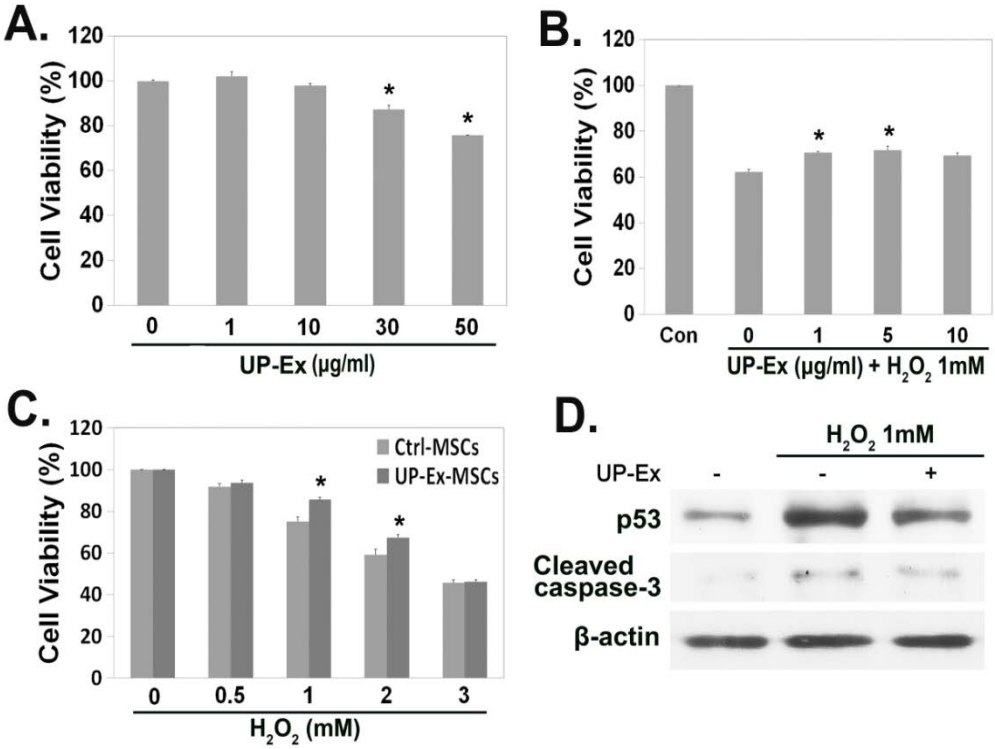

(Chapter 5) Fig. 1.

Figure 1. Cell-protective effects of *U. pinnatifida* extract (UP-Ex) in H_2O_2-treated MSCs.

(A) hBM-MSCs were treated with 0-50 μg/mL UP-Ex (UP-Ex-MSCs) for 24 h and evaluated by an MTT assay. (B) hBM-MSCs were treated with 1 mM H_2O_2 following pre-incubation with UP-Ex (0-10 μg/mL) for 24 h and cell viability was measured by MTT assay. (C) UP-Ex-MSCs (5 μg/mL for 24 h) were exposed to 0-3 mM H_2O_2 for 1 h and the cell viability was evaluated by an MTT assay. Cell viability was significantly improved in UP-Ex-MSCs. (D) 5 μg/mL UP-Ex-MSCs were incubated with 1 mM H_2O_2 for 1 h. Total protein was examined by immunoblot analysis with antibodies against the apoptotic proteins p53 and cleaved caspase-3. β-actin was used as the internal standard.

(2) Restriction of excessive ROS by UP-Ex in MSCs

Cellular damage induced by oxidative stress is caused by excessive iROS levels (Finkel and Holbrook, 2000). Since UP-Ex has protective effects in H_2O_2-treated hBM-MSCs, iROS levels were examined in the UP-Ex-MSCs. ROS levels were significantly reduced in H_2O_2-treated UP-Ex-MSCs compared with untreated hBM-MSCs (Fig. 2A; $p < 0.005$, n = 4), whereas the hBM-MSCs with/without UP-Ex treatment showed no change in the steady state (Fig. 2B). To further examine the modulation of iROS by UP-Ex, the levels of antioxidant enzymes were measured by immunoblot analysis. The expression of SOD1, SOD2, and catalase was decreased in H_2O_2-treated hBM-MSCs and restored by UP-Ex treatment (Fig. 2C). These data suggest that UP-Ex reduced excessive iROS through the recovery of antioxidant enzymes, SOD1, SOD2, and catalase in hBM-MSCs.

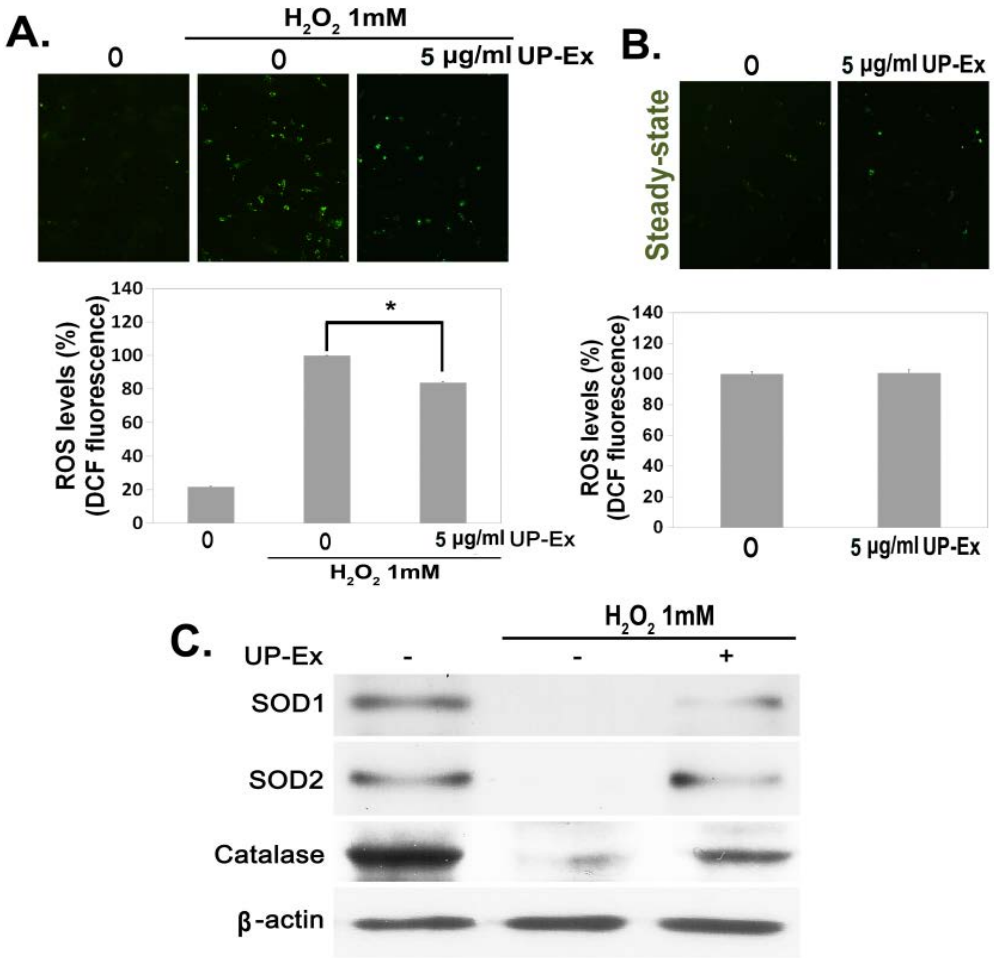

(Chapter 5) Fig. 2.

Figure 2. *U. pinnatifida* extract (UP-Ex) treatment reduces intracellular ROS levels in MSCs.

(A) UP-Ex-treated hBM-MSCs (UP-Ex-MSCs; 5 μg/mL for 24 h) were treated with 1 mM H_2O_2 for 1 h, and their iROS levels were observed by fluorescence microscopy (upper panel). Fluorescence levels were quantified with a fluorescence ELISA plate reader (lower panel). (B) Steady-state iROS levels were visualized in 0-5 μg/mL UP-Ex-MSCs (upper panel) and quantified by a fluorescence-based ELISA plate reader (lower panel). (C) UP-Ex-MSCs were treated with 1 mM H_2O_2 for 1 h. The expression of antioxidant enzymes SOD1, SOD2, and catalase was measured by immunoblot analysis. β-actin was used as the internal standard.

(3) Recovery of antioxidant enzymes by UP-Ex in replicative senescent MSCs

Previous study showed that stem cells made senescent by long-term expansion accumulate iROS and exhibit reduced antioxidant enzyme expression (Jeong and Cho, 2015a). To test whether the excessive ROS induced by long-term culture is reduced by UP-Ex treatment, hBM-MSCs were expanded up to P-17 and stained for the presence of iROS. The increased ROS in P-17 cells was significantly decreased in P-17 UP-Ex-MSCs (Fig. 3A; $p < 0.05$, n = 4). Immunoblot analysis of antioxidant enzymes showed that the expression of SOD1, SOD2, and catalase was decreased in P-17 cells and restored in P-17 UP-Ex-MSCs (Fig. 3B). In addition, the senescence proteins p53, p21, and p16 were increased in P-17 cells and this increase was reversed in P-17 UP-Ex-MSCs (Fig. 3C). These data suggest that UP-Ex reverses cellular senescence through recovery of antioxidant enzymes.

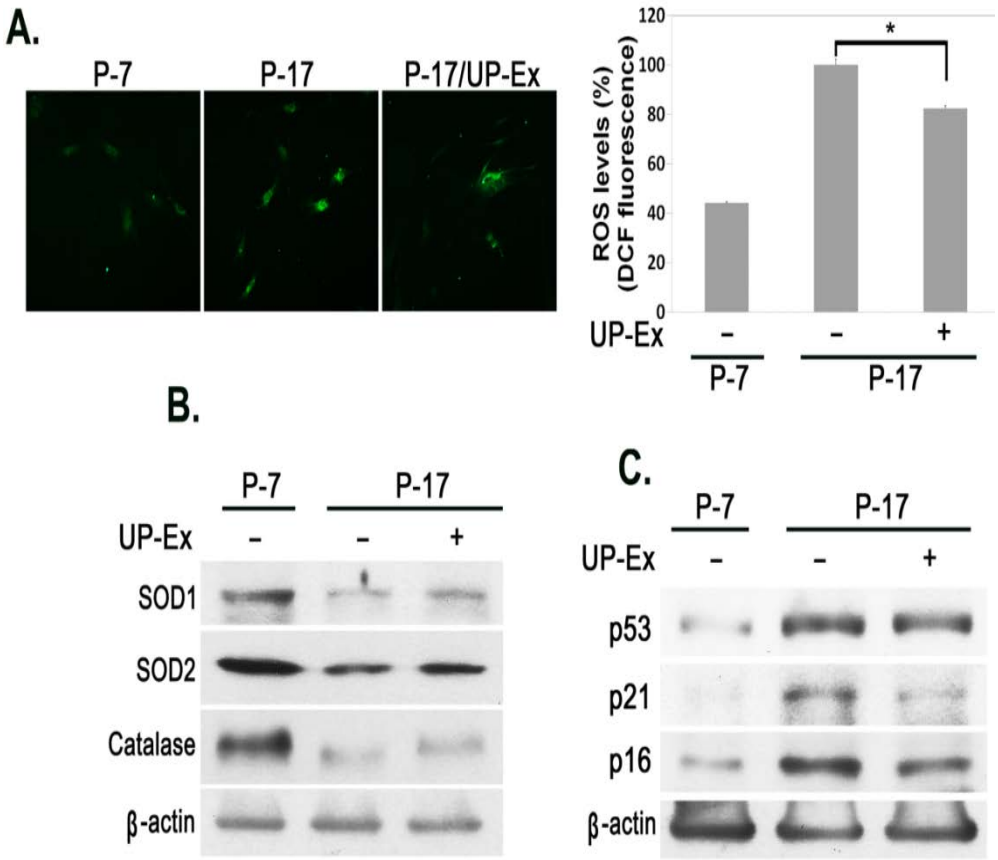

(Chapter 5) Fig. 3.

Figure 3. Restoration of antioxidant enzymes and reversal of senescence protein expression increases in *U. pinnatifida* extract (UP-Ex)-treated senescent MSCs.

(A) Intracellular reactive oxygen species were detected with DCFH-Da in passage (P)-7, P-17, and UP-Ex-treated P-17 hBM-MSCs by fluorescence microscopy (left panel) and quantified using a fluorescence-based ELISA plate reader (right panel). (B) Total protein from P-7, P-17, and UP-Ex-treated P-17 hBM-MSCs were examined by immunoblot analysis with antibodies against SOD1, SOD2, catalase, and β-actin. (C) The expression of the senescence proteins p53, p21, and p16 was examined by immunoblot analysis.

(4) Restoration of differentiation capacity by UP-Ex treatment

If UP-Ex has anti-senescence effects in replicative senescent stem cells, cells treated with UP-Ex may recover their differentiation potential. To confirm this hypothesis, long-term (P-17) cultured hBM-MSCs were treated with 5 μg/mL UP-Ex for 24 h and differentiated into osteocytes and adipocytes. P-17 hBM-MSCs exhibited reduced differentiation potential compared to P-7 cells, and UP-Ex treatment of P-17 cells restored this potential compared to untreated P-17 hBM-MSCs (Fig. 4). These results suggest that the decline in differentiation capacity caused by cellular senescence was at least partially reversed by UP-Ex treatment.

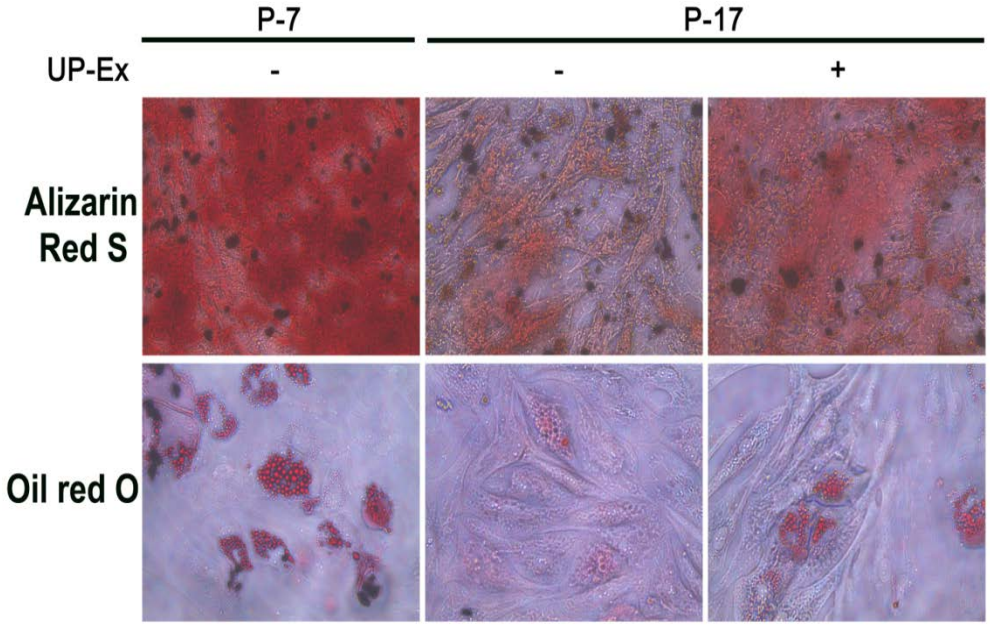

(Chapter 5) Fig. 4.

Figure 4. Improvement of differentiation potential in *U. pinnatifida* extract (UP-Ex)-treated senescent MSCs.

hBM-MSCs at passage (P)-7 or P-17, with or without UP-Ex treatment at P-17, were induced to differentiate into osteocytes (upper panels) and adipocytes (lower panels). Differentiation capacities were evaluated by alizarin red S or oil red O staining.

3. Discussion

Several useful compounds such as fucoxanthin and fucoidan have been isolated from *U. pinnatifida* (Deux et al., 2002; Maeda et al., 2005). Major benefits of these compounds have been demonstrated in arteriosclerosis, inflammation, fat metabolism, and antitumor therapy (Atashrazm et al., 2015; Kim and Lee, 2012; Kim et al., 2014b; Roux et al., 2012). In this study, to demonstrate the antioxidant and anti-senescence properties of *U. pinnatifida*, UP-Ex was used to treat hBM-MSCs, which were then evaluated for protection against senescence and oxidation. Treatment with UP-Ex resulted in enhanced protection against oxidative stress in hBM-MSCs (Fig. 1). The oxidation-sensitive protein p53 was increased upon H_2O_2 treatment, and this increase was partially reversed when hBM-MSCs were pretreated with UP-Ex. Similarly, expression of the apoptotic protein cleaved caspase-3 was reduced in UP-Ex-MSCs (Fig. 1D).

Antioxidant enzymes such as SOD1, SOD2, and catalase are known as major scavengers of iROS (Johnson and Giulivi, 2005). Expression of these enzymes is decreased in cells exposed to excessive oxidative stress, resulting in the accumulation of iROS (Huang and Tindall, 2007; Jeong and Cho, 2015b). Since I have shown that UP-Ex pretreatment protects against oxidative stress in hBM-MSCs, it is reasonable to assume that this protection is due to moderated iROS levels. To address this hypothesis, ROS levels were measured in H_2O_2-treated MSCs following pre-incubation

with UP-Ex. As expected, the increased ROS levels were moderated in UP-Ex-MSCs (Fig. 2A and B), which was likely caused by restoration of the ROS-scavenging enzymes SOD1, SOD2, and catalase (Fig. 2C).

Adult stem cells have been used for stem cell therapy in degenerative diseases (Barry and Murphy, 2013; Farini et al., 2014; Kim et al., 2014a). However, previous studies have shown that stem cells gradually display a senescent phenotype during long-term expansion following by accumulation of iROS (Jeong and Cho, 2015a; Oka et al., 2015; Su et al., 2015). Nevertheless, cell expansion is required to obtain sufficient amounts of donor stem cells for stem cell therapy (Wagner and Ho, 2007), which is a dilemma that needs to be resolved to obtain healthy donor stem cells. In this study, I showed that excessive iROS induced by long-term cell expansion was significantly decreased in UP-Ex-pretreated MSCs (Fig. 3A and B), which accompanied a significant reversal of the senescence-related proteins p53, p21, and p16 (Fig. 3C), suggesting that cellular senescence induced by cell expansion may be partly ameliorated by pre-incubation with UP-Ex.

If UP-Ex treatment downregulates excessive iROS accumulation and reduces the expression of senescence-related proteins in senescent stem cells (P-17), it may also improve the differentiation potential of stem cells. In support of this hypothesis, long-term cultured hBM-MSCs (P-17) pretreated with UP-Ex could be differentiated into osteocytes or adipocytes, confirming the differentiation potential of UP-Ex treated P-17

MSCs (Fig. 4). This result suggests that treatment with UP-Ex can recover the functional decline that is characteristic of replicative senescent stem cells.

In conclusion, I have shown that an ethanol extract of *U. pinnatifida* moderates excessive iROS and reverses replicative senescence with an increase in antioxidant enzymes in hBM-MSCs. This study has also shown that UP-Ex treatment restored the differentiation potential of replicative senescent (P-17) hBM-MSCs, suggesting that UP-Ex ameliorates the functional decline of senescent stem cells. Combined treatment with UP-Ex may provide better therapeutic efficacy in stem cell therapy.

Part II. Regulatory mechanism on neuronal differentiation

Chapter 1. The tubulin deacetylase sirtuin-2 regulates neuronal differentiation through the ERK/CREB signaling pathway

1. Introduction

Microtubules (MTs) are an important component of the cytoskeleton that can influence diverse aspects of cellular function such as cell migration, proliferation, development, and even differentiation (Bowne-Anderson et al., 2013; Gelfand and Bershadsky, 1991; Howard and Hyman, 2003). Furthermore, the determination of stem cell fate toward differentiation or self-renewal is regulated by modification of MTs and the motor protein dynein (Will and Steidl, 2014).

A previous study reported that exposing mesenchymal stem cells (MSCs) to taxol, which stabilizes β-tubulin (Amos and Lowe, 1999), resulted in a stabilized MT structure and a decreased ability to differentiate into adipocytes and osteocytes (Choron et al., 2015). Another study showed that treating MSCs with nocodazole, which disturbs MT dynamics, reduces the expression of osteogenic differentiation markers (Kallas et al., 2011; Rodriguez et al., 2004). These two drugs downregulated the differentiation capacities of MSCs by modifying the MT structure, suggesting that MTs are

involved in MSC differentiation into osteocytes and adipocytes. MTs also participate in regulating neuronal cell migration (Del Rio et al., 2004; Wen et al., 2004) and polarization (Witte et al., 2008), meaning that MT modification may regulate neuronal differentiation. However, the relationship between neuronal differentiation and MTs is still largely unknown.

MTs are complex structures consisting of asymmetric heterodimers of α- and β-tubulin, and the modification of MTs is mediated by post-translational modifications (PTM) of the tubulin subunits (α- and β-tubulin), such as acetylation, phosphorylation, detyrosination, and ubiquitination (de Forges et al., 2012; Mitchison and Kirschner, 1984). The acetylation/deacetylation of α-tubulin at lysine 40 (K40) contributes to MT modification (Al-Bassam and Corbett, 2012; Howes et al., 2014). A previous study reported that Ac-α-tubulin generally occurs in stable MT polymers and inhibits axon and neurite outgrowth from neurons (Creppe et al., 2009; Witte et al., 2008). Thus, α-tubulin modification is important for neuronal morphogenesis, suggesting that MT modification through α-tubulin acetylation/deacetylation may be a key process in neuronal differentiation.

The two major tubulin deacetylases, histone deacetylase 6 (HDAC6) (Hubbert et al., 2002; Zilberman et al., 2009) and sirtuin-2 (Sirt2) (North et al., 2003), which remove the acetyl group from α-tubulin at K40 (αK40), control MT modifications and are mostly localized to the cytoplasm.

HDAC6, a class II histone deacetylase, contributes to the regulation of MT growth and shrinkage velocity through α-tubulin deacetylation (Tapia et al., 2010). Inhibition of HDAC6 by a small molecule inhibitor or siRNA increases MT acetylation and reduces MT dynamics (Haggarty et al., 2003; Matsuyama et al., 2002; Zhang et al., 2008). Additionally, HDAC6 regulates MT dynamics by interacting with EB1, a microtubule plus-end-tracking protein (Zilberman et al., 2009). The other tubulin deacetylase, Sirt2, a class III NAD-dependent histone deacetylase (North et al., 2003), is primarily found in the central nervous system (CNS) and also localized in the cytoplasm, neurites, and their growth cones (Dent and Gertler, 2003; Maxwell et al., 2011). Sirt2 inhibits the collapse of neurite outgrowth and growth cones by increasing MT dynamics in post-mitotic hippocampal neurons (Pandithage et al., 2008). Furthermore, Sirt2 regulates the cell cycle (G2/M phase) through global deacetylation of Histone 4 (H4) in neuronal cells (Dryden et al., 2003). In degenerative stimulus-mice, Sirt2 reduces elevated levels of Ac-α-tubulin and ameliorates axon resistance (Suzuki and Koike, 2007).

MSCs have the potential to differentiate into neuronal cells (Jeong et al., 2013; Woodbury et al., 2000) and can be easily isolated from patients (Mahmood et al., 2001), allowing for patient-specific treatment of neurological disorders such as Parkinson's disease, Alzheimer's disease, and spinal cord injury. MT modification is involved in diverse cellular mechanisms, indicating that MSCs differentiation is also closely related to

MT modification. Therefore, the relationship between neuronal differentiation and MT modification needs to be investigated in MSCs. The tubulin deacetylases HDAC6 and Sirt2 can regulate MT modification, meaning that tubulin deacetylase and MT modification may be involved with neuronal differentiation in MSCs. In this study, I investigated the relationship between MTs and neuronal differentiation in MSCs and examined whether HDAC6 and Sirt2 regulate neuronal differentiation through their α-tubulin deacetylase activity.

2. Results and Discussion

(1) Alteration of acetylated α-tubulin during neuronal differentiation

Microtubule (MT) dynamics have profound functional effects on cellular transport, migration, differentiation, and division (Gelfand and Bershadsky, 1991). α-Tubulin is a major component of MTs and regulates MT dynamics through PTMs (Al-Bassam and Corbett, 2012; Howes et al., 2014). To examine the relationship between MT modification and neuronal differentiation, I determined the alteration of acetylated α-tubulin (Ac-α-tubulin) levels during neuronal differentiation. Ac-α-tubulin expression levels gradually decreased from 2–6 h upon incubation in induction medium and then returned to baseline at 12 h (Fig. 1A). The acetylation/deacetylation of α-tubulin is modulated by two major tubulin deacetylases, HDAC6 and Sirt2 (Dryden et al., 2003; Hubbert et al., 2002), suggesting that HDAC6 and Sirt2 may be related to neuronal differentiation. To investigate the association between tubulin deacetylase activity and neuronal differentiation, MSCs were incubated in neuronal induction media for 24 h. The mRNA expression of *HDAC6* and *Sirt2* was examined by real-time PCR. As shown in Figure 1B, *HDAC6* and *Sirt2* expression increased during neuronal differentiation compared to levels in non-induced MSCs (MSCs; *t*-test, $*p < 0.05$, mean ± SD, n = 3), indicating that Ac α-tubulin and tubulin deacetylase (HDAC6 and Sirt2) are related with neuronal differentiation.

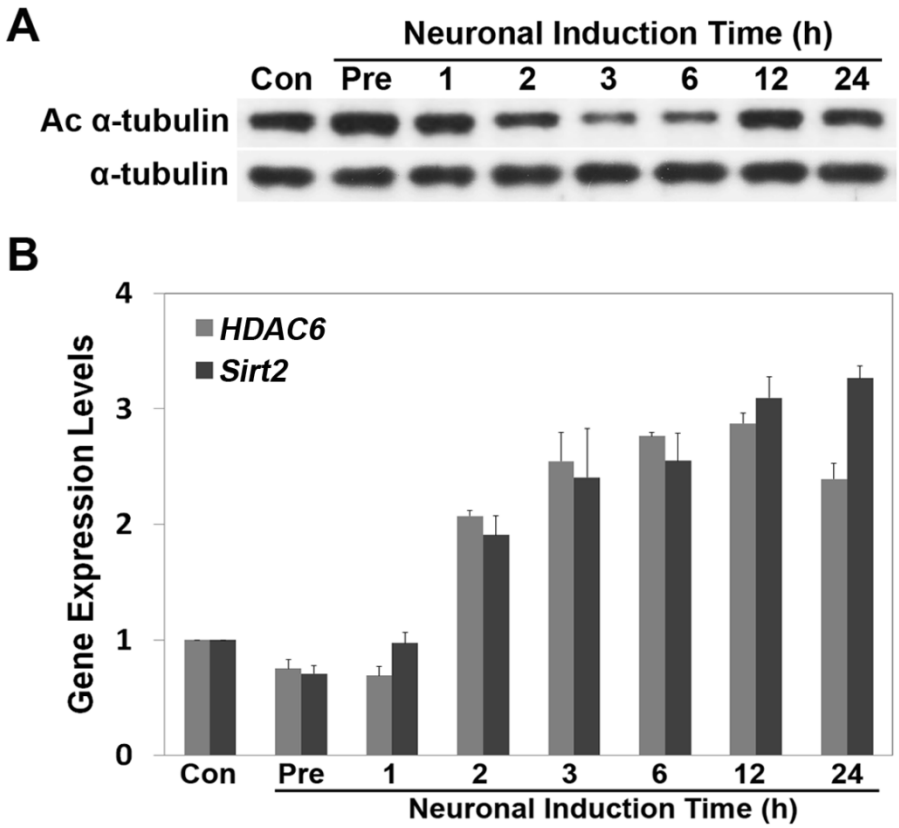

(Chapter 1) Fig. 1.

Figure 1. Changes in acetylated α-tubulin and tubulin deacetylase gene expression upon neuronal induction

(A) Cells were incubated in neuronal induction media for the indicated times (0, 1, 2, 3, 6, 12, and 24 h). Total proteins were examined by immunoblot analysis using antibodies to detect α-tubulin and acetylated α-tubulin (Ac-α-tubulin). (B) The mRNA expression of tubulin deacetylases *HDAC6* and *Sirt2* was measured by real-time PCR in MSCs incubated in neuronal differentiation media for the indicated times. β-actin was used as an internal standard.

(2) The activity of tubulin deacetylases HDAC6 and Sirt2 is involved with neuronal morphology

To confirm the relationship between tubulin deacetylase expression and MT modification during neuronal differentiation, I determined whether HDAC6 and Sirt2 could regulate neuronal differentiation by deacetylating α-tubulin. Prior to neuronal induction, cells were incubated with 3 μM tubastatin A (TubA), an HDAC6 inhibitor, or 10 μM AGK2, a Sirt2 inhibitor. Then, MSC differentiation (dMSC) was induced by exposing cells to neuronal induction media. TubA-treated dMSCs (TubA-dMSCs) showed increased Ac-α-tubulin levels compared to non-treated dMSCs (Con-dMSCs) (Fig. 2A). Similarly, I also detected increased levels of Ac-α-tubulin in AGK2-treated dMSCs (AGK2-dMSCs) compared to untreated control cells (Fig. 2B). This suggests that both HDAC6 and Sirt2 involved with alternation of α-tubulin deacetylation during neuronal differentiation.

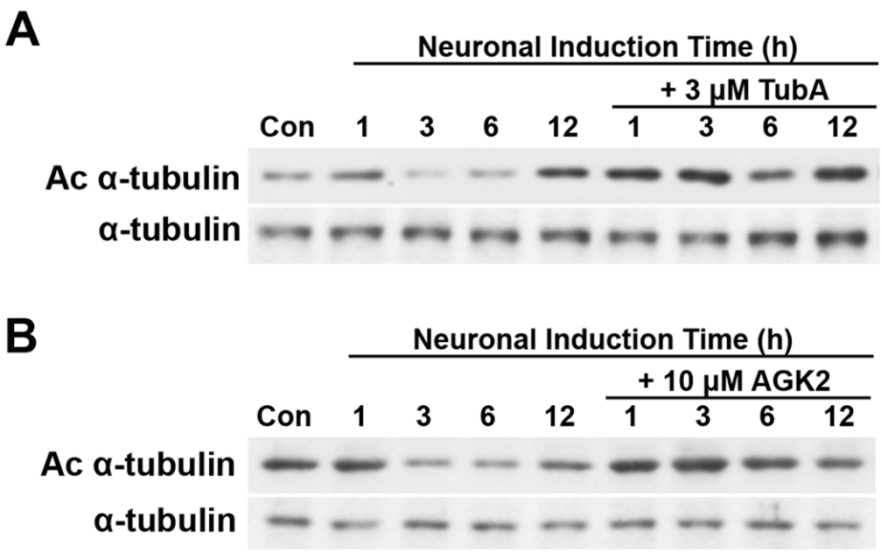

(Chapter 1) Fig. 2.

Figure 2. Effect of HDAC6 and Sirt2 on neuron-like morphology changes upon neuronal induction

Prior to induction, MSCs were incubated with media containing (A) 3 μM tubastatin A (TubA) or (B) 10 μM AGK2 for 24 h and then MSCs were exposed to neuronal induction media. Acetylated α-tubulin levels were measured by immunoblot analysis. (C) Control MSCs, TubA-exposed MSCs, and AGK2-exposed MSCs (Con-dMSCs, TubA-dMSCs, and AGK2-dMSCs, respectively) were differentiated into neuronal cells following incubation in neuronal induction media for 6 h.

(3) Sirt2 regulates the expression of neural-specific proteins during neuronal differentiation

Based on the above results, I hypothesized that inhibiting tubulin deacetylase activity impeded differentiation as a result of increased Ac-α-tubulin. To address this, I confirmed the expression changes of neural-specific markers NF-M and MAP-2 upon inhibition of HDAC6 or Sirt2. The expression of these neural-specific markers was determined by real-time PCR and immunoblot analysis in Con-dMSCs, TubA-dMSCs, and AGK2-dMSCs (Fig. 3A-D). Levels of the neural-specific genes and proteins examined were significantly decreased in AGK2-dMSCs compared to Con-dMSCs (Fig. 3C and 3D; *t*-test, $* p < 0.05$, mean ± SD, n = 5). However, contrary to expectations, TubA-dMSCs did not exhibit altered expression of neural-specific markers compared with Con-dMSCs (Fig. 3A and 3B). Consistent results were obtained from immunocytochemical staining using antibodies specific to NF-M and MAP-2 (Fig. 3E) in dMSCs for 6 h. These data suggest different roles for HDAC6 and Sirt2 during differentiation, with Sirt2 playing an important regulatory role in MSC neuronal differentiation.

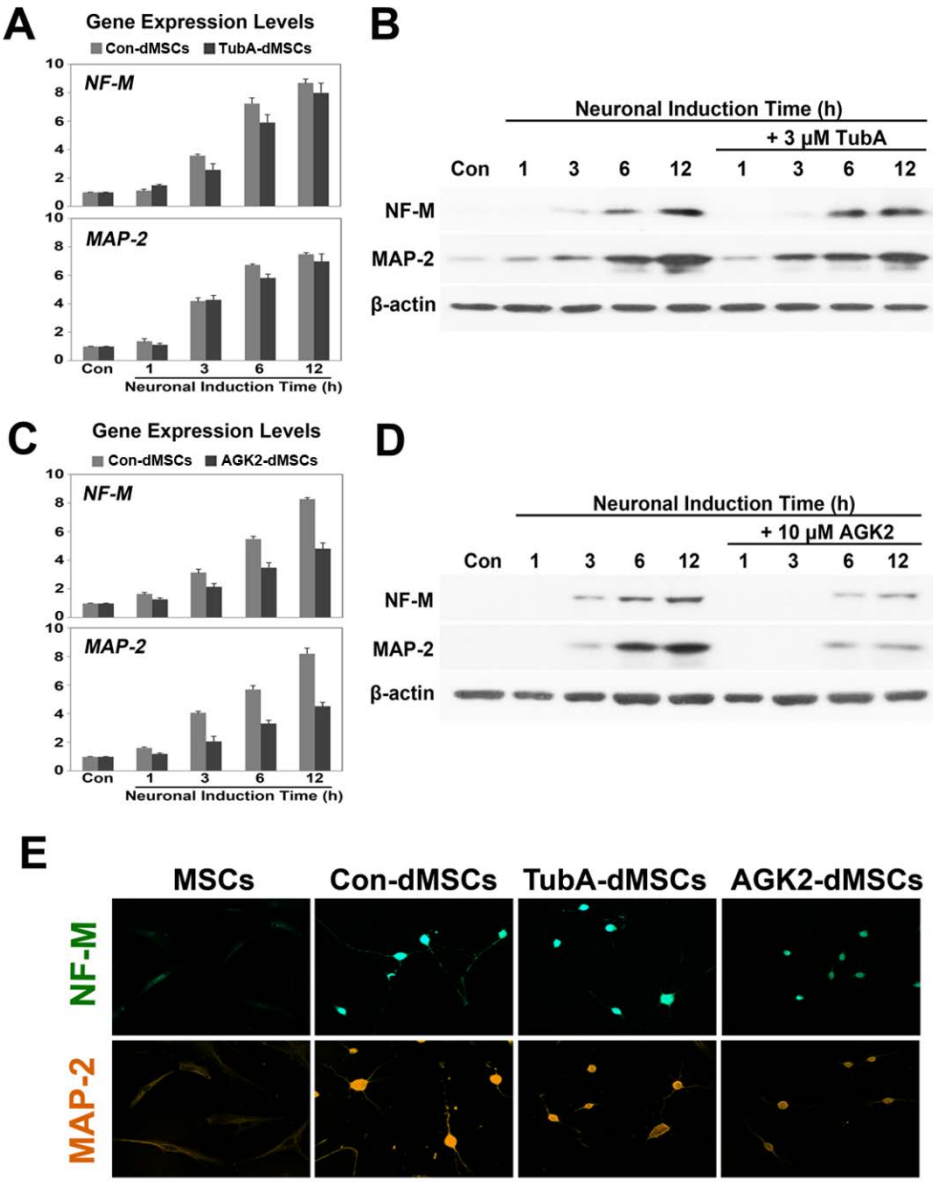

(Chapter 1) Fig. 3.

Figure 3. Neuronal-specific marker expression in differentiated MSCs treated with AGK2 or TubA

Neuronal differentiation was induced in MSCs by exposure to neuronal induction media for the indicated times. Changes in neuronal-specific marker levels were measured in control MSCs (Con-dMSCs) versus TubA-dMSCs or AGK2-dMSCs by real-time PCR (A,C) and immunoblotting with specific antibodies against NF-M, MAP-2, and β-actin (B,D). (E) MSCs and differentiated MSCs subjected to various pretreatments (Con-dMSCs, TubA-dMSCs, and AGK2-dMSCs) were fixed and stained with antibodies against NF-M (upper panel) and MAP-2 (lower panel), and detected by fluorescence microscopy.

(4) Sirt2 inhibition impairs the ERK-CREP signaling pathway in neuronal differentiation

The extracellular signal-regulated protein kinases 1 and 2 (ERK1/2), members of the mitogen-activated protein kinase (MAPK) pathway (Choi et al., 2013), regulate the stability and deacetylase activity of Sirt2, and blocking Sirt2 activity suppresses the phosphorylation of ERK (p-ERK) (Choi et al., 2013). Several studies have shown that ERK phosphorylation is a crucial event required for neuronal differentiation (Li et al., 2006; Moon et al., 2009). The ERK pathway is related with cAMP response element-binding protein (CREB) and increases CREB phosphorylation (p-CREB) (Impey et al., 1999). CREB is a major target of MAPK/ERK during differentiation (Canon et al., 2004), suggesting that Sirt2 may be involved with neuronal differentiation through the phosphorylation of ERK and CREB. To confirm this, I investigated the relationship between Sirt2 and ERK-CREB pathways. p-ERK levels gradually increased from 3-6 h during differentiation and then decreased from 12 h onward in Con-dMSCs. However, AGK2-dMSCs showed decreased p-ERK levels, while p-ERK levels in TubA-dMSCs were similar to levels in Con-dMSCs (Fig. 4A). Similar results were obtained from immunoblot analysis against phosphorylated CREB (p-CREB; Fig. 4B), indicating that Sirt2 regulates neuronal differentiation via ERK-CREB pathway, while HDAC6 does not.

In this study, I demonstrated that the Sirt2 plays an important role in

neuronal differentiation mechanisms. HDAC6 and Sirt2 control neuronal morphological changes by deacetylating α-tubulin. I found that Sirt2 regulates the expression of neural-specific proteins NF-M and MAP-2 via ERK-CREB pathway activation, but HDAC6 does not act in this manner. I was unable to confirm the differential mechanisms of Sirt2 and HDAC6 during neuronal differentiation. Therefore, specific roles of Sirt2 and HDAC6 in neuronal differentiation need to be further investigated. In conclusion, Sirt2 regulates MSC morphological changes during neural differentiation through the deacetylation of α-tubulin and controls the neuronal differentiation by modulating phosphorylation of the ERK-CREB pathway.

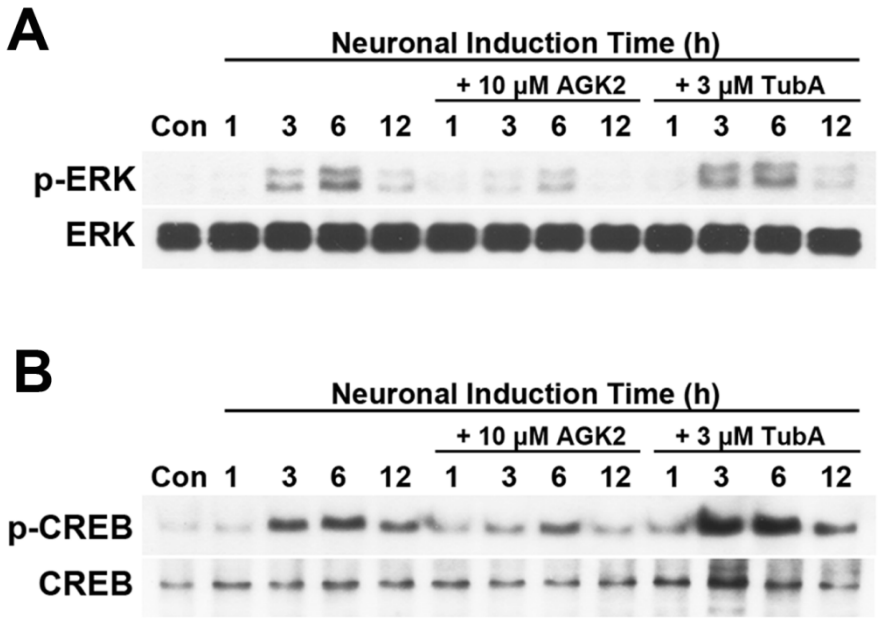

(Chapter 1) Fig. 4.

Figure 4. Correlation of ERK-CREB activation with Sirt2 in neuronal differentiation

(A) Cells were exposed to neuronal induction media for the indicated times (0, 1, 3, 6, and 12 h). Total proteins were extracted from control cells (Con-dMSCs), and cells pretreated with AGK2 (AGK2-dMSCs) or TubA (TubA-dMSCs). Proteins were detected by immunoblotting using specific antibodies against ERK, phosphorylated ERK (p-ERK), and β-actin. (B) Similarly, cells were subjected to immunoblot analyses with CREB and phosphorylated CREB (p-CREB) antibodies. β-actin was used as an internal standard.

Chapter 2. The assembly of stress granules during neuronal differentiation

1. Introduction

Gene expression is regulated by transcription and post-transcriptional system during neuronal differentiation (Black, 2003; Licatalosi and Darnell, 2006). RNA-binding proteins (RBP) play an important role in post-transcriptional processing, including splicing, RNA editing, and polyadenylation (Perrone-Bizzozero and Bolognani, 2002; Roegiers and Jan, 2004; Schaeffer et al., 2003). Previous studies have shown that RBP Ptbp1 expression levels are reduced in the development of nervous system. Ptbp1 knockdown induced the neuronal differentiation through the morphological change and functional change in non-neuronal cells (Linares et al., 2015). miR-124a is involved in the neuronal differentiation through the degradation of non-neuronal genes during the post-transcriptional process (Makeyev et al., 2007). miR-124a is coupled with an activity of epigenetic regulators such as RE1-silencing transcription factor (REST) and histone deacetylases (HDACs) family (Conaco et al., 2006). Thus, post-transcriptional and epigenetic regulation is largely responsible for the alteration of gene expression associated with neuronal differentiation.

RNA granules appear in various types in germ cells (germ cell granules)

(Schisa et al., 2001), somatic cells (stress granules and processing bodies) (Nover et al., 1989), and neurons (neuronal granules) (Kosik and Krichevsky, 2002; Krichevsky and Kosik, 2001). These granules play an important role at the post-transcriptional and epigenetic levels in the changes of gene expression. RNA granules contain the translation factors, RBP, ribosomal subunits, and decay enzymes and regulate the translation of RNA cargo (Anderson and Kedersha, 2006).

Stress granules (SGs), one of the RNA granules, are ribonucleoprotein (RNP) complexes consist of arrested translation initiation complexes (Anderson and Kedersha, 2008), RNA binding proteins, miRNAs, and various proteins involved with signaling of cell metabolisms (Anderson and Kedersha, 2009b). Cells continuously adapt to maintain their viability for environment changes due to oxidative stress, energy deprivation, glucose starvation, and viral infection (Yamasaki and Anderson, 2008). To adapt the changes of the environment, the cells regulate the translation of mRNA encoding protein. In this process, several mRNAs are delayed the translation until cues for the initiation of their translation (Anderson and Kedersha, 2009a), and the translationally delayed mRNAs are incorporated into cytoplasmic foci known as SGs (Emara et al., 2012). Thus, SGs are thought to regulate cellular metabolism by modulating post-transcription of mRNA under the changed environmental condition.

SGs assembly and translational repression occurred from an incomplete assembly of the eukaryotic initiation factor-4F (eIF4F) complexes

composed of eIF4E, 4G, 5A, and 43S pre-initiation complex (PIC) (Yamasaki and Anderson, 2008). 43S PIC is repressed by phosphorylation at serine 51 (S51) of eukaryotic initiation factor 2α (eIF2α), an important element of eIF2-GTP-$tRNA^{Met}$ ternary complex for assembly of 43S PIC (Yamasaki and Anderson, 2008). Previous study reported that the mutation at S51 of eIF2α, which is converted from the serine to alanine residue (S51A; non-phosphorylatable eIF2α), inhibits SGs assembly and repression of translation (Gerlitz et al., 2002; Sudhakar et al., 2000). Unlike this, mutation at S51 of eIF2α, which is replaced with aspartic acid (S51D; phosphomimetic eIF2α), induces the SGs assembly and inhibits the translation of mRNA (Costache et al., 2012). These results indicate that phosphorylation of eIF2α is necessary events to induce the SGs assembly and translation repression.

Human mesenchymal stem cells (hMSCs) possess the differentiation capacity into neuron, and are easily isolated from donor (Caplan, 2007; Jeong et al., 2013; Pittenger et al., 1999). For this reason, the use of hMSCs is an increasing interest as a source of treatment for neurological diseases, including Alzheimer's, Amyotrophic lateral sclerosis (ALS), and Parkinson's disease. Many researches showing the epigenetic modification and specific gene profiling to improve the differentiation efficacy have been reported. Thus, the research of differentiation mechanism into neuron has become an important aspect in therapy for neurological disease. However, their differentiation mechanism is still largely unknown. In the

present study, I observe the SGs assembly during neuronal differentiation and examine the correlation between SGs assembly and differentiation process in MSCs.

2. Results and Discussion

(1) SGs assembled during the neuronal differentiation

Cells have a conserved mechanism which can adjust to a change of environment induced by oxidative stress, ER stress, energy deprivation, glucose starvation, and reprogramming protein translation. The assembly of stress granules (SGs) is a representative mechanism adapting to the environmental changes in cells (Anderson and Kedersha, 2009a). Previous study reported that the translation of several mRNAs was delayed during neural stem cells (NSCs) differentiation, and various proteins exhibited the changes in their expression (Masakazu et al., 2016), suggesting that neuronal differentiation may be associated with SG assembly. The translational silencers TIA-1 and GTPase-activating protein SH3 domain binding protein (G3BP) are self-aggregating proteins essential for the assembly of SGs and contribute to the degradation of polysome (Pavel et al., 2011; Anderson et al., 2009). To detect the assembly of SGs during neuronal differentiation, SG markers G3BP and Tia-1 were observed by the immunocytochemical staining. I detected the SG assembly during differentiation process between 1 and 3 h (Fig. 1A). However, it may have been difficult to observe the SGs through a fluorescent staining because they are 100 ~ 200 nm in size. To clearly verify the relationship between the SGs and differentiation, I examined the phosphorylated eIF2α (p-eIF2α) expression levels. Immunoblot analysis was performed against translation initiation factor eIF2α protein. As shown in Figure 1B, p-eIF2α

expression levels were found to markedly increase similar to Figure 1A. To examine whether SGs assembly was induced by neuronal induction media, human U2OS osteosarcoma cells was incubated with same conditioned induction media. Unlike the MSCs, SGs were not observed in U2OS cells (Fig. 1C), and also the expression of p-eIF2α was not changed (Fig. 1D). These results indicate that SG assembly is not induced by stresses of induction media but occurs during processes of neuronal differentiation, meaning that the SG assembly may have any role in differentiation process into neuron in MSCs.

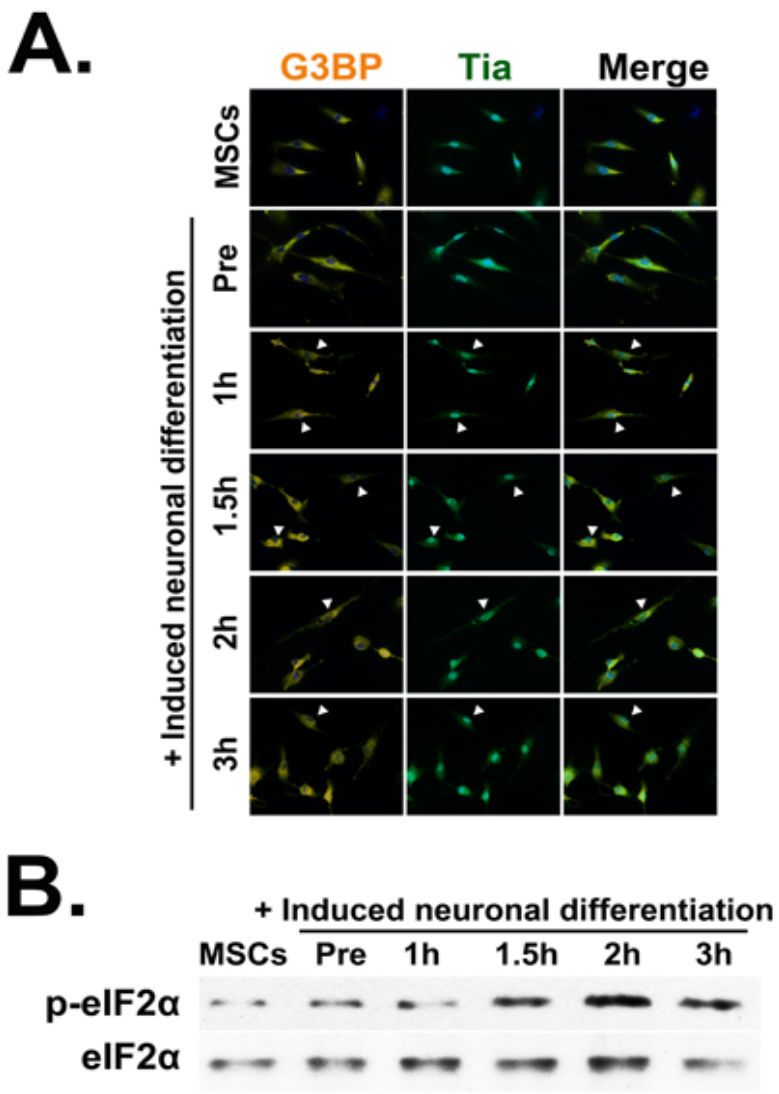

(Chapter 2) Fig. 1. (continued)

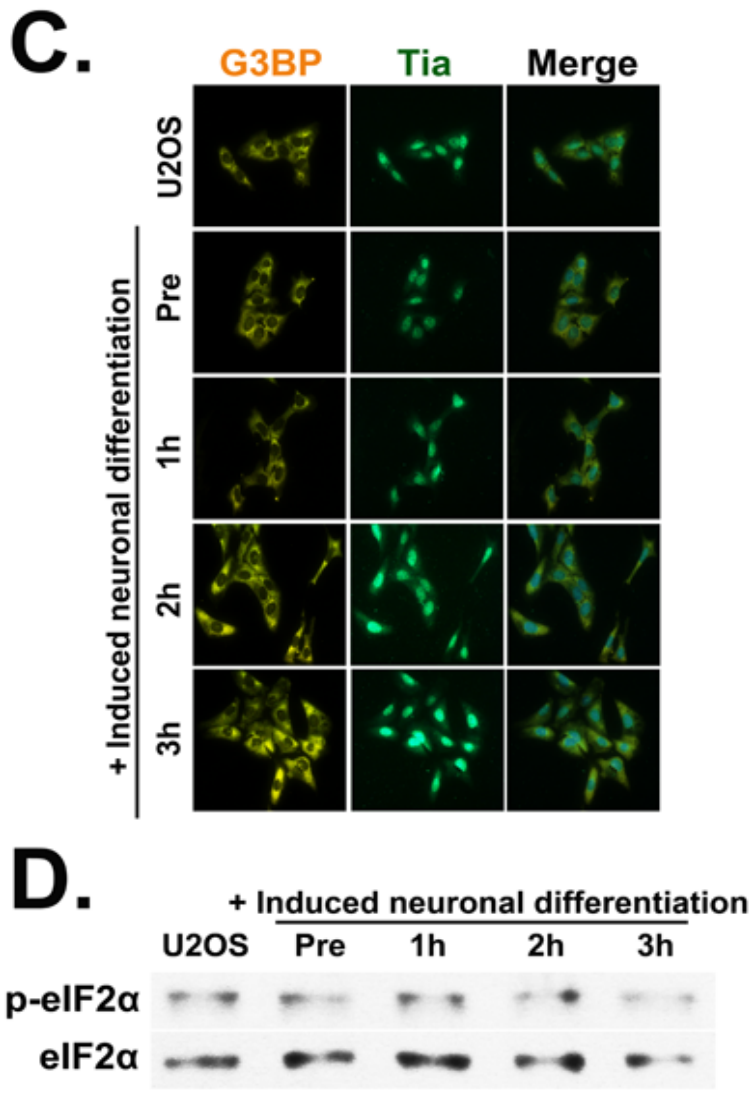

(Chapter 2) Fig. 1.

Figure 1. SGs are exhibited during neuronal differentiation

(A) MSCs were exposed to neuronal induction media for the indicated times (0, 1, 1.5, 2, and 3 h) prior to fixation and immunocytochemical staining for G3BP (orange) and Tia (green). SG assembled cells are indicated by arrow heads. (B) The protein expression of eIF2α and p-eIF2α was measured by immunoblot analysis in MSCs incubated with neuronal induction media for indicated times. (C) U2OS cells cultured on cover slips were incubated with neuronal induction media for the same condition with A. (D) Total proteins were measured by immunoblot analysis using antibodies to detect eIF2α and p-eIF2α in U2OS cells.

(2) SG assembly is not appeared in neural specific marker expressing cells

To examine the relationship between the SG assembly and neuronal differentiation, I examined the relationship by immunocytochemical staining using the antibodies against G3BP and neural specific marker NF-M. As shown in Figure 2A, SGs were detected during differentiation process from 1.5 to 4 h. The double labeling against G3BP and NF-M demonstrates that the expression level of NF-M in SGs existed cells was reduced. Similarly result obtained from Figure 2B. I observed the alteration of p-eIF2α and NF-M in differentiation process by immunoblot analysis. p-eIF2α levels were significantly increased until 2 h and were gradually decreased after 2 h, whereas NF-M expression was begun to increase after 6 h (Fig. 2B). SGs assembly and p-eIF2α trigger the repression of translation. Since SGs and p-eIF2α were observed during the differentiation process, the translation was observed by Click AHA detection. Translation was generally activated, whereas translation was markedly reduced from 2 to 3 h concurrently with SG assembly and phosphorylation of eIF2α (Fig. 2C), indicating that SGs may modulate the translation of mRNA involved in neuronal differentiation and influence the expression of neural specific marker.

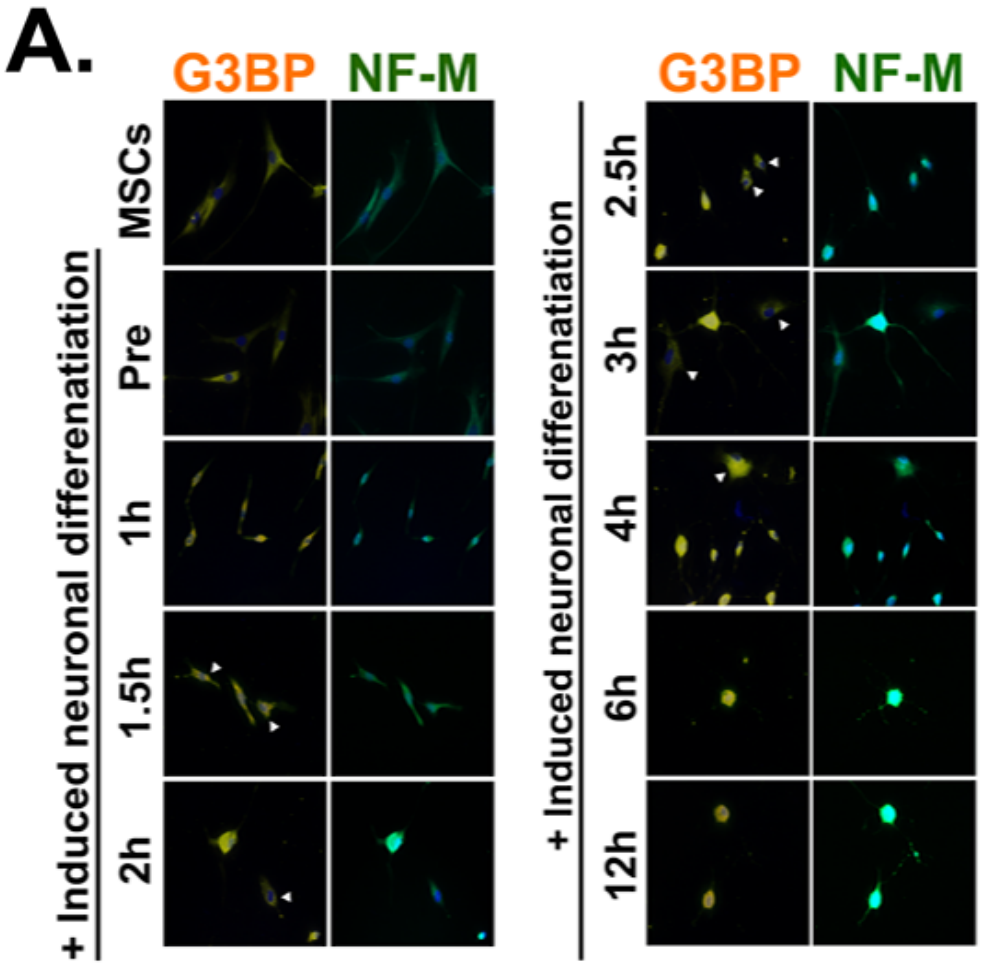

(Chapter 2) Fig. 2. (continued)

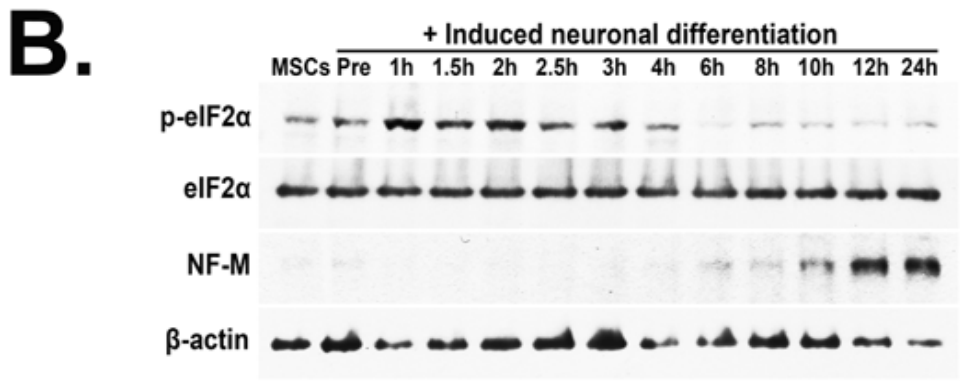

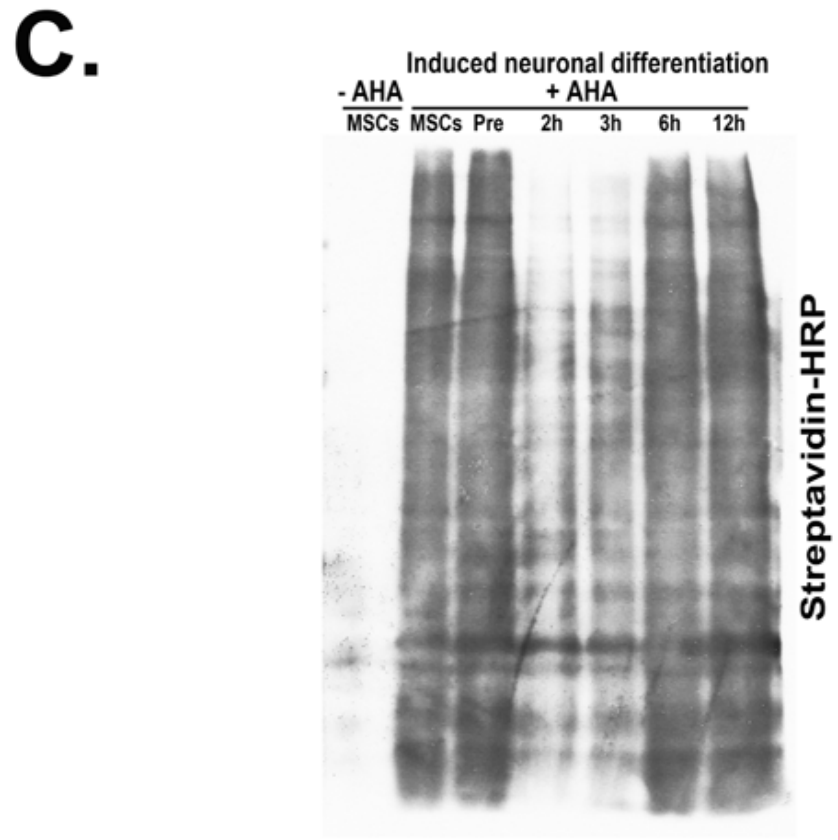

(Chapter 2) Fig. 1.

Figure 2. Effect of SG assembly on neural-specific protein expression in neuronal differerntiation

(A) MSCs were treated with neuronal induction media for the indicated times (0, 1, 1.5, 2, 2.5, 3, 4, 6, and 12 h). Cells were fixed and immunostained for G3BP (orange) and NF-M (green). SG assembled cells are indicated by arrow heads. (B) Changes in p-eIF2α and NF-M expression levels were measured by immunoblot analysis during neuronal differentiation for indicated times. (C) MSCs were labeled with 20 μM AHA for 4 h and then the cells were harvested at indicated times. Newly synthesized proteins were measured by immunoblot analysis for biotin-streptavidin conjugation. -AHA indicates not labeled with AHA.

(3) Inhibition of eIF2α dephosphorylation impede the process of neuronal differentiation

To examine the influence of eIF2α dephosphorylation in the differentiation process, 10 μM of salubrinal was treated to inhibit the dephosphorylation of eIF2α. As shown in Figure 3A, p-eIF2α levels were markedly increased until 6 h compared to salubrinal non-treated cells. Along with this, I also observed the significantly decrease of NF-M expression in salubrinal treated cells compared to non-treated cells._To confirm this result, salubrinal treated cells were stained for G3BP and Tia. Unlike the non-treated cells, I observed that SGs were remained until 6 h during differentiation process in salubrinal treated cells (Fig. 3B). The cells lead to change in the various cellular mechanisms, including transcription, translation, and histone modification, in order to adapt for the changed environment (Yamasaki et al., 2008). Since the both of eIF2α phosphorylation and SGs were maintained by treatment of salubrinal, I examined the alteration of translation using the Click AHA detection. During the neuronal differentiation, translation was dramatically reduced at 2 h and then gradually restored from 6 to 12 h in salubrinal treated cells compared with non-treated cells (Fig. 3C). These results suggest that SG assembly is involved in the expression of neural specific protein and interfere with the differentiation process.

Present study has demonstrated that the SG is involved in neuronal differentiation mechanisms. SG acts as a regulator of translation through

inhibition of polysome assembly in neuronal differentiation. I found that the inhibition of eIF2α dephosphorylation delays differentiation into neuron. These findings indicate that SG assembly may be an important mechanism which occurs during differentiation process. However, I could not confirm the role of SG assembly during neuronal differentiation. Therefore, definite role of SGs in differentiation into neuron need to be further investigated. In conclusion, SG regulates the expression of neural specific protein through the modulation of translation during neuronal differentiation.

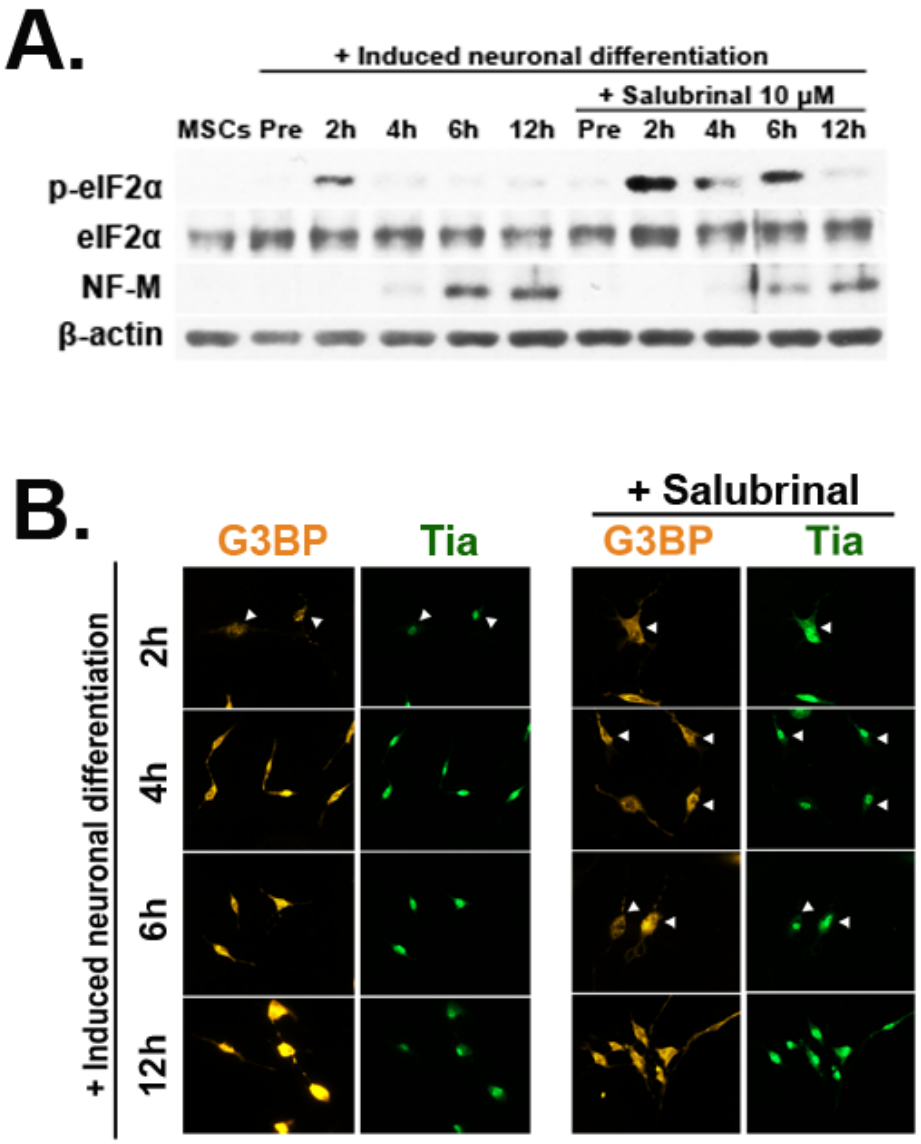

(Chapter 2) Fig. 3. (continued)

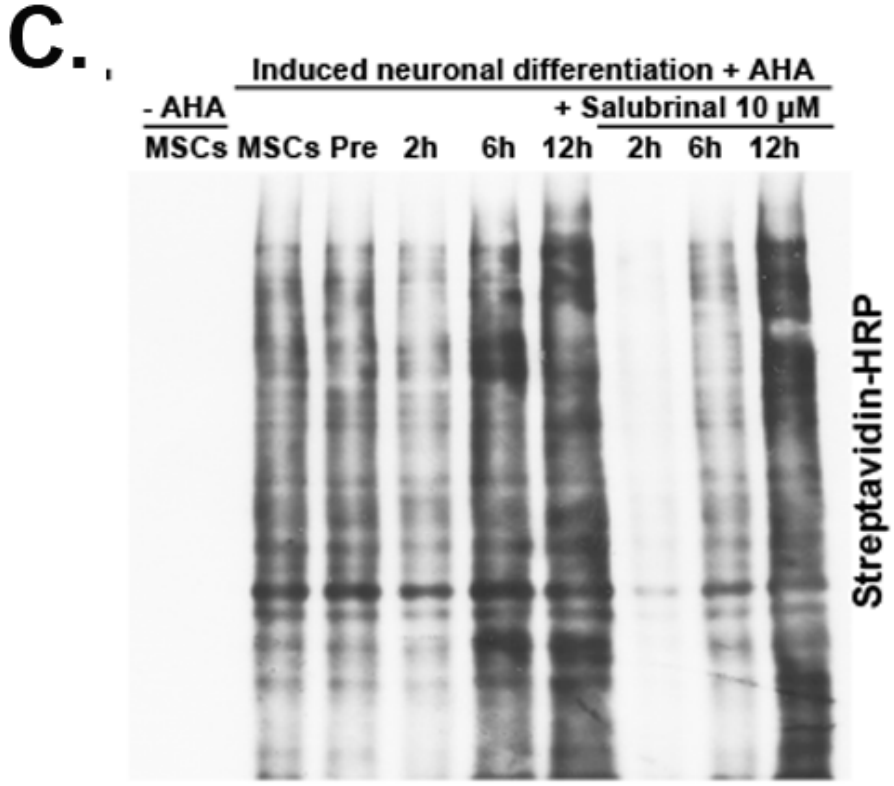

(Chapter 2) Fig. 3.

Figure 3. Alteration of SG assembly in neuronal differentiation treated with salubrinal

Neuronal differentiation induced by exposure to neuronal induction media for the indicated times. (A) Changes in p-eIF2α and NF-M expression levels were measured in non-treated differentiated MSCs versus salubrinal-treated differentiated MSCs by immunoblotting with specific antibodies. (B) Differentiated MSCs with (right panel) or without (left panel) treatment of salubrinal were fixed and stained with G3BP (orange) and Tia (green) antibodies, and observed by fluorescence microscopy. (C) Nascent proteins were measured by using the AHA labeling in differentiated MSCs with or without treatment of salubrinal.

IV. Conclusion

Cellular senescence is strongly associated with excessive intracellular ROS (Cadenas and Davies, 2000). ROS can cause cellular damage, which leads to loss of cell function or cell death when it exceeds the physiological concentration limit. In part I, I observed the increase of ROS levels and reduction of antioxidant proteins expression in long-term cultured MSCs, and identified the accumulation of apoptotic-resistant cells during stem cell expansion. Taken together, I propose that excessive intracellular ROS causes random damage to cellular molecules and induces apoptotic cell death. However, senescent cells that are accidently impaired by excessive ROS may avoid apoptosis and accumulate in long-term culture. These cells may accelerate the progressive senescence of healthy neighboring cells. Senescent cells were partially recovered by scavenging excess ROS by treatment with the TSA, UP-Ex, and GV-Ex. Thus, the control of senescent cells through the elimination of ROS may enable the accumulation of healthy stem cells during cell expansion. These cells may possess better stem cell potency, which may assure therapeutic efficacy in stem cell therapy.

MSCs, which have the potency to differentiate into neuronal cells, have been used as a source for therapy of neurological diseases. Neuronal differentiation leads to dynamic change in cell shape, metabolic function, and cellular signaling (Black, 2003; Licatalosi and Darnell, 2006). These changes are related to genetic and epigenetic modification. In part II, I

found that Sirt2 regulates the expression of neural-specific marker proteins NF-M and MAP-2 via ERK-CREB pathway activation, and observed that SGs are involved in neuronal differentiation through the post-transcriptional regulation. Thus, Sirt2 and SGs may play an important role in neuronal differentiation process. However, I was unable to confirm the mechanisms of Sirt2 and SGs during neuronal differentiation. Therefore, specific roles of Sirt2 and SGs in neuronal differentiation need to be further investigated.

V. References

Adachi, M., Osawa, Y., Uchinami, H., Kitamura, T., Accili, D., and Brenner, D.A. (2007). The forkhead transcription factor FoxO1 regulates proliferation and transdifferentiation of hepatic stellate cells. Gastroenterology *132*, 1434-1446.

Agudelo, M., Gandhi, N., Saiyed, Z., Pichili, V., Thangavel, S., Khatavkar, P., Yndart-Arias, A., and Nair, M. (2011). Effects of alcohol on histone deacetylase 2 (HDAC2) and the neuroprotective role of trichostatin A (TSA). Alcohol Clin Exp Res *35*, 1550-1556.

Al-Bassam, J., and Corbett, K.D. (2012). alpha-Tubulin acetylation from the inside out. Proceedings of the National Academy of Sciences of the United States of America *109*, 19515-19516.

Allsopp, R.C., Vaziri, H., Patterson, C., Goldstein, S., Younglai, E.V., Futcher, A.B., Greider, C.W., and Harley, C.B. (1992). Telomere length predicts replicative capacity of human fibroblasts. Proc Natl Acad Sci U S A *89*, 10114-10118.

Amos, L.A., and Lowe, J. (1999). How Taxol stabilises microtubule structure. Chemistry & biology *6*, R65-69.

Anderson, P., and Kedersha, N. (2006). RNA granules. The Journal of cell biology *172*, 803-808.

Anderson, P., and Kedersha, N. (2008). Stress granules: the Tao of RNA triage. Trends in biochemical sciences *33*, 141-150.

Anderson, P., and Kedersha, N. (2009a). RNA granules: post-

transcriptional and epigenetic modulators of gene expression. Nature reviews Molecular cell biology *10*, 430-436.

Anderson, P., and Kedersha, N. (2009b). Stress granules. Current biology : CB *19*, R397-398.

Atashrazm, F., Lowenthal, R.M., Woods, G.M., Holloway, A.F., and Dickinson, J.L. (2015). Fucoidan and cancer: a multifunctional molecule with anti-tumor potential. Marine drugs *13*, 2327-2346.

Augello, A., Tasso, R., Negrini, S.M., Cancedda, R., and Pennesi, G. (2007). Cell therapy using allogeneic bone marrow mesenchymal stem cells prevents tissue damage in collagen-induced arthritis. Arthritis Rheum *56*, 1175-1186.

Back, P., Braeckman, B.P., and Matthijssens, F. (2012). ROS in aging Caenorhabditis elegans: damage or signaling? Oxid Med Cell Longev *2012*, 608478.

Baker, D.J., Wijshake, T., Tchkonia, T., LeBrasseur, N.K., Childs, B.G., van de Sluis, B., Kirkland, J.L., and van Deursen, J.M. Clearance of p16Ink4a-positive senescent cells delays ageing-associated disorders. Nature *479*, 232-236.

Barry, F., and Murphy, M. (2013). Mesenchymal stem cells in joint disease and repair. Nature reviews Rheumatology *9*, 584-594.

Ben Mosbah, I., Mouchel, Y., Pajaud, J., Ribault, C., Lucas, C., Laurent, A., Boudjema, K., Morel, F., Corlu, A., and Compagnon, P. (2012). Pretreatment with mangafodipir improves liver graft tolerance to

ischemia/reperfusion injury in rat. PLoS One *7*, e50235.

Biteau, B., Hochmuth, C.E., and Jasper, H. (2011). Maintaining tissue homeostasis: dynamic control of somatic stem cell activity. Cell Stem Cell *9*, 402-411.

Black, D.L. (2003). Mechanisms of alternative pre-messenger RNA splicing. Annual review of biochemistry *72*, 291-336.

Bolden, J.E., Peart, M.J., and Johnstone, R.W. (2006). Anticancer activities of histone deacetylase inhibitors. Nat Rev Drug Discov *5*, 769-784.

Bowne-Anderson, H., Zanic, M., Kauer, M., and Howard, J. (2013). Microtubule dynamic instability: a new model with coupled GTP hydrolysis and multistep catastrophe. BioEssays : news and reviews in molecular, cellular and developmental biology *35*, 452-461.

Cadenas, E., and Davies, K.J. (2000). Mitochondrial free radical generation, oxidative stress, and aging. Free Radic Biol Med *29*, 222-230.

Canon, E., Cosgaya, J.M., Scsucova, S., and Aranda, A. (2004). Rapid effects of retinoic acid on CREB and ERK phosphorylation in neuronal cells. Molecular biology of the cell *15*, 5583-5592.

Caplan, A.I. (2007). Adult mesenchymal stem cells for tissue engineering versus regenerative medicine. J Cell Physiol *213*, 341-347.

Cerutti, P.A. (1985). Prooxidant states and tumor promotion. Science *227*, 375-381.

Chambers, S.M., Shaw, C.A., Gatza, C., Fisk, C.J., Donehower, L.A., and Goodell, M.A. (2007). Aging hematopoietic stem cells decline in

function and exhibit epigenetic dysregulation. PLoS Biol *5*, e201.

Chiarugi, P., and Buricchi, F. (2007). Protein tyrosine phosphorylation and reversible oxidation: two cross-talking posttranslation modifications. Antioxid Redox Signal *9*, 1-24.

Cho, G.W., Noh, M.Y., Kim, H.Y., Koh, S.H., Kim, K.S., and Kim, S.H. (2010). Bone marrow-derived stromal cells from amyotrophic lateral sclerosis patients have diminished stem cell capacity. Stem Cells Dev *19*, 1035-1042.

Choi, Y.H., Kim, H., Lee, S.H., Jin, Y.H., and Lee, K.Y. (2013). ERK1/2 regulates SIRT2 deacetylase activity. Biochemical and biophysical research communications *437*, 245-249.

Choron, R.L., Chang, S., Khan, S., Villalobos, M.A., Zhang, P., Carpenter, J.P., Tulenko, T.N., and Liu, Y. (2015). Paclitaxel impairs adipose stem cell proliferation and differentiation. The Journal of surgical research *196*, 404-415.

Chou, C.W., Wu, M.S., Huang, W.C., and Chen, C.C. (2011). HDAC inhibition decreases the expression of EGFR in colorectal cancer cells. PLoS One *6*, e18087.

Conaco, C., Otto, S., Han, J.J., and Mandel, G. (2006). Reciprocal actions of REST and a microRNA promote neuronal identity. Proceedings of the National Academy of Sciences of the United States of America *103*, 2422-2427.

Coppe, J.P., Patil, C.K., Rodier, F., Sun, Y., Munoz, D.P., Goldstein, J.,

Nelson, P.S., Desprez, P.Y., and Campisi, J. (2008). Senescence-associated secretory phenotypes reveal cell-nonautonomous functions of oncogenic RAS and the p53 tumor suppressor. PLoS Biol *6*, 2853-2868.

Costache, V., Bilotto, S., Laguerre, L., Belle, R., Cosson, B., Cormier, P., and Morales, J. (2012). Dephosphorylation of eIF2alpha is essential for protein synthesis increase and cell cycle progression after sea urchin fertilization. Developmental biology *365*, 303-309.

Creppe, C., Malinouskaya, L., Volvert, M.L., Gillard, M., Close, P., Malaise, O., Laguesse, S., Cornez, I., Rahmouni, S., Ormenese, S., *et al.* (2009). Elongator controls the migration and differentiation of cortical neurons through acetylation of alpha-tubulin. Cell *136*, 551-564.

de Almeida, C.L., Falcao Hde, S., Lima, G.R., Montenegro Cde, A., Lira, N.S., de Athayde-Filho, P.F., Rodrigues, L.C., de Souza Mde, F., Barbosa-Filho, J.M., and Batista, L.M. (2011). Bioactivities from marine algae of the genus Gracilaria. Int J Mol Sci *12*, 4550-4573.

de Candia, P., Blekhman, R., Chabot, A.E., Oshlack, A., and Gilad, Y. (2008). A combination of genomic approaches reveals the role of FOXO1a in regulating an oxidative stress response pathway. PLoS One *3*, e1670.

de Forges, H., Bouissou, A., and Perez, F. (2012). Interplay between microtubule dynamics and intracellular organization. The international journal of biochemistry & cell biology *44*, 266-274.

Del Rio, J.A., Gonzalez-Billault, C., Urena, J.M., Jimenez, E.M., Barallobre, M.J., Pascual, M., Pujadas, L., Simo, S., La Torre, A., Wandosell, F., *et al.* (2004). MAP1B is required for Netrin 1 signaling in neuronal migration and axonal guidance. Current biology : CB *14*, 840-850.

Dent, E.W., and Gertler, F.B. (2003). Cytoskeletal dynamics and transport in growth cone motility and axon guidance. Neuron *40*, 209-227.

Deux, J.F., Meddahi-Pelle, A., Le Blanche, A.F., Feldman, L.J., Colliec-Jouault, S., Bree, F., Boudghene, F., Michel, J.B., and Letourneur, D. (2002). Low molecular weight fucoidan prevents neointimal hyperplasia in rabbit iliac artery in-stent restenosis model. Arterioscler Thromb Vasc Biol *22*, 1604-1609.

Drevets, W.C. (2000). Neuroimaging studies of mood disorders. Biol Psychiatry *48*, 813-829.

Dryden, S.C., Nahhas, F.A., Nowak, J.E., Goustin, A.S., and Tainsky, M.A. (2003). Role for human SIRT2 NAD-dependent deacetylase activity in control of mitotic exit in the cell cycle. Molecular and cellular biology *23*, 3173-3185.

Emara, M.M., Fujimura, K., Sciaranghella, D., Ivanova, V., Ivanov, P., and Anderson, P. (2012). Hydrogen peroxide induces stress granule formation independent of eIF2alpha phosphorylation. Biochemical and biophysical research communications *423*, 763-769.

Evans, P., and Halliwell, B. (1999). Free radicals and hearing. Cause, consequence, and criteria. Ann N Y Acad Sci *884*, 19-40.

Fan, W., Cheng, K., Qin, X., Narsinh, K.H., Wang, S., Hu, S., Wang, Y., Chen, Y., Wu, J.C., Xiong, L., *et al.* (2013). mTORC1 and mTORC2 play different roles in the functional survival of transplanted adipose-derived stromal cells in hind limb ischemic mice via regulating inflammation in vivo. Stem Cells *31*, 203-214.

Farini, A., Sitzia, C., Erratico, S., Meregalli, M., and Torrente, Y. (2014). Clinical applications of mesenchymal stem cells in chronic diseases. Stem Cells Int *2014*, 306573.

Fehrer, C., Laschober, G., and Lepperdinger, G. (2006). Aging of murine mesenchymal stem cells. Ann N Y Acad Sci *1067*, 235-242.

Finkel, T., and Holbrook, N.J. (2000). Oxidants, oxidative stress and the biology of ageing. Nature *408*, 239-247.

Gambino, V., De Michele, G., Venezia, O., Migliaccio, P., Dall'Olio, V., Bernard, L., Minardi, S.P., Della Fazia, M.A., Bartoli, D., Servillo, G., *et al.* (2013). Oxidative stress activates a specific p53 transcriptional response that regulates cellular senescence and aging. Aging Cell *12*, 435-445.

Geissler, S., Textor, M., Kuhnisch, J., Konnig, D., Klein, O., Ode, A., Pfitzner, T., Adjaye, J., Kasper, G., and Duda, G.N. (2012). Functional comparison of chronological and in vitro aging: differential role of the cytoskeleton and mitochondria in mesenchymal stromal cells. PLoS One *7*, e52700.

Gelfand, V.I., and Bershadsky, A.D. (1991). Microtubule dynamics:

mechanism, regulation, and function. Annual review of cell biology *7*, 93-116.

Gerlitz, G., Jagus, R., and Elroy-Stein, O. (2002). Phosphorylation of initiation factor-2 alpha is required for activation of internal translation initiation during cell differentiation. European journal of biochemistry *269*, 2810-2819.

Govindarajan, N., Rao, P., Burkhardt, S., Sananbenesi, F., Schluter, O.M., Bradke, F., Lu, J., and Fischer, A. (2013). Reducing HDAC6 ameliorates cognitive deficits in a mouse model for Alzheimer's disease. EMBO Mol Med *5*, 52-63.

Guaiquil, V.H., Vera, J.C., and Golde, D.W. (2001). Mechanism of vitamin C inhibition of cell death induced by oxidative stress in glutathione-depleted HL-60 cells. J Biol Chem *276*, 40955-40961.

Haggarty, S.J., Koeller, K.M., Wong, J.C., Grozinger, C.M., and Schreiber, S.L. (2003). Domain-selective small-molecule inhibitor of histone deacetylase 6 (HDAC6)-mediated tubulin deacetylation. Proceedings of the National Academy of Sciences of the United States of America *100*, 4389-4394.

Harley, C.B., Futcher, A.B., and Greider, C.W. (1990). Telomeres shorten during ageing of human fibroblasts. Nature *345*, 458-460.

Hart, R.W., and Setlow, R.B. (1974). Correlation between deoxyribonucleic acid excision-repair and life-span in a number of mammalian species. Proc Natl Acad Sci U S A *71*, 2169-2173.

Hayflick, L. (1965). The Limited in Vitro Lifetime of Human Diploid Cell Strains. Exp Cell Res *37*, 614-636.

Heeschen, C., Lehmann, R., Honold, J., Assmus, B., Aicher, A., Walter, D.H., Martin, H., Zeiher, A.M., and Dimmeler, S. (2004). Profoundly reduced neovascularization capacity of bone marrow mononuclear cells derived from patients with chronic ischemic heart disease. Circulation *109*, 1615-1622.

Hoidal, J.R. (2001). Reactive oxygen species and cell signaling. Am J Respir Cell Mol Biol *25*, 661-663.

Honda, Y., and Honda, S. (1999). The daf-2 gene network for longevity regulates oxidative stress resistance and Mn-superoxide dismutase gene expression in Caenorhabditis elegans. FASEB J *13*, 1385-1393.

Howard, J., and Hyman, A.A. (2003). Dynamics and mechanics of the microtubule plus end. Nature *422*, 753-758.

Howes, S.C., Alushin, G.M., Shida, T., Nachury, M.V., and Nogales, E. (2014). Effects of tubulin acetylation and tubulin acetyltransferase binding on microtubule structure. Molecular biology of the cell *25*, 257-266.

Huang, H., and Tindall, D.J. (2007). Dynamic FoxO transcription factors. J Cell Sci *120*, 2479-2487.

Hubbert, C., Guardiola, A., Shao, R., Kawaguchi, Y., Ito, A., Nixon, A., Yoshida, M., Wang, X.F., and Yao, T.P. (2002). HDAC6 is a microtubule-associated deacetylase. Nature *417*, 455-458.

Hussain, S.P., Amstad, P., He, P., Robles, A., Lupold, S., Kaneko, I., Ichimiya, M., Sengupta, S., Mechanic, L., Okamura, S., *et al.* (2004). p53-induced up-regulation of MnSOD and GPx but not catalase increases oxidative stress and apoptosis. Cancer Res *64*, 2350-2356.

Impey, S., Obrietan, K., and Storm, D.R. (1999). Making new connections: role of ERK/MAP kinase signaling in neuronal plasticity. Neuron *23*, 11-14.

Irani, K. (2000). Oxidant signaling in vascular cell growth, death, and survival : a review of the roles of reactive oxygen species in smooth muscle and endothelial cell mitogenic and apoptotic signaling. Circ Res *87*, 179-183.

Jeong, S.G., and Cho, G.W. (2015a). Endogenous ROS levels are increased in replicative senescence in human bone marrow mesenchymal stromal cells. Biochem Biophys Res Commun *460*, 971-976.

Jeong, S.G., and Cho, G.W. (2015b). Trichostatin A modulates intracellular reactive oxygen species through SOD2 and FOXO1 in human bone marrow-mesenchymal stem cells. Cell biochemistry and function *33*, 37-43.

Jeong, S.G., and Cho, G.W. (2015b). Trichostatin A modulates intracellular reactive oxygen species through SOD2 and FOXO1 in human bone marrow-mesenchymal stem cells. Cell Biochem Funct *33*, 37-43.

Jeong, S.G., Ohn, T., Kim, S.H., and Cho, G.W. (2013). Valproic acid

promotes neuronal differentiation by induction of neuroprogenitors in human bone-marrow mesenchymal stromal cells. Neurosci Lett *554*, 22-27.

Joe, I.S., Jeong, S.G., and Cho, G.W. (2015). Resveratrol-induced SIRT1 activation promotes neuronal differentiation of human bone marrow mesenchymal stem cells. Neuroscience letters *584*, 97-102.

Johnson, F., and Giulivi, C. (2005). Superoxide dismutases and their impact upon human health. Mol Aspects Med *26*, 340-352.

Johnson, T.M., Yu, Z.X., Ferrans, V.J., Lowenstein, R.A., and Finkel, T. (1996). Reactive oxygen species are downstream mediators of p53-dependent apoptosis. Proc Natl Acad Sci U S A *93*, 11848-11852.

Jung, K.H., Han, D.M., Jeong, S.G., Choi, M.R., Chai, Y.G., and Cho, G.W. (2015). Proteomic analysis reveals KRIT1 as a modulator for the antioxidant effects of valproic acid in human bone-marrow mesenchymal stromal cells. Drug Chem Toxicol *38*, 286-292.

Jung, M.S., Jin, D.H., Chae, H.D., Kang, S., Kim, S.C., Bang, Y.J., Choi, T.S., Choi, K.S., and Shin, D.Y. (2004). Bcl-xL and E1B-19K proteins inhibit p53-induced irreversible growth arrest and senescence by preventing reactive oxygen species-dependent p38 activation. J Biol Chem *279*, 17765-17771.

Kallas, A., Pook, M., Maimets, M., Zimmermann, K., and Maimets, T. (2011). Nocodazole treatment decreases expression of pluripotency markers Nanog and Oct4 in human embryonic stem cells. PloS one *6*,

e19114.

Kan, I., Ben-Zur, T., Barhum, Y., Levy, Y.S., Burstein, A., Charlow, T., Bulvik, S., Melamed, E., and Offen, D. (2007). Dopaminergic differentiation of human mesenchymal stem cells--utilization of bioassay for tyrosine hydroxylase expression. Neurosci Lett *419*, 28-33.

Khan, M.N., Cho, J.Y., Lee, M.C., Kang, J.Y., Park, N.G., Fujii, H., and Hong, Y.K. (2007). Isolation of two anti-inflammatory and one pro-inflammatory polyunsaturated fatty acids from the brown seaweed Undaria pinnatifida. J Agric Food Chem *55*, 6984-6988.

Kim, E.K., Lim, S., Park, J.M., Seo, J.K., Kim, J.H., Kim, K.T., Ryu, S.H., and Suh, P.G. (2012). Human mesenchymal stem cell differentiation to the osteogenic or adipogenic lineage is regulated by AMP-activated protein kinase. J Cell Physiol *227*, 1680-1687.

Kim, H.Y., Kim, H., Oh, K.W., Oh, S.I., Koh, S.H., Baik, W., Noh, M.Y., Kim, K.S., and Kim, S.H. (2014). Biological markers of mesenchymal stromal cells as predictors of response to autologous stem cell transplantation in patients with amyotrophic lateral sclerosis: an investigator-initiated trial and in vivo study. Stem Cells *32*, 2724-2731.

Kim, J.H., Park, S.G., Song, S.Y., Kim, J.K., and Sung, J.H. (2013). Reactive oxygen species-responsive miR-210 regulates proliferation and migration of adipose-derived stem cells via PTPN2. Cell Death

Dis *4*, e588.

Kim, K.J., and Lee, B.Y. (2012). Fucoidan from the sporophyll of Undaria pinnatifida suppresses adipocyte differentiation by inhibition of inflammation-related cytokines in 3T3-L1 cells. Nutrition research *32*, 439-447.

Kim, M.J., Jeon, J., and Lee, J.S. (2014b). Fucoidan prevents high-fat diet-induced obesity in animals by suppression of fat accumulation. Phytotherapy research : PTR *28*, 137-143.

Koch-Weser, J., and Browne, T.R. (1980). Drug therapy: Valproic acid. N Engl J Med *302*, 661-666.

Koga, H., Kaushik, S., and Cuervo, A.M. (2011). Protein homeostasis and aging: The importance of exquisite quality control. Ageing Res Rev *10*, 205-215.

Kondo, Y., Masutomi, H., Noda, Y., Ozawa, Y., Takahashi, K., Handa, S., Maruyama, N., Shimizu, T., and Ishigami, A. (2014). Senescence marker protein-30/superoxide dismutase 1 double knockout mice exhibit increased oxidative stress and hepatic steatosis. FEBS Open Bio *4*, 522-532.

Kosik, K.S., and Krichevsky, A.M. (2002). The message and the messenger: delivering RNA in neurons. Science's STKE : signal transduction knowledge environment *2002*, pe16.

Krichevsky, A.M., and Kosik, K.S. (2001). Neuronal RNA granules: a link between RNA localization and stimulation-dependent translation.

Neuron *32*, 683-696.

Kuilman, T., Michaloglou, C., Mooi, W.J., and Peeper, D.S. (2010). The essence of senescence. Genes Dev *24*, 2463-2479.

Kujoth, G.C., Hiona, A., Pugh, T.D., Someya, S., Panzer, K., Wohlgemuth, S.E., Hofer, T., Seo, A.Y., Sullivan, R., Jobling, W.A., *et al.* (2005). Mitochondrial DNA mutations, oxidative stress, and apoptosis in mammalian aging. Science *309*, 481-484.

Kuroda, J., Ago, T., Matsushima, S., Zhai, P., Schneider, M.D., and Sadoshima, J. (2010). NADPH oxidase 4 (Nox4) is a major source of oxidative stress in the failing heart. Proc Natl Acad Sci U S A *107*, 15565-15570.

Lee, H.S., Hwang, C.Y., Shin, S.Y., Kwon, K.S., and Cho, K.H. (2014). MLK3 is part of a feedback mechanism that regulates different cellular responses to reactive oxygen species. Sci Signal *7*, ra52.

Li, Z., Theus, M.H., and Wei, L. (2006). Role of ERK 1/2 signaling in neuronal differentiation of cultured embryonic stem cells. Development, growth & differentiation *48*, 513-523.

Licatalosi, D.D., and Darnell, R.B. (2006). Splicing regulation in neurologic disease. Neuron *52*, 93-101.

Linares, A.J., Lin, C.H., Damianov, A., Adams, K.L., Novitch, B.G., and Black, D.L. (2015). The splicing regulator PTBP1 controls the activity of the transcription factor Pbx1 during neuronal differentiation. eLife *4*, e09268.

Liu, B., Chen, Y., and St Clair, D.K. (2008). ROS and p53: a versatile partnership. Free Radic Biol Med *44*, 1529-1535.

Liu, L., and Rando, T.A. (2011). Manifestations and mechanisms of stem cell aging. The Journal of cell biology *193*, 257-266.

Liu, S.P., Ding, D.C., Wang, H.J., Su, C.Y., Lin, S.Z., Li, H., and Shyu, W.C. (2010). Nonsenescent Hsp27-upregulated MSCs implantation promotes neuroplasticity in stroke model. Cell Transplant *19*, 1261-1279.

Liu, Y., Li, P., Liu, K., He, Q., Han, S., Sun, X., Li, T., and Shen, L. (2014). Timely inhibition of Notch signaling by DAPT promotes cardiac differentiation of murine pluripotent stem cells. PLoS One *9*, e109588.

Lu, T., and Finkel, T. (2008). Free radicals and senescence. Experimental cell research *314*, 1918-1922.

Ludlow, A.T., Spangenburg, E.E., Chin, E.R., Cheng, W.H., and Roth, S.M. (2014). Telomeres shorten in response to oxidative stress in mouse skeletal muscle fibers. J Gerontol A Biol Sci Med Sci *69*, 821-830.

Machado-Vieira, R., Ibrahim, L., and Zarate, C.A., Jr. (2011). Histone deacetylases and mood disorders: epigenetic programming in gene-environment interactions. CNS Neurosci Ther *17*, 699-704.

Macip, S., Igarashi, M., Fang, L., Chen, A., Pan, Z.Q., Lee, S.W., and Aaronson, S.A. (2002). Inhibition of p21-mediated ROS accumulation can rescue p21-induced senescence. EMBO J *21*, 2180-2188.

Maeda, H., Hosokawa, M., Sashima, T., Funayama, K., and Miyashita, K.

(2005). Fucoxanthin from edible seaweed, Undaria pinnatifida, shows antiobesity effect through UCP1 expression in white adipose tissues. Biochem Biophys Res Commun *332*, 392-397.

Maegawa, S., Hinkal, G., Kim, H.S., Shen, L., Zhang, L., Zhang, J., Zhang, N., Liang, S., Donehower, L.A., and Issa, J.P. (2010). Widespread and tissue specific age-related DNA methylation changes in mice. Genome Res *20*, 332-340.

Mahmood, A., Lu, D., Wang, L., Li, Y., Lu, M., and Chopp, M. (2001). Treatment of traumatic brain injury in female rats with intravenous administration of bone marrow stromal cells. Neurosurgery *49*, 1196-1203; discussion 1203-1194.

Makeyev, E.V., Zhang, J., Carrasco, M.A., and Maniatis, T. (2007). The MicroRNA miR-124 promotes neuronal differentiation by triggering brain-specific alternative pre-mRNA splicing. Molecular cell *27*, 435-448.

Marcus, A.J., Coyne, T.M., Rauch, J., Woodbury, D., and Black, I.B. (2008). Isolation, characterization, and differentiation of stem cells derived from the rat amniotic membrane. Differentiation; research in biological diversity *76*, 130-144.

Mastri, M., Shah, Z., McLaughlin, T., Greene, C.J., Baum, L., Suzuki, G., and Lee, T. (2012). Activation of Toll-like receptor 3 amplifies mesenchymal stem cell trophic factors and enhances therapeutic potency. Am J Physiol Cell Physiol *303*, C1021-1033.

Matsuyama, A., Shimazu, T., Sumida, Y., Saito, A., Yoshimatsu, Y., Seigneurin-Berny, D., Osada, H., Komatsu, Y., Nishino, N., Khochbin, S., *et al.* (2002). In vivo destabilization of dynamic microtubules by HDAC6-mediated deacetylation. The EMBO journal *21*, 6820-6831.

Maxwell, M.M., Tomkinson, E.M., Nobles, J., Wizeman, J.W., Amore, A.M., Quinti, L., Chopra, V., Hersch, S.M., and Kazantsev, A.G. (2011). The Sirtuin 2 microtubule deacetylase is an abundant neuronal protein that accumulates in the aging CNS. Human molecular genetics *20*, 3986-3996.

Mazarrasa, I., Olsen, Y.S., Mayol, E., Marba, N., and Duarte, C.M. (2014). Global unbalance in seaweed production, research effort and biotechnology markets. Biotechnology advances *32*, 1028-1036.

Minucci, S., and Pelicci, P.G. (2006). Histone deacetylase inhibitors and the promise of epigenetic (and more) treatments for cancer. Nat Rev Cancer *6*, 38-51.

Mitchison, T., and Kirschner, M. (1984). Dynamic instability of microtubule growth. Nature *312*, 237-242.

Moll, U.M., and Petrenko, O. (2003). The MDM2-p53 interaction. Mol Cancer Res *1*, 1001-1008.

Moon, B.S., Yoon, J.Y., Kim, M.Y., Lee, S.H., Choi, T., and Choi, K.Y. (2009). Bone morphogenetic protein 4 stimulates neuronal differentiation of neuronal stem cells through the ERK pathway. Experimental & molecular medicine *41*, 116-125.

Murata, M., Sano, Y., Ishihara, K., and Uchida, M. (2002). Dietary fish oil and Undaria pinnatifida (wakame) synergistically decrease rat serum and liver triacylglycerol. The Journal of nutrition *132*, 742-747.

Nagai, A., Kim, W.K., Lee, H.J., Jeong, H.S., Kim, K.S., Hong, S.H., Park, I.H., and Kim, S.U. (2007). Multilineage potential of stable human mesenchymal stem cell line derived from fetal marrow. PLoS One *2*, e1272.

Nguyen, A., Leblond, F., Mamarbachi, M., Geoffroy, S., and Thorin, E. (2016). Age-Dependent Demethylation of Sod2 Promoter in the Mouse Femoral Artery. Oxidative medicine and cellular longevity *2016*, 8627384.

North, B.J., Marshall, B.L., Borra, M.T., Denu, J.M., and Verdin, E. (2003). The human Sir2 ortholog, SIRT2, is an NAD+-dependent tubulin deacetylase. Molecular cell *11*, 437-444.

Nover, L., Scharf, K.D., and Neumann, D. (1989). Cytoplasmic heat shock granules are formed from precursor particles and are associated with a specific set of mRNAs. Molecular and cellular biology *9*, 1298-1308.

Oka, S., Hirai, J., Yasukawa, T., Nakahara, Y., and Inoue, Y.H. (2015). A correlation of reactive oxygen species accumulation by depletion of superoxide dismutases with age-dependent impairment in the nervous system and muscles of Drosophila adults. Biogerontology *16*, 485-501.

Owusu-Ansah, E., and Banerjee, U. (2009). Reactive oxygen species

prime Drosophila haematopoietic progenitors for differentiation. Nature *461*, 537-541.

Pandithage, R., Lilischkis, R., Harting, K., Wolf, A., Jedamzik, B., Luscher-Firzlaff, J., Vervoorts, J., Lasonder, E., Kremmer, E., Knoll, B., *et al.* (2008). The regulation of SIRT2 function by cyclin-dependent kinases affects cell motility. The Journal of cell biology *180*, 915-929.

Pani, G., Koch, O.R., and Galeotti, T. (2009). The p53-p66shc-Manganese Superoxide Dismutase (MnSOD) network: a mitochondrial intrigue to generate reactive oxygen species. Int J Biochem Cell Biol *41*, 1002-1005.

Passos, J.F., and von Zglinicki, T. (2005). Mitochondria, telomeres and cell senescence. Exp Gerontol *40*, 466-472.

Pellettieri, J., and Sanchez Alvarado, A. (2007). Cell turnover and adult tissue homeostasis: from humans to planarians. Annual review of genetics *41*, 83-105.

Perrone-Bizzozero, N., and Bolognani, F. (2002). Role of HuD and other RNA-binding proteins in neural development and plasticity. Journal of neuroscience research *68*, 121-126.

Piazza, N., Hayes, M., Martin, I., Duttaroy, A., Grotewiel, M., and Wessells, R. (2009). Multiple measures of functionality exhibit progressive decline in a parallel, stochastic fashion in Drosophila Sod2 null mutants. Biogerontology *10*, 637-648.

Pittenger, M.F., Mackay, A.M., Beck, S.C., Jaiswal, R.K., Douglas, R.,

Mosca, J.D., Moorman, M.A., Simonetti, D.W., Craig, S., and Marshak, D.R. (1999). Multilineage potential of adult human mesenchymal stem cells. Science *284*, 143-147.

Pryor, W.A., Houk, K.N., Foote, C.S., Fukuto, J.M., Ignarro, L.J., Squadrito, G.L., and Davies, K.J. (2006). Free radical biology and medicine: it's a gas, man! Am J Physiol Regul Integr Comp Physiol *291*, R491-511.

Rajkowska, G. (2000). Postmortem studies in mood disorders indicate altered numbers of neurons and glial cells. Biol Psychiatry *48*, 766-777.

Rodier, F., and Campisi, J. (2011). Four faces of cellular senescence. J Cell Biol *192*, 547-556.

Rodriguez, J.P., Gonzalez, M., Rios, S., and Cambiazo, V. (2004). Cytoskeletal organization of human mesenchymal stem cells (MSC) changes during their osteogenic differentiation. Journal of cellular biochemistry *93*, 721-731.

Rodriguez, K.A., Gaczynska, M., and Osmulski, P.A. (2010). Molecular mechanisms of proteasome plasticity in aging. Mech Ageing Dev *131*, 144-155.

Roegiers, F., and Jan, Y.N. (2004). Asymmetric cell division. Current opinion in cell biology *16*, 195-205.

Rogawski, M.A., and Loscher, W. (2004). The neurobiology of antiepileptic drugs. Nat Rev Neurosci *5*, 553-564.

Rossi, D.J., Bryder, D., Seita, J., Nussenzweig, A., Hoeijmakers, J., and

Weissman, I.L. (2007). Deficiencies in DNA damage repair limit the function of haematopoietic stem cells with age. Nature *447*, 725-729.

Rossi, D.J., Jamieson, C.H., and Weissman, I.L. (2008). Stems cells and the pathways to aging and cancer. Cell *132*, 681-696.

Rota, M., LeCapitaine, N., Hosoda, T., Boni, A., De Angelis, A., Padin-Iruegas, M.E., Esposito, G., Vitale, S., Urbanek, K., Casarsa, C., *et al.* (2006). Diabetes promotes cardiac stem cell aging and heart failure, which are prevented by deletion of the p66shc gene. Circ Res *99*, 42-52.

Roux, N., Brakenhielm, E., Freguin-Bouillant, C., Lallemand, F., Henry, J.P., Boyer, O., Thuillez, C., and Plissonnier, D. (2012). Progenitor cell mobilizing treatments prevent experimental transplant arteriosclerosis. The Journal of surgical research *176*, 657-665.

Saito, S., Goodarzi, A.A., Higashimoto, Y., Noda, Y., Lees-Miller, S.P., Appella, E., and Anderson, C.W. (2002). ATM mediates phosphorylation at multiple p53 sites, including Ser(46), in response to ionizing radiation. J Biol Chem *277*, 12491-12494.

Schaeffer, C., Beaulande, M., Ehresmann, C., Ehresmann, B., and Moine, H. (2003). The RNA binding protein FMRP: new connections and missing links. Biology of the cell *95*, 221-228.

Schisa, J.A., Pitt, J.N., and Priess, J.R. (2001). Analysis of RNA associated with P granules in germ cells of C. elegans adults. Development *128*, 1287-1298.

Schultz Moreira, A.R., Benedi, J., Bastida, S., Sanchez-Reus, I., and Sanchez-Muniz, F.J. (2013). Nori- and sea spaghetti- but not wakame-restructured pork decrease the hypercholesterolemic and liver proapototic short-term effects of high-dietary cholesterol consumption. Nutricion hospitalaria *28*, 1422-1429.

Sharpless, N.E., and DePinho, R.A. (2004). Telomeres, stem cells, senescence, and cancer. J Clin Invest *113*, 160-168.

Singh, S.R. (2012). Stem cell niche in tissue homeostasis, aging and cancer. Curr Med Chem *19*, 5965-5974.

Song, H., Cha, M.J., Song, B.W., Kim, I.K., Chang, W., Lim, S., Choi, E.J., Ham, O., Lee, S.Y., Chung, N., *et al.* (2010). Reactive oxygen species inhibit adhesion of mesenchymal stem cells implanted into ischemic myocardium via interference of focal adhesion complex. Stem Cells *28*, 555-563.

Stenderup, K., Justesen, J., Clausen, C., and Kassem, M. (2003). Aging is associated with decreased maximal life span and accelerated senescence of bone marrow stromal cells. Bone *33*, 919-926.

Strasser, A., O'Connor, L., and Dixit, V.M. (2000). Apoptosis signaling. Annu Rev Biochem *69*, 217-245.

Su, S., Zhu, X., Lin, L., Chen, X., Wang, Y., Zi, J., Dong, Y., Xie, Y., Zhu, Y., Zhang, J., *et al.* (2015). Lowering endogenous cathepsin D abundance results in ROS accumulation and cell senescence. Molecular & cellular proteomics : MCP.

Sudhakar, A., Ramachandran, A., Ghosh, S., Hasnain, S.E., Kaufman, R.J., and Ramaiah, K.V. (2000). Phosphorylation of serine 51 in initiation factor 2 alpha (eIF2 alpha) promotes complex formation between eIF2 alpha(P) and eIF2B and causes inhibition in the guanine nucleotide exchange activity of eIF2B. Biochemistry *39*, 12929-12938.

Suzuki, K., and Koike, T. (2007). Mammalian Sir2-related protein (SIRT) 2-mediated modulation of resistance to axonal degeneration in slow Wallerian degeneration mice: a crucial role of tubulin deacetylation. Neuroscience *147*, 599-612.

Tapia, M., Wandosell, F., and Garrido, J.J. (2010). Impaired function of HDAC6 slows down axonal growth and interferes with axon initial segment development. PloS one *5*, e12908.

Tepper, O.M., Galiano, R.D., Capla, J.M., Kalka, C., Gagne, P.J., Jacobowitz, G.R., Levine, J.P., and Gurtner, G.C. (2002). Human endothelial progenitor cells from type II diabetics exhibit impaired proliferation, adhesion, and incorporation into vascular structures. Circulation *106*, 2781-2786.

Thannickal, V.J., and Fanburg, B.L. (2000). Reactive oxygen species in cell signaling. American journal of physiology Lung cellular and molecular physiology *279*, L1005-1028.

van Ginneken, V.J., Helsper, J.P., de Visser, W., van Keulen, H., and Brandenburg, W.A. (2011). Polyunsaturated fatty acids in various macroalgal species from North Atlantic and tropical seas. Lipids

Health Dis *10*, 104.

Vanhaecke, T., Papeleu, P., Elaut, G., and Rogiers, V. (2004). Trichostatin A-like hydroxamate histone deacetylase inhibitors as therapeutic agents: toxicological point of view. Curr Med Chem *11*, 1629-1643.

Vehvilainen, P., Koistinaho, J., and Gundars, G. (2014). Mechanisms of mutant SOD1 induced mitochondrial toxicity in amyotrophic lateral sclerosis. Front Cell Neurosci *8*, 126.

Voog, J., and Jones, D.L. (2010). Stem cells and the niche: a dynamic duo. Cell Stem Cell *6*, 103-115.

Wagner, W., and Ho, A.D. (2007). Mesenchymal stem cell preparations--comparing apples and oranges. Stem cell reviews *3*, 239-248.

Wagner, W., Bork, S., Horn, P., Krunic, D., Walenda, T., Diehlmann, A., Benes, V., Blake, J., Huber, F.X., Eckstein, V., *et al.* (2009). Aging and replicative senescence have related effects on human stem and progenitor cells. PLoS One *4*, e5846.

Walensky, L.D. (2006). BCL-2 in the crosshairs: tipping the balance of life and death. Cell Death Differ *13*, 1339-1350.

Wang, P., Liu, Z., Liu, X., Teng, H., Zhang, C., Hou, L., and Zou, X. (2014). Anti-metastasis effect of fucoidan from Undaria pinnatifida sporophylls in mouse hepatocarcinoma Hca-F cells. PloS one *9*, e106071.

Wang, P., Zhang, P., Huang, J., Li, M., and Chen, X. (2013). Trichostatin A protects against cisplatin-induced ototoxicity by regulating

expression of genes related to apoptosis and synaptic function. Neurotoxicology *37*, 51-62.

Watanabe, K., Shibuya, S., Ozawa, Y., Nojiri, H., Izuo, N., Yokote, K., and Shimizu, T. (2014). Superoxide dismutase 1 loss disturbs intracellular redox signaling, resulting in global age-related pathological changes. Biomed Res Int *2014*, 140165.

Wen, Y., Eng, C.H., Schmoranzer, J., Cabrera-Poch, N., Morris, E.J., Chen, M., Wallar, B.J., Alberts, A.S., and Gundersen, G.G. (2004). EB1 and APC bind to mDia to stabilize microtubules downstream of Rho and promote cell migration. Nature cell biology *6*, 820-830.

Will, B., and Steidl, U. (2014). Stem cell fate regulation by dynein motor protein Lis1. Nature genetics *46*, 217-218.

Witte, H., Neukirchen, D., and Bradke, F. (2008). Microtubule stabilization specifies initial neuronal polarization. The Journal of cell biology *180*, 619-632.

Wollert, K.C., Meyer, G.P., Lotz, J., Ringes-Lichtenberg, S., Lippolt, P., Breidenbach, C., Fichtner, S., Korte, T., Hornig, B., Messinger, D.*, et al.* (2004). Intracoronary autologous bone-marrow cell transfer after myocardial infarction: the BOOST randomised controlled clinical trial. Lancet *364*, 141-148.

Woodbury, D., Schwarz, E.J., Prockop, D.J., and Black, I.B. (2000). Adult rat and human bone marrow stromal cells differentiate into neurons. Journal of neuroscience research *61*, 364-370.

Xuan, A., Long, D., Li, J., Ji, W., Hong, L., Zhang, M., and Zhang, W. (2012). Neuroprotective effects of valproic acid following transient global ischemia in rats. Life Sci *90*, 463-468.

Yamasaki, S., and Anderson, P. (2008). Reprogramming mRNA translation during stress. Current opinion in cell biology *20*, 222-226.

Yang, J.I., Yeh, C.C., Lee, J.C., Yi, S.C., Huang, H.W., Tseng, C.N., and Chang, H.W. (2012). Aqueous extracts of the edible Gracilaria tenuistipitata are protective against H(2)O(2)-induced DNA damage, growth inhibition, and cell cycle arrest. Molecules *17*, 7241-7254.

Yildirim, F., Gertz, K., Kronenberg, G., Harms, C., Fink, K.B., Meisel, A., and Endres, M. (2008). Inhibition of histone deacetylation protects wildtype but not gelsolin-deficient mice from ischemic brain injury. Exp Neurol *210*, 531-542.

Yoo, Y.E., and Ko, C.P. (2011). Treatment with trichostatin A initiated after disease onset delays disease progression and increases survival in a mouse model of amyotrophic lateral sclerosis. Exp Neurol *231*, 147-159.

You, B.R., and Park, W.H. (2013). Trichostatin A induces apoptotic cell death of HeLa cells in a Bcl-2 and oxidative stress-dependent manner. Int J Oncol *42*, 359-366.

Zhang, Y., Kwon, S., Yamaguchi, T., Cubizolles, F., Rousseaux, S., Kneissel, M., Cao, C., Li, N., Cheng, H.L., Chua, K., *et al.* (2008). Mice lacking histone deacetylase 6 have hyperacetylated tubulin but

are viable and develop normally. Molecular and cellular biology *28*, 1688-1701.

Zilberman, Y., Ballestrem, C., Carramusa, L., Mazitschek, R., Khochbin, S., and Bershadsky, A. (2009). Regulation of microtubule dynamics by inhibition of the tubulin deacetylase HDAC6. Journal of cell science *122*, 3531-3541.

VI. Acknowledgements

박사학위를 시작한지 얼마 되지 않은 것 같은데 벌써 졸업 날이 다 되어 갑니다. 아직은 박사라는 학위를 받기에는 부족한 점이 많은데 부끄러울 뿐입니다. 지금까지 박사학위를 무사히 마칠 수 있도록 도와주신 분들께 감사의 인사를 드립니다. 먼저 저를 낳아주시고 길러주시고 세상에 두려움 없이 맞서도록 도와주신 아버지, 어머니 정말 감사 드립니다. 그리고 옆에서 항상 힘내라는 말과 함께 든든하게 지켜줬던 가족들 정말 감사합니다. 앞으로도 좀 더 저의 꿈을 향한 그리고 발전을 위한 길을 계속 가려 합니다. 끝까지 믿고 지켜봐 주세요.

석사부터 박사 학위 생활까지 항상 앞장서서 지도해주시고 이끌어 주신 저의 Boss 조광원 교수님 항상 감사 드립니다. 교수님의 첫 제자로서 부끄럽지 않도록 그리고 진취적인 사람이 되고자 항상 노력하겠습니다. 아직은 부족한 점이 많지만 계속해서 노력하여 부족한 부분들을 하나하나 채워가도록 하겠습니다. 그리고 저에 대학 생활부터 대학원 생활까지 지켜봐 주시고 가르쳐 주시고 인도해주신 김영곤 교수님, 박현용 교수님께 감사의 말씀을 드리고 저에 학위 생활 동안 많은 가르침을 주신 윤성명 교수님, 조태오 교수님, 전택중 교수님, 이준식 교수님, 송상기 교수님께도 진심으로 감사의 말씀을 드립니다. 또한 항상 지도 학생처럼 아낌없는 조언과 지도를 해주신 온탁범 교수님 정말 감사 드립니다. 그리고 정신적인 지주로 자주 뵙진 못하였지만 항상 좋은 말, 그리고 생각할 수 있도록 도와주신 정은이 누나 항상 감사합니다. 지금은 떨어져있지만 학위 과정 동안 항상 힘이 되어주셨던 라영이 누나, 그리고 아라빈스에게도 고맙다는 말씀을 드립니다. 저의 학위 과정 동안 항상 옆에서 함께 해왔던 우리 실험실 식구들, 윤서, 이슬이, 호태,

민지, 영찬이, 향이 항상 고맙게 생각한다는 마음을 이 자리에서 전합니다. 아울러 비록 같은 실험실 생활을 하진 않았지만 항상 많은 것을 느끼고 깨닫게 해준 김미은 박사님, 소영이, 종국이 형, 현기 형, 항상 발전해 가는 모습을 보면서 많은 것을 느끼고 배울 수 있었습니다. 그리고 다른 어리지만 항상 열심히 하는 모습을 통해 저한테 배움을 준 혜선이, 주용이, 푸름이, 주원이, 동엽이, 방헌이, 영빈이, 길옥이, 항상 고마워. 아울러 저를 지지해 주고 버팀목이 되어준 대학 동기 동환이, 병호, 정선, 석희, 종배, 진태, 영희, 기수, 지일이에게 정말 고맙다는 말을 전하고 싶습니다. 그리고 항상 의지하고 힘들 때 조언을 아끼지 않은 공민이형에게도 고맙다는 말을 전합니다. 그리고 힘들 때 고민을 들어주고 든든한 버팀목이 되어준 고등학교 친구들 길근이, 재우, 영표, 백진, 의연, 슬기, 그리고 지금은 함께 할 수 없지만 항상 곁에 있는 친구 세훈이에게 항상 고맙게 생각하고 있음을 전하고 싶습니다. 모든 소중한 분들이 있었기에 제가 지금 이 순간까지 버티며 전진해 나갈 수 있었습니다. 다시 한번 감사의 말씀을 드리며 또 다른 시작을 준비하는 만큼 여러분께 부끄럽지 않은 사람이 되도록 노력하겠습니다. 항상 노력하고 멈추지 않고 정진하는 정신구가 되도록 하겠습니다. 감사합니다.